The roles of hippocampal and neocortical learning mechanisms in the human brain

Samuel Charles Berens

University of Sussex

Thesis submitted for the degree of Doctor of Philosophy

November 2015

Declaration

This thesis is the result of my own work and includes nothing which is the outcome of work done in collaboration except where specifically indicated in the text.

The thesis conforms to an ‘article format’ in which the middle chapters consist of discrete articles written in a style that is appropriate for publication in peer-reviewed journals. The first and final chapters’ present overviews and discussions of the field and the research undertaken.

I hereby declare that this thesis has not been and will not be, submitted in whole or in part to another University for the award of any other degree.

Acknowledgments

First and foremost, I owe a great deal to my supervisor, Chris Bird. His experience, knowledge, insight and support have been invaluable at each stage of my research.

For the funding that I have received over the course of my doctoral training, thanks are due to the Economic and Social Research Council and the University of Sussex. Additionally, I would like to thank Neil Harrison for inviting me to run an exciting project which was funded by his research grant.

A special thanks goes to my fellow lab members (James Keidel, Chrissi Oedekoven, and Gemma Campbell) along with all those who have shared an office with me. I am grateful for your friendship, support, and willingness to discuss my work with me.

For your support and reminders that there is more to life than work, thanks to the FOMO collective and all those who I have had the pleasure of calling friends while living in Brighton.

To my mother and father, thank you for the education and opportunities you have provided me with. To my brother Daniel, thank you for your interest in my work and the enthusiastic discussions that we have together.

Finally, I wish to thank Charlotte. For your love, companionship and encouragement, I am truly blessed. You never fail to lift my spirits.

Summary

Contemporary models of declarative memory state that when initially learned, all novel information is encoded by the hippocampal system before being consolidated or transformed to depend on neocortical structures subserving semantic memory. Based on observations with functional magnetic resonance imaging (fMRI), this thesis presents evidence that novel associations may be directly encoded by the semantic system in humans. While the hippocampus is often involved in information processing at the early stages of learning, the semantic system is seen to encode associative memory traces in the first instance (chapter 2). Furthermore, it is proposed that the hippocampus is not involved in learning when associative information is gradually accumulated across a series of ambiguous events. This is characteristic of cross-situational learning (xSL) which allows for the acquisition of word-object associations (i.e. nouns) during infancy. It is shown that xSL is not well accounted for by a prominent model of contextual learning - the temporal context model (chapter 3). Additionally, fMRI data suggest that neocortical structures rather than components of the hippocampal system are preferentially involved in xSL compared to traditional methods of training (chapter 4). Finally, it is suggested that rapid hippocampal learning mechanisms rely on specialised neuronal-microglial interactions. The administration of a microglial inhibitor (minocycline) was found to modulate hippocampal function and bias its use when other learning systems would have been more advantageous (chapter 5). Collectively, these findings suggest that the hippocampal system is specialised for rapidly encoding information that is explicitly provided, yet may not be recruited when associative information is collated across ambiguous events. At the same time, the neocortical semantic system may be able to learn new information at faster rates than previously thought. As such, it is hypothesised that amnestic patients may be able to acquire some forms of declarative material if presented in an appropriate manner.

Table of contents

List of abbreviations

The follow table lists various abbreviations used throughout this thesis.

AAL	Automated Anatomical Labelling
AC-PC	Anterior commissure to posterior commissure axis
AD	Alzheimer's disease
AFC	Alternative forced choice
AG	Angular gyrus
AMPA	α-amino-3-hydroxy-5-methyl-4-isoxazolepropionic acid
ANOVA	Analysis of variance
BA	Brodmann area
BIC	Bayesian information criterion
BOLD	Blood-oxygen-level dependent
Cau	Caudate
DARTEL	Diffeomorphic anatomical registration through exponentiated lie algebra
EE	Explicit encoding
EEG	Electroencephalogram
EM	Expectation–maximisation
EPI	Echo planar imaging
FA	Flip angle
FM	Fast mapping
fMRI	Functional magnetic resonance imaging
FoV	Field of view
Fus	Fusiform gyrus
FWE	Family-wise error
FWHM	Full width at half maximum
GLM	General linear model
H_0	Null hypothesis
H_1	Alternative hypothesis
HRF	Hemodynamic response function
IFG	Inferior frontal gyrus
IGF	insulin-like growth factor
IL-1(β)	Interleukin 1 (beta)
IL-6	Interleukin 6

Ins	Insula cortex
IPL	Inferior parietal lobule
IPS	Intraparietal sulcus
ITG	Inferior temporal gyrus
ITI	Inter-trial interval
ITL	Inferior temporal lobe
JMPT	Joint multinomial process tree
LTD	Long term depression
LTP	Long term potentiation
MFG	Middle frontal gyrus
MNI	Montreal neurological institute
MP-RAGE	Magnetization-prepared rapid gradient echo
MR	Magnetic resonance
MTL	Medial temporal lobe
MTT	Multiple trace theory
MVPA	Multi-voxel pattern analysis
NMDA	N-methyl-D-aspartate
PAI	Paired associates inference
PCA	Principal component analysis
PFC	Prefrontal cortex
PHG	Parahippocampal gyrus
PPI	Psychophysiological interaction
Put	Putamen
REMERGE	Recurrency and episodic memory results in generalisation
ROC	Receiver operating characteristic
ROI	Region of interest
SCT	Standard consolidation theory
SD	Standard deviation
SFG	Superior frontal gyrus
SM	Source memory
SMA	Supplementary motor area
SMG	Superior medial gyrus
SPM	Statistical parametric mapping
STG	Superior temporal gyrus
SVM	Support vector machine

TCM	Temporal context model
TE	Echo time
TGF-β1	Transforming growth factor beta 1
TH	Transformation hypothesis
TNFα	Tumour necrosis factor alpha
TR	Repetition time
UKCRN	United Kingdom Clinical Research Network
VAS	Visual analogue scale
VM	Virtual metres
vmPFC	Ventromedial prefrontal cortex
VR	Virtual reality
xSL	Cross-situational learning

Chapter 1

General introduction

1.1 The declarative memory hypothesis

Humans possess a remarkable ability to quickly encode large amounts of information and access it on demand. Importantly, learning and memory functions are not unitary. Classic neuropsychological evidence highlights that different types of information are represented in memory by different brain systems. For instance, amnesia resulting from damage to the hippocampal system has been characterised as a strong dissociation between spared non-declarative memory (e.g. procedural learning and priming) and impaired declarative memory (learning for consciously accessible information; Cohen & Squire, 1980). Observations such as these led to the declarative memory hypothesis. This states that the hippocampal system is specialised for encoding declarative material (Squire, Knowlton, & Musen, 1993). Critically however, the hypothesis postulates a time-limited role of the hippocampal system as it is clear that not all declarative information is continually represented by the region. Amnestic patients often show a temporal gradient to their memory dysfunction; memories for distant events are relatively intact compared to memories for more recent events (e.g. Squire, Slater, & Chace, 1975). Furthermore, whilst new vocabulary acquisition appears very difficult, patients with amnesia still retain premorbid levels of language function (e.g. Corkin, 1984). Given this, the declarative memory hypothesis suggests that while all declarative details are initially encoded by the medial temporal lobe (MTL), they eventually become independent of this system by a slow and gradual process of memory consolidation.

1.2 System consolidation and memory transformation

According to standard consolidation theory (SCT; McClelland, McNaughton, & O'Reilly, 1995; Squire & Alvarez, 1995), neocortical learning mechanisms are characterised by a slow rate of acquisition. As such, multiple repeated instantiations of a particular activation pattern are required to form stable memory traces. This is thought important as the neocortex is responsible for coding all accumulated knowledge and rapid learning would result in catastrophic interference - that is, the abolition of previously established memory traces (O'Reilly & McClelland, 1994; McClelland & Goddard, 1996). In place of rapid learning by the neocortex, the hippocampal system is thought to underpin an initial learning mechanism which quickly records a compressed form of neocortical activation patterns. During encoding, pattern separation processes within the hippocampus may act to avoid interference (see Yassa & Stark, 2011). SCT further suggests that compressed patterns coded by a hippocampal-neocortical ensemble may be repeatedly reactivated over long

periods (weeks to years). Each reactivation results in minor synaptic changes within the neocortex thereby enabling consolidation. Importantly, this process avoids catastrophic interference as neocortical patterns that could potentially interfere with one another are activated in an interleaved manner. Such interleaving means that overlaps between cortical patterns is adequately encoded rather than causing interference.

Similar to SCT, the transformation hypothesis (TH) also states that hippocampally mediated memory traces gradually become independent of the hippocampus (Winocur & Moscovitch, 2011). However, when this happens, memories are stripped of their contextual detail becoming "schematized". This transformation of memory structure is thought to occur because the hippocampus is specialised for coding contextually rich information while the neocortex represents information in a gist-like manner (Wiltgen & Silva, 2007; Winocur, Moscovitch, & Sekeres, 2007; Winocur, Frankland, Sekeres, Fogel & Moscovitch, 2009). As such, recalling mnemonic information with a contextual component (e.g. episodic recall) always requires the hippocampus since contextual details cannot be represented by neocortical structures alone. In support of this, amnestic patients do not always show a temporal gradient to their memory dysfunction, particularly when memory assessments involve contextual recall (e.g. Warrington & Duchen, 1992).

The TH further states that when a hippocampal memory trace is reactivated, a new representation of that memory is formed by a distinct hippocampal-neocortical enable (so-called multiple trace theory; Nadel & Moscovitch, 1997). These multiple traces are thought to play an important role in memory transformation. Specifically, because multiple traces may code similar units of information, the process by which they form may result in the development of neocortical representations that are hippocampally independent. Furthermore, because memory traces relating to the same information are likely formed within different contexts, the neocortex may only encode information common across traces (i.e. the conceptual structure, or 'gist') while contextual details are disregarded.

1.3 Schema-assisted learning

As discussed above, SCT and the TH suggest that neocortical learning processes are slow, requiring hippocampal codes to be repeatedly re-activated before neocortical traces are fully formed. Recently however, evidence has emerged to suggest that the neocortex is capable of more rapid learning than previously thought. Tse et al. (2007) observed that when rats learn novel smell-location associations in a well-known environment, the newly learned associations become hippocampally independent within 24 hours. Furthermore, these rapidly consolidated associations did not require multiple learning instances - acquisition occurred during a single rewarded trial. This phenomenon has been termed "schema-assisted learning" and is where pre-existing knowledge

acts as a cognitive model (i.e. a schema) that facilitates fast neocortical acquisition. Although seemingly at odds with the aforementioned models, this finding can be incorporated into the pre-existing consolidation framework. Specifically, when new information is consistent with pre-established schemas, its encoding may not necessarily cause catastrophic interference meaning that neocortical learning can take place sooner (McClelland, 2013). Furthermore, the medial prefrontal cortex has been implicated in detecting schema-consistent information in aid of accelerated neocortical acquisition (van Kesteren, Ruiter, Fernandez, & Henson, 2010). As such, the critical role of the hippocampus in learning may be limited to the acquisition of information that is completely novel where no pre-established schema of relevance exists.

1.4 Aims of this thesis

1.4.1 Chapter 2

While the declarative memory hypothesis appears well suited to account for amnesia, the model suffers a major pitfall. Specifically, it lacks a high degree of specificity and predictive power as the concept of "declarative memory" is poorly defined. It is often found that learning which may fit this general label need not depend on the hippocampus at all. For example, while trace conditioning in rodents is sensitive to hippocampal damage, delay conditioning is not (Thompson & Kim, 1996; McEchron, Bouwmeester, Tseng, Weiss & Disterhoft, 1998; Clark et al., 2002). Despite this, it is not clear why the former should be more declarative than the latter. Other models have attempted to provide more specific definitions regarding the types of information that the hippocampal system is critical for. These include the relational memory hypothesis which suggests that the hippocampus is specialised for coding associative relationships between separate items (Cohen & Eichenbaum, 1993; Eichenbaum, Otto & Cohen, 1994). Additionally, the dual-process model of MTL function suggests that the hippocampus underpins episodic recollection which supports the retrieval of contextual details (Aggleton & Brown, 1999, 2006). While these more specific construct definitions represent an improvement over the declarative memory hypothesis, they too encounter problems associated with a lack of specificity. Not all relational learning or recollective memory processes are found to be critically dependent on the hippocampus (e.g. Saksida, Bussey, Buckmaster, & Murray, 2007; Cipolotti et al., 2006).

An alternative approach to the characterisation of hippocampal function is to define the precise contribution of the region in operational terms - that is, definitions stipulating the differences between tasks that necessarily require the hippocampus, and tasks that do not. In doing so, hypotheses founded on this approach offer greater specificity and predictive power. One such attempt was made by Rudy and colleagues who posited that the hippocampus forms a vital part of the configural learning system (Sutherland & Rudy, 1989; Rudy & Sutherland, 1995). Configural

memories are defined as representations that bind separate and distinct stimulus elements in memory to form a unique stimulus array. Importantly, they contrast with elemental (or featural) memories which simply code for the occurrence of a single item. As such, tests of configural learning have the defining property that they cannot be subserved via elemental means (that is, by simply learning the significance of single items). In operational terms, this entails learning that a given stimulus is predictive of an event (e.g. reward) when it occurs in some circumstances (e.g. the presence of an accompanying stimulus), but not others.

Initially, lesion studies in rats provided some evidence in favour of the configural hypothesis by showing that hippocampal damage produces a dissociation between spared elemental and impaired configural learning (e.g. Alvarado & Rudy, 1995). However, it was also found that both animals and humans with hippocampal lesions can sometimes acquire configural tasks at normal rates (Gallagher & Holland, 1992; Barense et al., 2005). One study even showed that hippocampal damage can actually aid configural learning by reducing proactive interference from competitor contingencies (Han, Gallagher, & Holland, 1998). Given this, the hypothesis that configural learning depends on the hippocampus is now considered falsified. More recent investigations have implicated the perirhinal cortex as the critical structure underpinning configural learning (Bussey, Saksida & Murray, 2002; Saksida, Bussey, Buckmaster & Murray, 2007; Eacott, Machin, & Gaffan, 2001). Furthermore, it has been suggested that the hippocampus is specialised for a particular class of configural learning referred to as structural learning (Aggleton, Sanderson & Pearce, 2007). More than simply representing the conjunction of stimulus features, structural memory codes specify the spatial or temporal arrangement of stimuli. As such, tests of structural learning require discriminating stimuli composed of the same elemental features that are ordered distinctly in space or time. Some initial evidence for this structural hypothesis has been provided from studies in rodents (Sanderson, Pearce, Kyd & Aggleton, 2006), However, no formal tests have been conducted in humans. As such, the experiment in chapter 2 used fMRI to investigate how structural learning is underpinned by the brain in comparison to configural learning that does not have a structural component.

1.4.2 Chapters 3 and 4

While SCT is able to account for rapid neocortical learning in the context of a pre-established schema, there is evidence to suggest that learning completely novel associations can take place independently of the hippocampal system altogether. Patients with developmental amnesia (i.e. having hippocampal damage at birth) are able to acquire semantic knowledge sufficient to support normal levels of language function (Martins, Guillery-Girard, Jambaqué, Dulac, & Eustache, 2006; Vargha-Khadem, Gadian, & Mishkin, 2001). Furthermore, patients with acquired amnesia are able to learn new labels for unfamiliar shapes when the labels are decided on through collaborative

discussion (Duff, Hengst, Tranel & Cohen, 2005). Recently, it has been suggested that an incidental learning procedure termed “fast mapping” (FM) may be particularly able to elicit hippocampally independent semantic learning (Sharon, Moscovitch & Gilboa, 2011).

On each trial of the FM procedure, two objects or animals are simultaneously presented, only one of which is previously known. Participants are then asked a simple yes/no question regarding the visual appearance of one of these items. If the question refers to the unknown stimulus by name, the name-item association must be deduced in order to respond (Carey & Bartlett, 1978; see Figure 1-1A). Sharon et al. reported that four amnestic patients with hippocampal system damage were capable of learning novel word-referent associations via FM and retaining them over the course of a week. At the same time, these patients were severely impaired at learning other word-referent associations using standard learning instructions. As a result, it was proposed that FM may be a direct route to neocortical semantic learning that is independent of the hippocampus - perhaps because the novel association is learned in the context of a previously known association.

Despite the findings by Sharon et al., at least two attempted replications have failed to find any evidence that learning via FM is spared in amnesia (Smith, Urgolites, Hopkins & Squire, 2014; Warren & Duff, 2014). Additionally, Greve, Cooper and Henson (2014) have reported that healthy adults with reduced hippocampal volume do not exhibit a relative sparing of FM when compared to standard associative learning techniques. In light of this, it seems unlikely that FM is sufficient to induce neocortical learning independent of the hippocampus. Nevertheless, 16 month old infants can use FM to rapidly acquire word-object associations despite not having a fully developed hippocampal system (Friedrich & Friedrich, 2008; Bauer, 2008). This observation formed part of the original motivation for testing FM in amnesia. However, while infants are indeed able to deduce novel associations through FM, even 24 month olds exhibit very poor rates of retention for delays as little as 5 minutes (Horst & Samuelson, 2008). This raises the possibility that other learning procedures that operate in infancy may be better suited to evoke neocortical learning as long as they confer higher rates of retention. One learning procedure with such a potential is known as cross-situational learning (xSL; see Yu & Smith, 2007).

Like FM, xSL involves acquiring associations that are not explicitly given but must be extracted by the learner. On each xSL trial, multiple unknown word-object pairs (typically 3 or 4) are presented simultaneously (see figure 1-1B). Because of this, there is a high degree of “referential ambiguity” regarding the correspondences between words and objects. However, trials are constructed so that each word-object pair is repeatedly presented, each time alongside different non-corresponding stimuli. As such, learners may be able to extract the word-object co-occurrences across trials in order to infer the underlying mappings. Investigations have shown that adults (Yu &

Smith, 2007), and 12 month old infants (Smith & Yu, 2008) can quickly acquire multiple word-object associations via xSL. Additionally, this learning method is known to support the acquisition of one-to-many and many-to-many mappings which are the basic cognitive structures necessary to support linguistic categories (Gangwani, Kachergis & Yu, 2010). Given this, xSL has been implicated as a primary route to semantic memory formation in infancy.

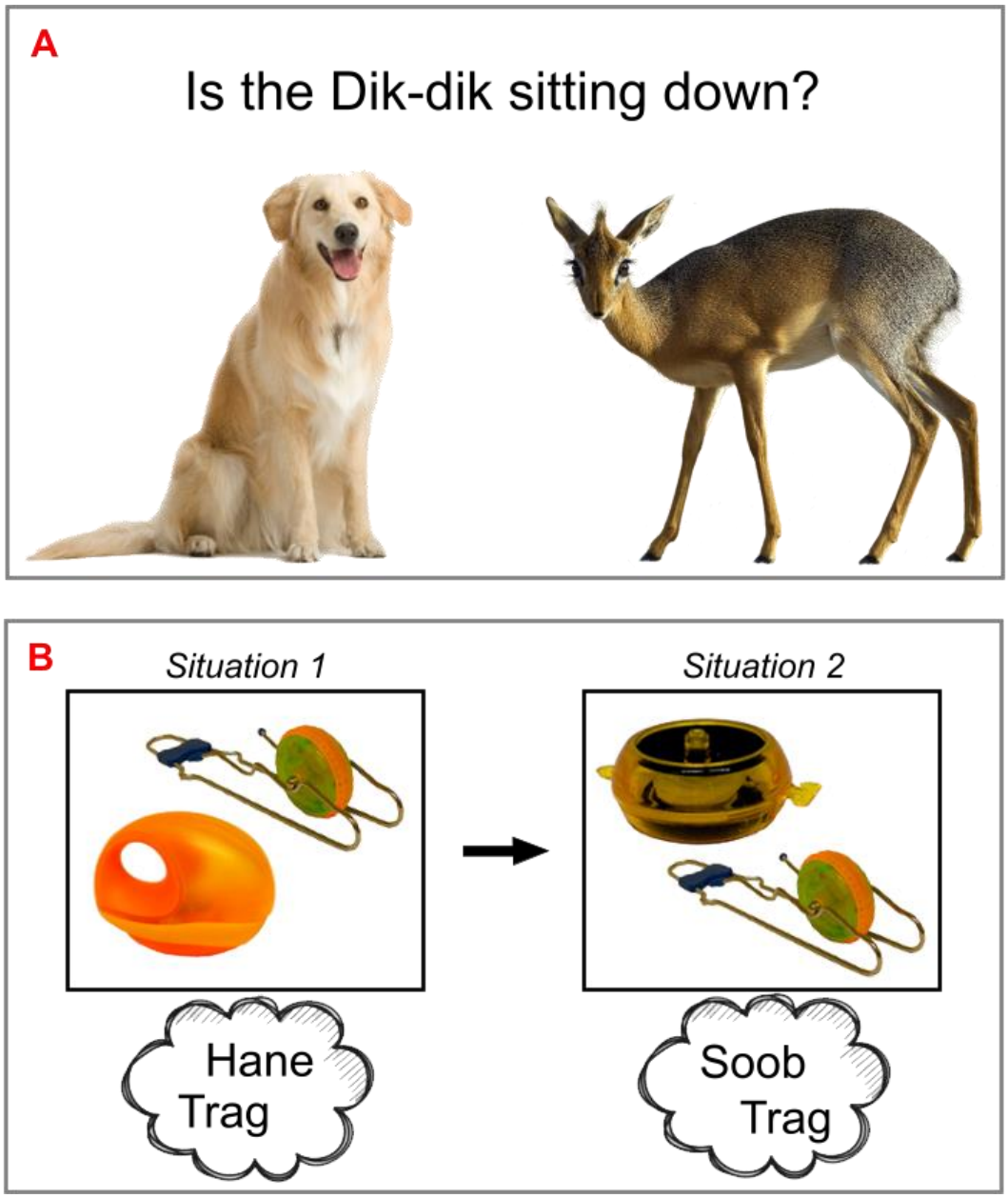

Figure 1-1. *Examples of fast mapping (FM; panel **A**), and cross-situational learning (xSL; panel **B**). During FM, two objects (or animals) are simultaneously presented, only one of which is known by name. A yes/no question is then posed. If the question refers to the novel object by name, the object-name association must be deduced in order to respond. This can lead to incidental learning (see Carey & Bartlett, 1978). During xSL, each study instance (or situation) simultaneously presents two or more unknown objects alongside their corresponding names. Since each object is unknown, there is referential ambiguity regarding the object-name mappings. However, each learning instance will tend to present object-name pairs in the context of different, non-corresponding stimuli. Learners can therefore extract the object-name mappings by tracking co-occurrences across trials (see Yu and Smith, 2007).*

Importantly, xSL differs from FM in that it requires associative information to be maintained across study events and involves more demanding inference operations. Due to this greater processing demand, xSL is likely to result in higher rates of long-term retention for the inferred mappings. Since it is also thought to play a role in semantic memory formation by infants, we hypothesised that xSL may offer a direct route to neocortical learning that is independent of the hippocampus. As noted above, current models suggest that the neocortical system learns by abstracting statistical regularities across multiple hippocampal traces (Winocur & Moscovitch, 2011). One reason why xSL may engage neocortical learning mechanisms directly is that it requires approximately tracking co-occurrence information in a statistical manner (see Kachergis, Yu & Shiffrin, 2012a/b). Furthermore, because xSL involves a high degree of referential ambiguity, individual study events convey a relatively small amount of referential information which the hippocampus may not be suited to encode.

In chapter 3, we first examined whether a model of hippocampal associative learning is able to account for performance during xSL. Specifically, we tested a behavioural prediction regarding the way in which word-object co-occurrence information is accumulated as described by the temporal context model (TCM; Howard & Kahana 2002; Howard, Fotedar, Datey, & Hasselmo, 2005; Howard, 2004). If this prediction is found to be accurate, it would constitute good evidence that xSL is not independent of the hippocampus. In chapter 4, we examined the brain regions involved in xSL using fMRI. Participants were scanned as they acquired word-object associations through the learning procedure. Learning rates were tracked with intermittent test trials in order to identify brain regions showing increases in activity corresponding to information acquisition.

1.4.3 Chapter 5

Regardless of whether associative information can be learned in the absence of hippocampal function, amnesia clearly demonstrates that the hippocampus draws on specialised mechanisms for rapid encoding. This leads to the question of what particular processes in the hippocampus enable rapid synaptic changes. Recently, immune functions within the brain have been implicated in underpinning learning and memory operations (Yirmiya & Goshen, 2011). In particular, microglia are thought to regulate long-term potentiation/depression (LTP/LDP; Zhong et al., 2010) and adult neurogenesis (Ekdahl et al. 2009), both of which are believed to be critical for pattern separation operations and synaptic plasticity (Yassa & Stark, 2011; Deng et al., 2010; Leuner & Gould, 2010). In support of this, peripheral inflammation (which modulates microglial function) is known to impair hippocampally dependent memory while leaving other learning systems unaffected (Harrison, Doeller, Voon, Burgess, & Critchley, 2014). However, peripheral inflammation affects many immune cells within the brain (e.g. astrocytes; Carson, Thrash, & Walter, 2006) and also increases

the concentration of immunological signalling proteins (cytokines; Woodroofe, 1995). Because of this, it remains unclear whether the influence of inflammation on memory really reflect altered microglial function.

In chapter 5 we investigated whether a pharmacological manipulation of microglial activity was sufficient to induce selective changes in hippocampal memory function. Minocycline is an antibiotic known to inhibit the activity of microglia via mechanisms distinct from its antimicrobial action (Hinwood et al., 2012; He, Appel, & Le, 2001; Sriram, Miller, & O'Callaghan, 2006). We hypothesised that microglial inhibition by minocycline would result in selective changes in hippocampal function as measured behaviourally and using fMRI.

Chapter 2

Configural learning in the human brain

2.1 Abstract

Configural learning entails forming a conjunctive representation of features. Structural learning, a configural learning subtype, additionally specifies the temporal or spatial arrangement of features. These processes are thought to be critical to the formation of episodic memories that link multiple mnemonic elements into a contextually rich memory code. While non-structural configural learning may be subserved by the perirhinal cortex, lesion studies in rodents suggest that structural learning is dependent on the hippocampus. However, as yet, this hypothesis remains to be adequately tested in humans. We used event-related fMRI to investigate the brain regions involved in structural and non-structural configural learning. Fifteen right-handed participants engaged in a virtual reality trial-and-error learning task with spatial-structural and non-structural trials. The inferior temporal lobes (bilaterally), left angular gyrus and basal forebrain (bilaterally) all exhibited monotonic increases in BOLD activity alongside both structural and non-structural memory acquisition. Contrary to predictions, no areas within the medial temporal lobes (including the hippocampus and perirhinal cortex) exhibited similar effects or the predicted learning effects for structural trials alone. Nonetheless, a multi-voxel pattern analysis indicated that the hippocampal, parahippocampal, perirhinal, and entorhinal cortices did contain trial relevant information both before and after learning had taken place. Furthermore, the strength of this information predicted subsequent behavioural performance towards the end of the task. Finally, in a test of discrimination transitivity (i.e. generalisation) for the structural associations, behavioural performance positively correlated with BOLD activity in the right posterior hippocampus. Taken together, these findings suggest that humans rapidly encode configural information into neocortical semantic areas. As well as being involved in visually processing such information prior to acquisition, the hippocampus may reintegrate learned configurations when generalising between them.

2.2 Introduction

Configural learning is a fundamental process supporting the formation of episodic memories. It entails binding separate and distinct mnemonic elements in memory to form conjunctive representations of sensory features (Sutherland & Rudy, 1989). Importantly, this contrasts with featural learning which simply requires encoding information about single items. As such, tests of configural learning require discriminating stimuli that share elemental features (e.g. stimuli 'AB' and 'CD' are rewarded, but 'AC' and 'BD' are not). Structural learning, a sub-type of configural learning, additionally specifies the spatial or temporal arrangement of features in a configuration (Aggleton, Sanderson & Pearce, 2007). As such, tests of structural learning require discriminating stimuli composed of the same elements that are ordered distinctly in space or time (e.g. stimulus 'XY' is rewarded but 'YX' is not).

The perirhinal and hippocampal cortices may be principally responsible for coding non-structural and structural configurations respectively (Saksida & Bussey, 2010; Aggleton, Sanderson & Pearce, 2007). Perirhinal damage impairs non-structural configuration learning but not structural learning (Bussey, Saksida & Murray, 2002; Aggleton, Albasser, Aggleton, Poirier & Pearce, 2010). In contrast, damage to the hippocampus of rats has been observed to elicit the opposite dissociation, impaired structural but not non-structural learning (Sanderson, Pearce, Kyd & Aggleton, 2006). Additionally, various lines of evidence further implicate the hippocampus in generalising across previously learned configural contingencies, e.g. transitively inferring associations that were not explicitly trained (e.g. Eichenbaum, 1999; DeVito, Kanter, Eichenbaum, 2010; Aggleton et al., 2007).

Despite this evidence, the contribution of each medial temporal lobe (MTL) subregion to configural learning and generalisation remains controversial. Some investigations have failed to find any configural learning deficits in rodents with perirhinal damage (Davies, Machin, Sanderson, Pearce & Aggleton, 2007). Furthermore, the findings from studies of humans are also mixed. For example, Kumaran et al. (2007) found that hippocampal damage disrupted all forms of configural learning. However, other studies suggest that if stimuli are sufficiently meaningful, configural learning can be supported by neocortical structures associated with semantic memory, even in the context of hippocampal amnesia (Moses, Ostreicher, Rosenbaum & Ryan, 2008; Moses et al., 2009).

While information that is consistent with pre-existing semantic knowledge may be assimilated relatively quickly (Tse et al., 2007; McClelland, 2013), prominent models suggest that neocortical learning for completely novel information occurs much more gradually (McClelland, McNaughton, & O'Reilly, 1995). In particular, multiple repeated instances of an activation pattern are thought required to form stable synaptic changes in the neocortex. Nonetheless, it remains unclear

precisely how quickly neocortical learning can take place for novel configurations. Furthermore, while the hippocampus may be involved in mnemonic generalisation, there has been much debate concerning how this process is underpinned. Some accounts suggest that the hippocampus principally acts to encode generalised memory representations at the point of encoding (e.g. Howard & Kahana, 2002). In contrast, other accounts suggest that the hippocampus pattern separates representations at encoding and then engages in 'on-the-fly' generalisation processes at the point of retrieval (e.g. Kumaran & McClelland, 2012).

Using event-related fMRI in humans, we aimed to identify the brain regions involved in structural and non-structural configural learning and generalisation. Participants learned structural and non-structural contingencies (termed structural- and transverse- patterning respectively) for novel stimuli via a trial-and-error task. Performance was analysed with a state-space smoothing algorithm to produce learning curves of each configural sub-type (Smith et al., 2004). Learning-curve information was then used to identify brain regions showing monotonic increases in activity indicative of greater involvement at retrieval. Additionally, using a multi-voxel pattern analysis (MVPA), we probed whether regions of the MTL exhibited distinct BOLD patterns to structural and non-structural stimuli at various stages of learning. The presence of distinct BOLD patterns would indicate that a region is representing some form of stimulus specific information and is thus is functionally involved in the task. Finally, an inference test for the structural configurations was administered to reveal areas involved in configural generalisation.

2.3 Methods

2.3.1 Subjects

Twenty-three right-handed students were recruited from the University of Sussex (UK) by way of online advertisement. All gave written informed consent to take part and were compensated for their time. Subjects had either normal or corrected-to-normal vision and reported no history of neurological or psychiatric illness. Of those who participated, 8 did not exhibit sufficient levels of learning to be included in analyses with the remainder of the sample (see Data Analysis section below). As such, analyses reported here used data from 15 subjects (7 male) with a mean age of 23.8 years (*SD* = 4.14). The study was approved by the Brighton and Sussex Medical School's Research Governance and Ethics Committee.

2.3.2 In-scanner Task

A forced-choice trial-and-error learning task was developed to concurrently probe structural and non-structural configural learning. Unreal Development Kit (Epic Games, 2012) was used to generate a number of unique scenes within a first-person virtual reality environment (see Figure 2-1 for examples). On each trial, one of these scenes was presented displaying two buildings positioned equidistantly from a start location. One building concealed a pile of virtual gold (reinforcement) and the only features that predicted the rewarded location were the wall textures rendered onto the towers of each building. In total, six different wall textures were used and these were combined to form 6 binary concurrent discriminations; 3 non-structural configural and 3 structural (see Figure 2-1). Importantly, each rewarded texture combination was rendered onto the left and right buildings an equal number of times. This ensured that the use of non-target strategies (e.g. relying on the absolute rather than the relative locations of wall textures) would not result in above chance performance.

A schematic illustration of the experimental procedure is shown in figure 2-2. All trials started with the presentation of a still image taken at a scene's start location for a maximum of 3 seconds. During this time subjects were required to select the building they believed contained the gold via a left/right button press (decision period). Immediately following a response, a 5 second animation was played depicting the subject approaching their chosen building and opening its central door to reveal whether or not it contained gold (feedback period). If no response was made within the 3 second response window, a 5 second red fixation cross was shown in place of the feedback video. Subsequently, a variable (uniformly distributed) inter-trial interval (ITI) occurred for between 300 and 1300 ms.

In all, the task consisted of 144 structural and 144 non-structural trials with each discrimination listed in Figure 2-1 being repeated 48 times. Additionally, 24 non-memory control discriminations were included (location of gold visible at trial onset). All trials progressed in a semi-random permuted block structure where no more than 8 trials of any one type occurred consecutively. This design was chosen to provide an effective trade-off between BOLD signal estimation and detection (see Liu, 2004). Finally, 12 'transitivity trials' were run to tap cross-discrimination integration of the structural contingencies. Here, the texture combinations used in structural trials were rearranged to produce discriminations between rewarded and unrewarded combinations that had not been previously paired together (see figure 2-3; note: this could not be done with the non-structural discriminations since every possible stimulus pairing was explicitly trained). As such, these trials involved the generalisation of stored memory representations that had been previously learned in parallel. All experimental periods were carried out in the scanner. Prior to scanning, participants were briefed on the experimental procedure but were not given any details regarding the number or type of discriminations that they would be required to learn. Instead, they were simply told that (excluding control trials) the wall textures were the only features that predicted reward.

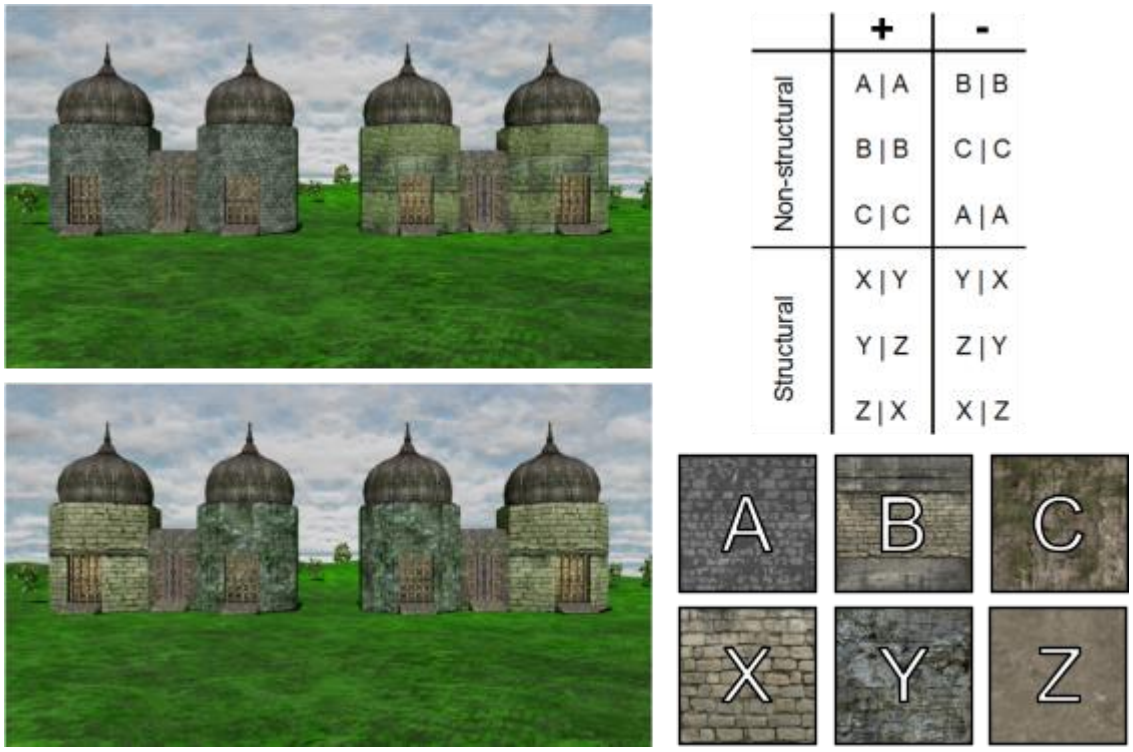

Figure 2-1. *Left: Examples of the virtual-reality reality environment on non-structural (top) and structural (bottom) trials. Right: Lists of the configural contingencies and wall texture used in the task. Each row of the contingency list corresponds to a unique discrimination and vertical bars (i.e. |) indicate spatial arrangements ("X | Y" = "X" to the left of "Y"). The "+" column denotes wall texture combinations that were rewarded while the "-" column denotes wall texture combinations that were unrewarded. Note: Each rewarded texture combination was rendered onto the left and right buildings an equal number of times.*

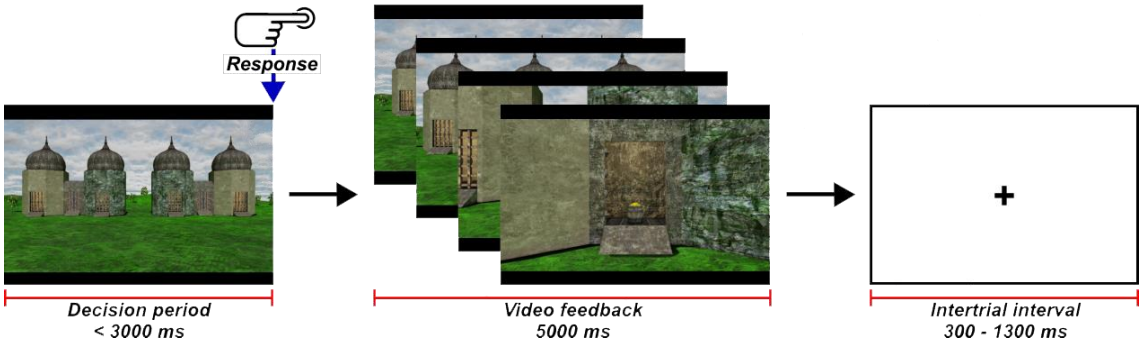

Figure 2-2. *Structure of each trial.*

	+	-
Transitive inference	X | Y	X | Z
	Y | Z	Y | X
	Z | X	Z | Y
	X | Y	Z | Y
	Y | Z	X | Z
	Z | X	Y | X

Figure 2-3. *Transitive inference discriminations.*

2.3.3 MRI Acquisition

All images were acquired in a 1.5 Tesla Siemens Avanto scanner equipped with a 32-channel phased array head coil. During the task, gradient-echo T2*-weighted scans were acquired using echo-planar imaging (EPI) recording 34 axial slices (approximately 30° to AC-PC line; ascending interleaved) and the following parameters; TR = 2520 ms, TE = 43 ms, flip angle (FA) = 90°, slice thickness = 3 mm, inter-slice gap = 0.6 mm in-plane resolution = 3 x 3 mm & acquisition matrix = 64 x 64. To allow for T1 equilibrium, the first 5 EPI volumes were acquired before the task started and then discarded. A field map scan was also acquired to correct inhomogeneity-based distortions (see Image Preprocessing section below). Finally, for purposes of coregistration and image normalisation, a whole-brain T1-weighted structural scan was acquired with a 1mm^3 resolution using an MP-RAGE pulse sequence.

2.3.4 Image Preprocessing

Image preprocessing was performed in SPM8 (www.fil.ion.ucl.ac.uk/spm) and using custom written code in MATLB. First, each subject's EPI volumes were corrected for inter-slice acquisition delay and spatially realigned to the first image in the time series. At the same time, images were corrected for field inhomogeneity based geometric distortions (as well as the interaction between motion and such distortions) using the Realign and Unwarp algorithms in SPM (Andersson et al. 2001; Hutton et al. 2002). For the univariate analyses, EPI time series data were warped to MNI space with transformation parameters derived from the structural scans (using the DARTEL toolbox; Ashburner, 2007). Subsequently, the EPI volumes were spatially smoothed with an isotropic 8 mm FWHM Gaussian kernel prior to GLM analysis. For the MVPA, data were not normalised or smoothed but were detrended with motion parameters and a vector coding for drift in

the MR signal (computed as mean white matter intensity after voxel-wise z-scoring). Prior to MVPA classifier training/test, volumes acquired when the structural/non-structural decision period HRF was above 40% of maximum were averaged together and z-scored producing a single input volume per trial. This threshold guaranteed there to be at least two EPI volumes per trial that could be averaged together.

2.3.5 Data Analysis

2.3.5.1 Behavioural data

Behavioural outputs were reaction times and binary correct/incorrect responses for each trial. Trials were coded as incorrect when no response was made within the 3 second response window. Responses to experimental trials were separated into two ordered binary strings according to trial type (i.e. non-structural and structural). These were then converted into learning curves giving trial-by-trial estimates of memory strength using a logistic regression algorithm developed by Brown and colleagues (Smith & Brown, 2003; Smith et al., 2004; and as used by Law et al. 2005). Here learning curves are defined as the probability of a correct response (*pC*) as a function of trial number and are estimated by a state-space smoothing algorithm using expectation maximization to compute a maximum likelihood estimate of the learning curve along with its associated confidence intervals (see figure 2-4 for an example). All subjects selected for analysis produced learning curves demonstrating a highly significant and persistent level of memory acquisition that was similar for both structural and non-structural contingencies (i.e. the lower 95% confidence bound of each learning curve exceeded chance level [$pC = 0.5$] for at least 50 trials). For purposes of analysing the imaging data, trial-by-trial learning curve statistics were then categorised into one of three memory strengths relative to chance level - Str1 ($pC \leq 33\%$ of max), Str2 (*pC* between 33% and 66% of max), and Str3 ($pC \geq 66\%$ of max) – similar to Law et al. (2005).

2.3.5.2 Analysis of univariate BOLD activations

For the univariate analyses, first-level general linear models of the fMRI data were produced. These separately modelled the decision periods of structural and non-structural trials for each level of memory strength. Additionally, the decision periods of control and transitivity trials were included as their own event types. Separate regressors modelling periods of feedback for each type of decision were also included in the model but were not analysed. As well as HRF amplitude estimates, temporal and dispersion derivatives pertaining to all of these periods were modelled. Nuisance regressors included motion parameters and a vector coding for drift in the MR signal. To examine group-wide BOLD differences as a function of structural and non-structural learning, a two factor model was generated at second-level. Here, the HRF amplitude estimates of structural and non-structural trials for each memory strength were entered into a 3x2 repeated measures ANOVA

(factor 1: memory strength; factor 2: trial type). Further to this, HRF amplitude estimates of the transitivity trials were correlated with participants' behavioural performance on these trials (i.e. proportion correct) in a between-subject linear regression analysis (note: for these transitivity analyses, data from one participant had be excluded due to problems with fMRI data acquisition during the generalisation test).

Based on our strong a priori hypotheses that effects of interest would be observed in the medial temporal lobes, a region of interest (ROI) encompassing the hippocampal, parahippocampal, perirhinal and entorhinal cortices was generated by combining binary masks of these structures (Tzourio-Mazoyer et al., 2002; Holdstock et al., 2009). Within this ROI, reported activations survive an uncorrected height threshold of $p < .001$ and a spatial extent threshold of 5 contiguous voxels (135 mm^3). We also report activations that survive a map-wide height threshold of $p < .001$ (uncorrected) and a spatial extent threshold of 30 contiguous voxels (810 mm^3). Where fMRI activations are plotted graphically, percent signal change was calculated by scaling beta estimates with the corresponding GLM regressor heights, and normalising the resultant values with the constant term (as implemented in the MarsBaR toolbox; Brett, Anton, Valabregue & Poline, 2002).

2.3.5.3 Multi-voxel pattern analysis

For the MVPA, an equal number of structural and non-structural input volumes were generated (as described above) for memory strengths Str1 and Str3. Data from Str2 were not used as this category contained too few trials (commonly less than 20). To examine whether multivariate BOLD patterns within distinct MTL subregions could significantly discriminate the two trial types, input volumes were separately masked with bilateral hippocampal, parahippocampal (Tzourio-Mazoyer et al., 2002), perirhinal (Holdstock et al., 2009) and entorhinal (Maldjian, Laurienti, Kraft & Burdette, 2003) ROIs that had been warped to native space for each subject. Subsequently, for Str1 and Str3 data separately, input patterns were grouped into 5 equally sized chunks. Following a t-test based feature selection ($p < .05$), these chunks were then entered into 5 N-minus-1 training-test iterations (4 chunks for training, 1 chunk for test) using an SVM classifier running in the Princeton MVPA toolbox (csbmb.princeton.edu/mvpa). Classifier performance was then taken as the mean classification accuracy across the five iterations. To ensure that above chance classifier performance actually depended on differential BOLD patterns rather than some arbitrary property of the ROI under test, we performed a control MVPA analysis. This was run in the same way as discussed above except that the trial type labels (i.e. non-structural vs structural) for data in the training set were randomly shuffled prior to each training-test iteration.

2.3.5.4 Bayesian methods

Where statistical tests are non-significant and the absence of an effect is of theoretical interest, we report the results of follow-up a Bayesian analysis as described by Masson (2011). This tests the relative strength of evidence in favour of the null hypothesis (H_0) compared to the alternative hypothesis (H_1) by computing a Bayesian information criterion (BIC). The BIC statistic is calculated by contrasting the total variance in the data against the variance accounted for by the effect of interest. In comparison to other Bayesian methods (e.g. Dienes, 2011), this has the advantage that a prior expectation regarding the size of the effect need not be specified. Both H_0 and H_1 are assumed to be equally likely a priori.

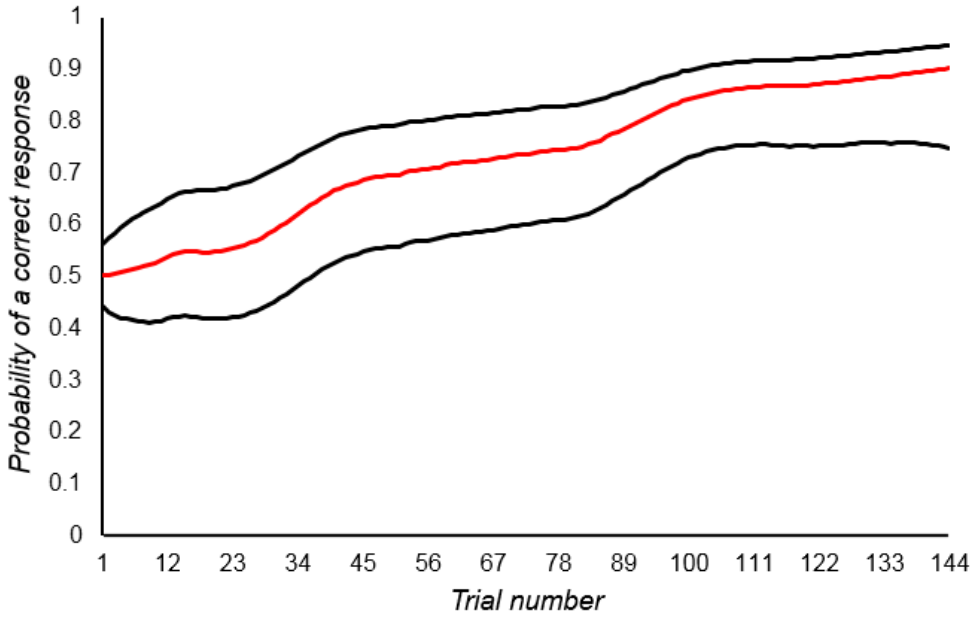

Figure 2-4. *An example learning curve displaying trial-by-trial pC estimates along with associated confidence intervals.*

2.4 Results

2.4.1 Behavioural data

To quantify the peak level of behavioural performance achieved by each subject, maximum *pC* statistics (*max_pCs*) were taken from both structural and non-structural learning curves. Despite structural trials being more computationally demanding, the numerical difference in *max_pCs* between trial types did not reach significance; $t(14) = 1.875$, $p = .082$. However, the correlation between structural and non-structural *max_pCs* was highly significant; $r(13) = .779$, $p < .001$, indicating that levels of performance across trial types were strongly related.

Reaction times to correct responses as a function of memory strength and trial type are displayed in figure 2-5. A 3x2 ('memory strength' x 'trial type') repeated-measures ANOVA revealed a trend towards a main effect of memory strength; $F(2,28) = 2.841$, $p = .075$. Closer examination of this reveals that mean reaction times to Str1 and Str2 trials were fairly similar and then dropped in Str3. This pattern is consistent with previously reported data (Law et al, 2005) and suggests more rapid processing once memory codes had been fully formed. Given the small size and nonlinear nature of this effect, and that reaction times decreased in the condition where BOLD signals are predicted to be strongest, any observed learning effects in the fMRI data that follow the predicted pattern are highly unlikely to be the results of differences in reaction time.

The ANOVA further revealed a strong main effect of trial type, $F(1,14) = 28.231$, $p < .001$, indicating greater processing times to structural trials (mean difference = 209 ms). Importantly however, there was no significant memory strength by trial type interaction; $F(2,28) = 0.049$, $p = .952$, and a Bayesian analysis revealed substantially more evidence in favour of the null hypothesis for this interaction term; $p(H_0|Data) = .936$. Again, this suggests that the predicted interactions between trial type and memory strength are unlikely to be the results of differences in reaction time. Furthermore, the result suggests that as structural and non-structural memory codes gradually form, differential processing times in memory activation do not emerge. It therefore follows that the greater response latencies for structural trials are reflective of differences in processing occurring before learning has taken place (i.e. at the level of visual encoding rather than at the level of memory activation).

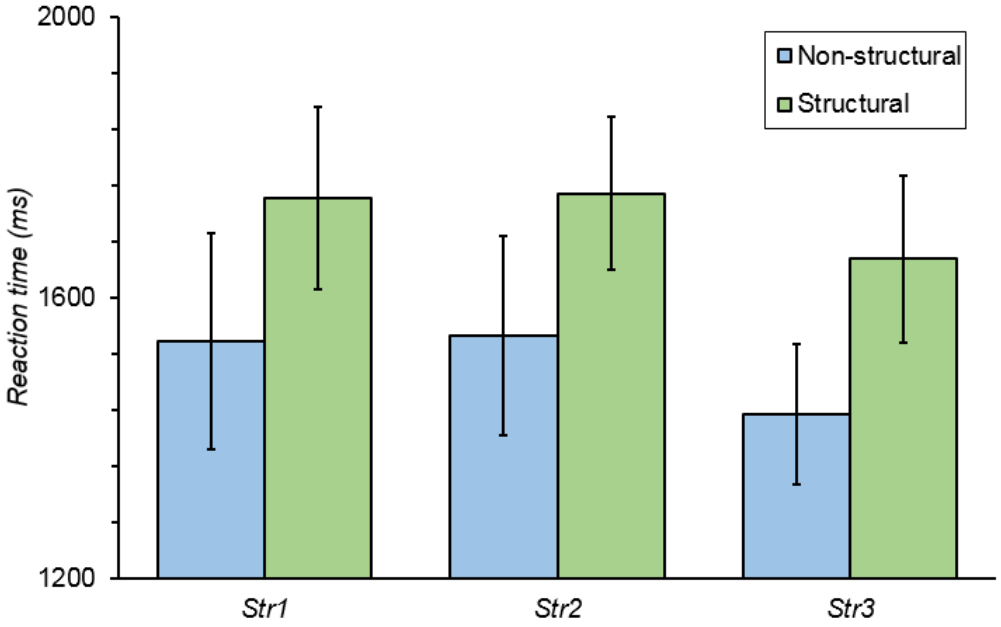

Figure 2-5. *Reaction times to correct responses grouped by memory strength and trial type. Errors bars indicate 95% confidence intervals corrected for the within subject-error term.*

2.4.2 Univariate imaging results

2.4.2.1 Main effect of memory strength

The 3x2 repeated-measures ANOVA on the imaging data initially revealed a wide range of brain regions demonstrating a main effect of memory strength (suprathreshold activations listed in table 2-1). Examination of model parameter estimates showed the majority of these regions (but not the left angular gyrus, left inferior temporal and left mid orbital cortices) exhibited heightened BOLD activity in Str1 which either dropped to a consistent level in Str2 and Str3, or systematically decreased across memory strengths. These BOLD patterns do not accord with our hypothesised learning effects (i.e. gradually strengthening memory representations). Instead, they likely represent generalised task difficulty or familiarisation processes. In order to identify regions showing increases in BOLD activity in accordance with learning, we performed a t-contrast to highlight areas showing higher activity in Str3 over Str1 (i.e. “Str3 > Str1” averaged across structural and non-structural trial types). This revealed four suprathreshold clusters (listed in table 2-2 and displayed in figure 2-6). An ANOVA trend analysis across Str levels 1, 2 and 3 confirmed that each of these clusters exhibited a strong linear relationship between memory strength and BOLD activity (see table 2-2).

Table 2-1. *Regions showing a main effect of memory strength. Asterisks denote significance at p(peak-FWE) < .05. Daggers denote significance at p(cluster-FWE) < .05.*

Region	***MNI***	***Peak F***	***Cluster size***
Right Insula	[+33 -24 +12]	18.22 *	471 †
Left Area 6	[-24 -21 +54]	17.65 *	45 †
Middle Cingulate	[+06 -12 +45]	16.37 *	56 †
Left Mid Orbital	[-09 +24 -06]	15.97	93 †
Left Superior Temporal Gyrus	[-54 -18 +06]	15.38	96 †
Right Supramarginal Gyrus	[+54 -39 +42]	14.58	104 †
Left Angular Gyrus	[-42 -72 +45]	12.69	65 †
Left Inferior Temporal Gyrus	[-39 -03 -33]	12.66	53
Left Middle Orbital Gyrus	[-36 +57 +03]	12.48	32
Right Postcentral Gyrus	[+45 -24 +54]	10.94	33
Left Parahippocamal Gyrus	[-30 -37 -18]	9.27	13

Table 2-2. *Regions revealed by the "Str3 > Str1" contrast. Daggers denote significance at p(cluster-FWE) < .05.*

Region	***MNI***	***Peak t***	***Cluster size***	***Linear F(1,14)***
Left Angular Gyrus	[-42 -75 +42]	4.71	118 †	19.70
Left InferiorTemporal Gyrus	[-45 -09 -30]	4.68	76 †	16.40
Left Superior Orbital Gyrus	[-15 +21 -15]	4.61	45	16.15
Right InferiorTemporal Gyrus	[+48 -09 -27]	4.47	44	13.43

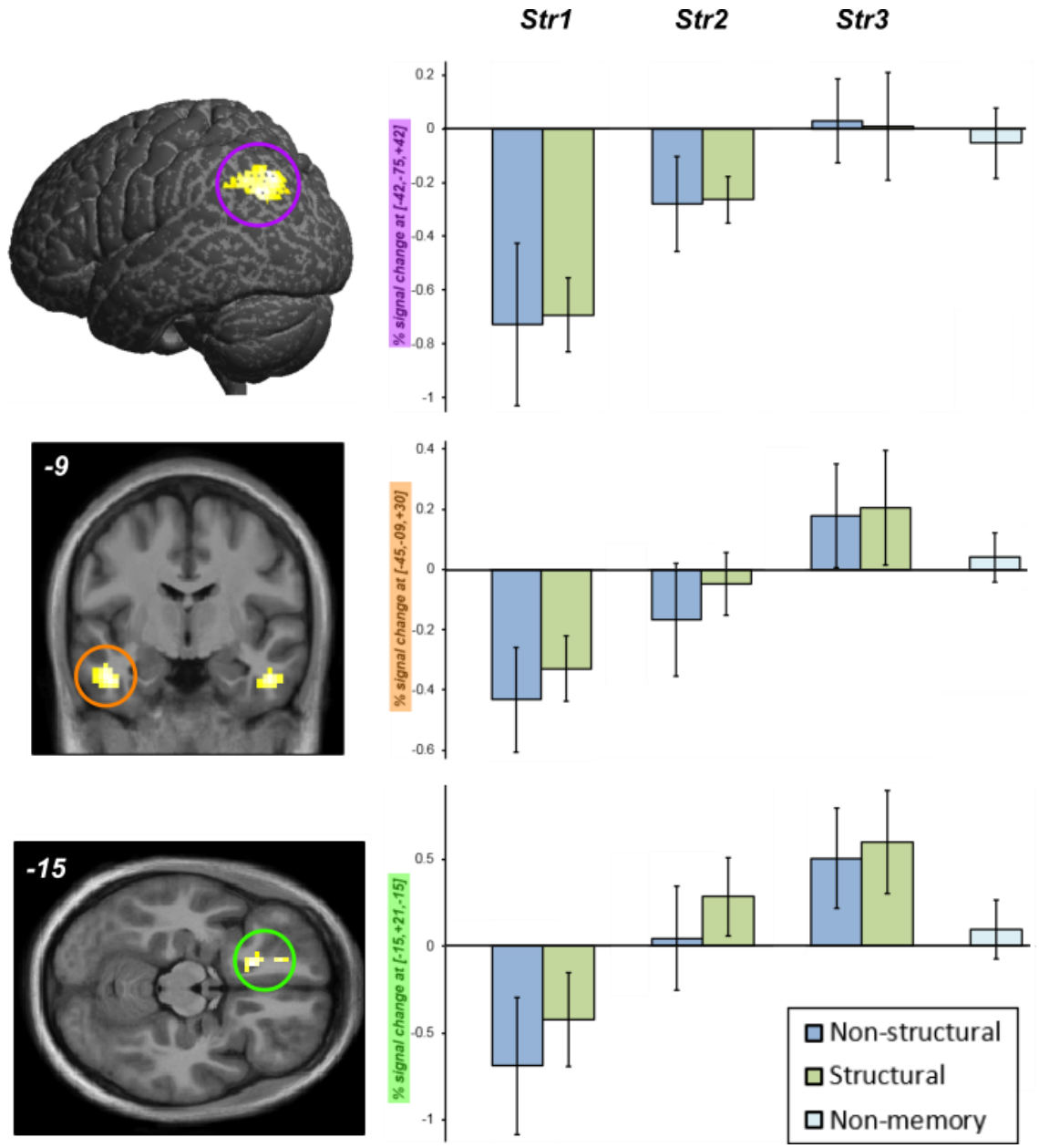

Figure 2-6. *Clusters revealed by the "Str3 > Str1" contrast. Error bars indicate 95% confidence intervals corrected for the within subject-error term.*

2.4.2.2 Main effect of trial type

A main effect of trial type was detected in eight clusters which all exhibited greater BOLD activity to structural trials (suprathreshold activations listed in table 2-3). Of these clusters, the left inferior parietal, right superior frontal and right supramarginal activations also demonstrated a strong main effect of memory strength (all *F*'s > 5.32, uncorrected *p*'s < .01) where BOLD activity systematically decreased across memory strengths. Given that structural discriminations are more computationally demanding than their non-structural counterparts, and processing demands to

both trial types are likely vary as a function of learning stage, activations showing a main effect of each factor, such as these, likely reflect differences in task difficulty or attentional processing. In contrast, the right middle occipital and right inferior frontal activations both showed greater BOLD activity to structural trials which remained relatively consistent across memory strengths; $p(H_0|Data) > .933$ for the main effect of memory strength in each cluster. As such, these effects may be indicative of fundamental differences in processing between the two the trial types.

Table 2-3. *Regions showing a main effect of trial type. Asterisks denote significance at p(peak-FWE) < .05. Daggers denote significance at p(cluster-FWE) < .05.*

Region	MNI	Peak F	Cluster size
Left Middle Occipital Gyrus	[-33 -84 +21]	40.44 *	331
Left Inferior Parietal Lobule	[-33 -39 +42]	32.69 *	217
Right Superior Frontal Gyrus	[+27 +00 +57]	27.51 *	42
Right Supramarginal Gyrus	[+39 -36 +45]	24.79	53
Left Inferior Temporal Gyrus	[-51 -66 -03]	23.39	65 †
Right Middle Occipital Gyrus	[+39 -81 +12]	22.21	165 †
Right Inferior Frontal Gyrus (BA 44)	[+54 +09 +36]	20.08	86 †
Left Middle Frontal Gyrus	[-24 +00 +60]	18.83	40

2.4.2.3 'Memory strength' x 'trial type' interaction

No areas demonstrated a significant memory strength by trial type interaction. However, for completeness, we conducted the above mentioned "Str3 > Str1" *t*-contrast separately for structural and non-structural trials to identify learning effects that may be specific to each trial type. The resultant activation maps are presented in figure 2-7 and show that the gradual learning effects for each trial type are highly overlapping.

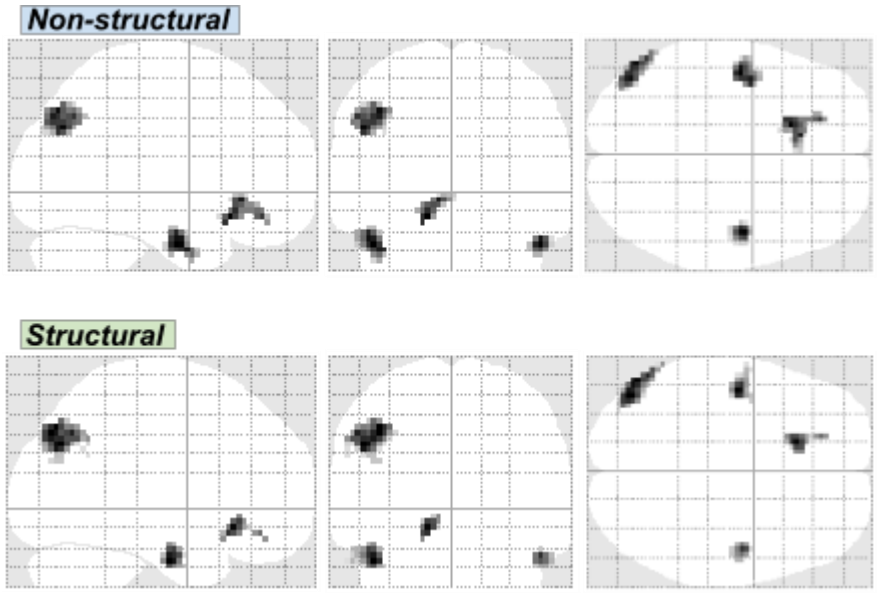

Figure 2-7. *"Str3 > Str1" broken down by trial type.*

2.4.2.4 Analysis of transitivity data

Although each subject included in the analysis showed a high degree of learning on the structural contingencies, performance on the transitivity trials (which directly relates to these contingencies) was highly variable; mean proportion correct: 0.732, range: 0.333 - 0.916. Nonetheless, there was a significant correlation between *max_pCs* for structural discriminations and transitive performance; $r(13) = .541$, $p = .019$. The correlation between transitivity trial performance and BOLD amplitude estimates revealed one suprathreshold activation in the right posterior hippocampus (see figure 2-8); $t(12) = 7.62$, $p(peak\text{-}FWE) = .005$ (within the MTL ROI), $k = 21$. In this analysis, the performance of one subject was numerically below chance (i.e. less than 0.5). Given that any level of at or below chance performance should be equally indicative of a lack memory activation, we wished to examine whether the observed effect was robust to capping performance scores at the 0.5 level. Even when proportion correct scores were adjusted in this way, the hippocampal activation remained; $t(12) = 6.59$, $p(peak\text{-}FWE) = .019$, $k = 14$.

This brain-behaviour correlation may reflect the online integration of distinct structural representation as required for generalisation (Kumaran & McClelland, 2012; DeVito, Kanter & Eichenbaum, 2010; Zalesak & Heckers, 2009; Heckers, Zalesak, Weiss, Ditman & Titone, 2004; Preston, Shrager, Dudukovic & Gabrieli, 2004). Alternately, the effect may result from the activation of hippocampal memory codes that were instantiated during learning, but not identified in the aforementioned ANOVA (see Frank, Rudy & O'Reilly, 2003; Shohamy & Wagner, 2008; Zeithamova & Preston, 2010; Greene, Gross, Elsinger & Rao, 2006; Van der Jeugd et al., 2009).

To address this possibility, we focused on the peak voxel in the hippocampal cluster in two follow-up analyses. Firstly, we tested whether transitive performance (behaviour) correlated with BOLD activity during learning (structural trials only) – that is, did hippocampal activity at encoding predict subsequent transitive performance. A positive association was indeed found across all memory strengths together, $F(1,13)$ = 6.647, p = .023, and individually; Str1 [$r(13)$ = .543, p = .018], Str2 [$r(13)$ = .595, p = .010], Str3 [$r(13)$ = .172, p = .270]. The differences in these regression slopes were statistically nonsignificant; $F(2,26)$ = 1.325, p = .283, $p(H_0|Data)$ = .879. Secondly, we examined whether the hippocampal cluster exhibited monotonic learning effects in the main task after accounting for (i.e. partialling out) subsequent transitive performance. To do this we contrasted the Str1, Str2, and Str3 parameter estimates (for structural trials alone) in a one-way ANCOVA with a z-scored transitive performance covariate. This returned a non-significant effect of memory strength, $F(2,26)$ = 0.734, p = .490. Moreover, a Bayesian analysis revealed substantially more evidence in favour of the null hypothesis for this effect, $p(H_0|Data)$ = .909 and the tested BOLD pattern constituted neither a monotonic increase or decrease. Taken together, these results suggest that hippocampal activity at encoding is associated with subsequent transitive performance even though the region does not appear to store configural codes in memory.

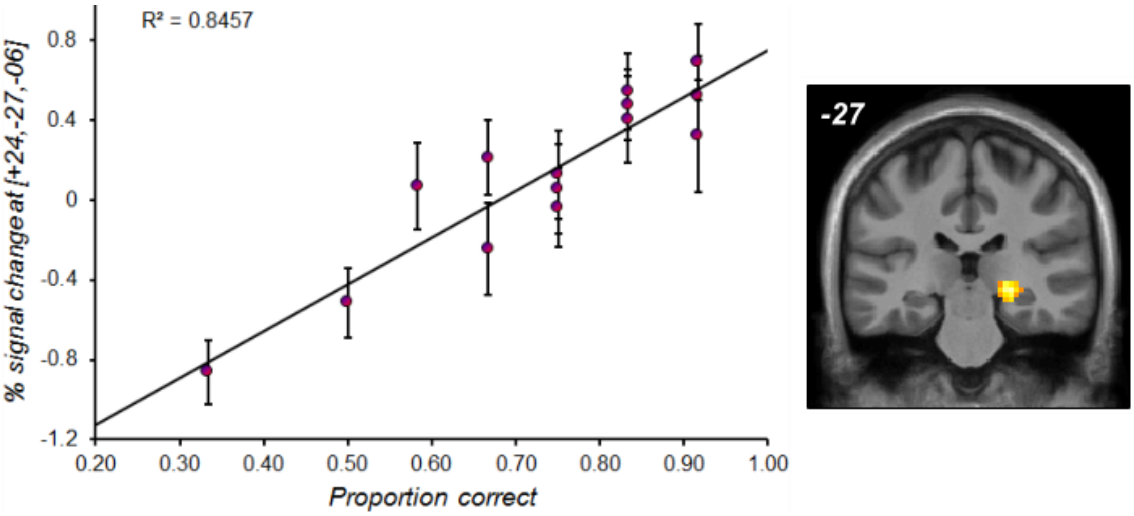

Figure 2-8. *Correlation between transitive performance and right hippocampal activity. Error bars indicate 95% confidence intervals for each signal change statistic.*

2.4.3 MVPA results

As well as examining whether each MTL ROI contained trial relevant information in Str1 and Str3, we wished to explore whether an overall measure of 'learning success' predicted the decodability (i.e. classifier performance) of multivariate BOLD patterns. Given the strong association between structural and non-structural max_pCs reported above, this was done by averaging *max_pCs* across trial types and dichotomizing them by median split to produce a between-subjects categorical variable denoting low vs high subsequent performance. For the hippocampal, parahippocampal, perirhinal and entorhinal data separately, MVPA classification accuracy scores were then entered into a 2x2x2 mixed-measures ANOVA (factor 1: data integrity [i.e. shuffled vs unshuffled data labels]; factor 2: memory strength [i.e. Str1 vs St3]; factor 3: learning success [low vs high subsequent performance]). Figure 2-9 displays MVPA classification accuracy scores broken down by each factor of interest and table 2-4 displays ANOVA output statistics for the four model parameters of interest. These were; 1) the main effect of data integrity [whether the ROI contained trial-relevant BOLD information], 2) the memory strength by data integrity interaction [whether the level of trial-relevant BOLD information differed between memory strengths], 3) the learning success by data integrity interaction [whether the level of trial-relevant BOLD information was related to participants subsequent behavioural performance], and 4) the three-way interaction between memory strength, learning success, and data integrity [whether the association between trial-relevant BOLD information and memory strength depended on participants subsequent behavioural performance].

Table 2-4. *2x2x2 ANOVA output statistics for MVPA classification accuracy scores. All model terms have degrees of freedom (1,13).*

Region	***Data Integrity***	***Str x Data Integrity***	***Learning Success x Data Integrity***	***Str x Learning Success x Data Integrity***
Hippocampus	F = 16.774 p = .001 *	F = 2.072 p = .174	F = 6.677 p = .023 *	F = 9.363 p = .009 *
Parahippocampal cortex	F = 9.349 p = .009 *	F = 1.598 p = .228	F = 4.971 p = .044 *	F = 3.851 p = .071
Perirhinal cortex	F = 7.410 p = .017 *	F = 2.958 p = .109	F = 10.055 p = .007 *	F = 2.729 p = .122
Entorhinal cortex	F = 9.289 p = .009 *	F = 0.396 p = .540	F = 3.229 p = .096	F = 7.144 p = .019 *

The ANOVAs revealed a very similar pattern of results for each ROI. All four ROIs demonstrated a significant main effect of data integrity indicating that, overall, each region did contain trial-relevant information. Moreover, excluding the entorhinal cortex, all ROIs exhibited a significant learning success by data integrity interaction. This indicated that MVPA classifier accuracy was generally higher for participants who achieved a greater level of behavioural performance (see figure 2-9). Although the memory strength by data integrity interaction was consistently nonsignificant across regions, both the hippocampus and the entorhinal cortex showed a significant three-way interaction between memory strength, learning success, and data integrity. Examination of this effect revealed that, within memory strength Str1, the hippocampus and entorhinal cortex only displayed significant levels of trial-relevant information for participants who subsequently showed a greater level of behavioural performance in Str3. In other words, for hippocampal and entorhinal data, greater levels of trial-relevant information at the early stage of the experiment predicted better behavioural performance at the end of the experiment.

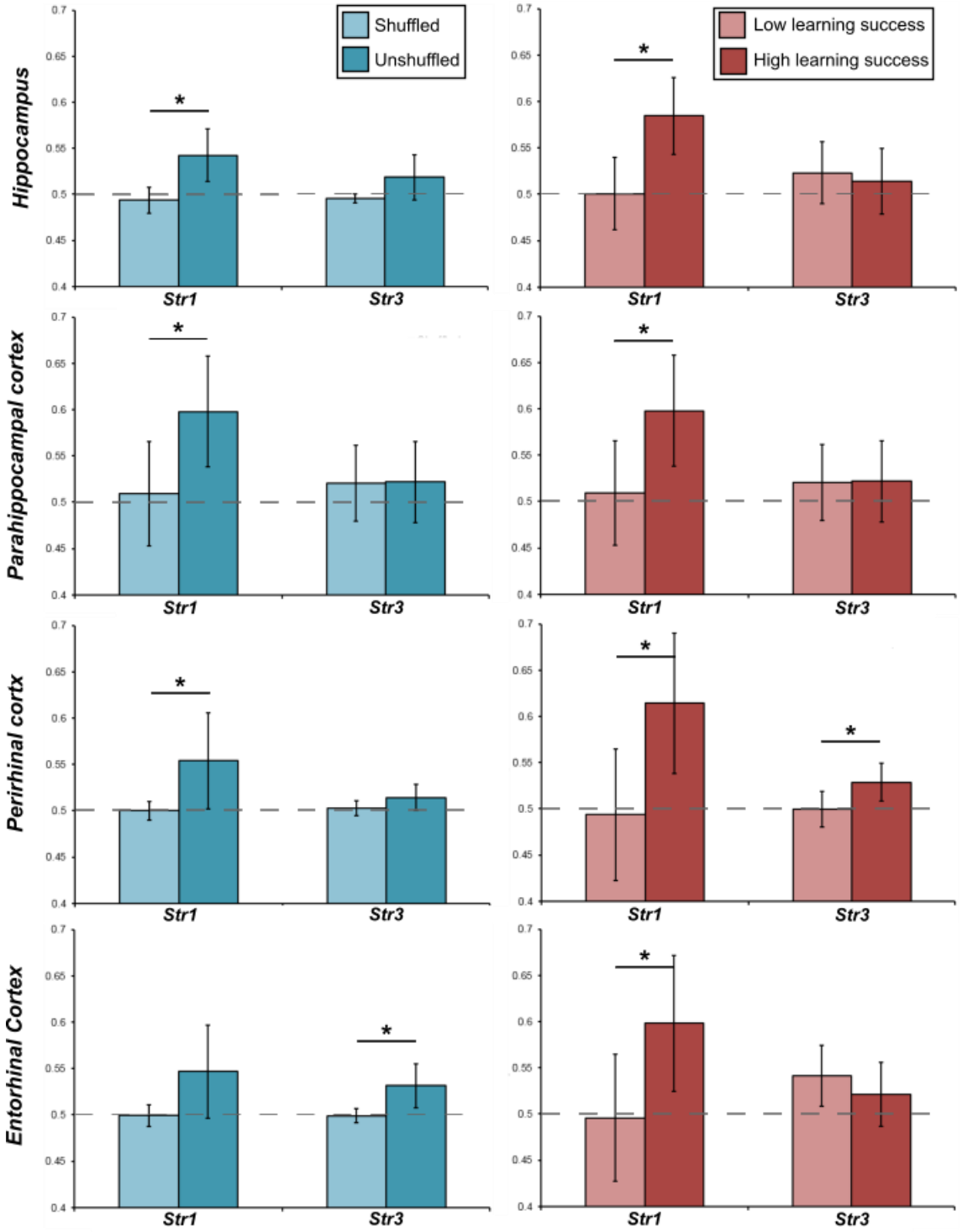

Figure 2-9. *MVPA classification accuracy scores broken down by memory strength, data integrity (blue bars) and learning success (red bars). Error bars indicate 95% confidence intervals corrected for the within subject-error term.*

2.5 Discussion

We investigated the brain regions involved in configural memory formation and generalisation. Using trial-and-error, participants gradually acquired two different types of configural contingency; non-structural configurations (learning feature conjunctions) and structural patterning (learning feature conjunctions and spatial arrangements). We observed clear monotonic increases in BOLD activity as a function of both learning types in the inferior temporal lobes (bilaterally), left angular gyrus and left orbital gyrus. Learning of this sort has been hypothesised to depend on regions within the MTL (namely the perirhinal and hippocampal cortices for non-structural and structural respectively; Saksida & Bussey, 2010; Aggleton, Sanderson & Pearce, 2007), yet we observed no gradual learning effects in these areas. Nonetheless, an MVPA highlighted that both of these structures, and the parahippocampal and entorhinal cortices, did contain task relevant information that was present both before and after the contingencies had been learned. Furthermore, during the early stages of learning, the strength of this information in the hippocampus and entorhinal cortex was predictive of subsequent behavioural performance - a finding which indicates that the decoded BOLD patterns are functionally relevant to learning. Finally, in a test of cross-discrimination transitivity requiring generalising between the structural discriminations, participants' performance was strongly related to BOLD activity in the right posterior hippocampus. This suggests that even after configural representations have been well learned, the hippocampus may be required to integrate and generalise between them.

Both the left inferior temporal gyrus and the left angular gyrus (lAG) are commonly co-activated in fMRI studies tapping semantic knowledge and semantic processing (Binder Desai, Graves & Conant, 2009). As such, they are assumed to be key components of the semantic memory system and so we suggest that that humans can use this system to store and retrieve configural contingencies. Specifically, the inferior temporal gyrus has been implicated in the storage of semantic facts. Evidence for this has come from neuropsychological observations that damage to this region results in substantial category-specific deficits in semantic knowledge (Warrington, 1975; Warrington & Shallice, 1984; Lambon Ralph, Lowe & Rogers, 2007; Noppeney et al., 2007). Given this, we propose that configural contingencies can be encoded by this region in the form of explicit rule-like (i.e. semantised) memory representations.

In contrast, the lAG has been implicated in integrating semantic and perceptual elements during schema retrieval and comprehension (e.g. Wagner et al., 2015; Humphries, Binder, Medler & Liebenthal, 2007). The region has also been associated with stimulus-driven (i.e. bottom-up) attentional mechanisms that aid episodic memory retrieval (Cabeza, Ciaramelli, Olson & Moscovitch, 2008). Notably, the lAG may be particularly involved in selectively mapping perceptual feature conjunctions to specific memory representations when there is interference from

overlapping representations (see Ansari, 2008; De Visscher, Berens, Kidel, Noël & Bird, 2015). This represents a core operation when making configural discriminations as, by definition, configural learning entails forming a number of distinct representations with overlapping features. As a result, non-target memory representations may be erroneously activated during discrimination if they share common features with the target. For instance, in a non-structural task, while the target memory representation may be “A > B”, non-target representations “B > C” and “C > A” may be activated given the featural overlap. Consequently, it may be necessary to have a retrieval control process which only selects memory codes containing features that wholly or maximally intersect with the perceptually presented configuration (i.e. “A ∩ B”).

The proposed role of the angular gyrus in semantic and perceptual integration makes it a prime candidate for such a retrieval control process. In support of this view, the angular gyrus is thought to play a part in selectively retrieving arithmetic facts (learned arithmetic rules such as “2 x 2 = 4”; van Eimeren et al., 2010). Arithmetic facts are memory traces for configurations that contain overlapping features (i.e. the digits 0 - 9), and so these memory codes are susceptible to interference at retrieval (De Visscher & Noël, 2014). Previous work has shown the left angular gyrus to be activated when retrieving arithmetic facts and to be modulated by the level of digit interference specifically (Grabner et al., 2009; De Visscher, Berens, Kidel, Noël & Bird, 2015). Concordant with this, the symbol-referent mapping hypothesis posits that the left angular gyrus acts to map multiple perceptual features to overlapping memory representations (Ansari, 2008).

The final region that showed monotonic increases in BOLD activity as a function of configural memory strength was the left orbital gyrus. Studies of reinforcement learning have shown BOLD activity within this area to be positively correlated with participants’ expectations of how rewarding a stimulus is predicted to be (Wunderlich, Rangel, & O’Doherty, 2010; Glascher, Hampton, & O’Doherty, 2009; Tanaka et al., 2004). Given that expectations of reward should directly relate to task proficiency and thus configural memory strength, our observed increases in orbital BOLD activity may be indicative of increasing reward anticipation. However, as well as encoding the value of an expected reward, the orbitofrontal region is known to signal reward value per se (i.e. positive feedback once as decision has actually been made; Sescousse et al., 2010). Since decision periods were always directly followed by feedback periods during the in-scanner task, we are not able to distinguish between these two processes with the current dataset. In any case, these reward-related signals are likely to provide an input to credit assignment and memory update processes that facilitate learning (Rushworth, Noonan, Boorman, Walton & Behrens, 2011).

The view that configural learning can make use of the semantic memory system is at odds with studies of learning in non-human animals. Most of the previous literature has focused on rodents

and rhesus monkeys and has emphasised the roles of MTL structures (e.g. Aggleton et al., 2007; Bussey, Saksida, Murray, 2002). In the present study, the only univariate BOLD effect in the MTL occurred in the left parahippocampal cortex. However, this area exhibited an activation pattern indicative for gaining initial familiarity with the task environment rather than learning the configural contingencies themselves. As discussed above, the angular gyrus did show involvement in configural learning yet this structure is phylogenetically recent and so not present in non-humans other than the higher primates (Brodmann, 1994/1909). This suggests that humans can employ a fundamentally different brain system to most animals when acquiring configural contingencies. Consistent with this, Moses et al. (2008) has shown that configural learning in the context of hippocampal amnesia can be supported by semantic processes as evidenced by spared performance when using semantically meaningful stimuli. Additionally, magnetoencephalography has demonstrated that increasing the semantic meaningfulness of configural stimuli leads to reduced reliance on the hippocampus and increasing reliance on brain regions associated with semantic knowledge (namely the anterior temporal, left prefrontal and inferior frontal cortices; Moses et al., 2009). Here we further demonstrate that semantic system may be involved in configural learning even when there is no semantic component.

A further point of divergence between previous work and the present study lies in the cognitive models suggested by each. Models of configural learning in animals often assume that memory representations are built up hierarchically (see Saksida & Bussey, 2010). On this view, a network of cytoarchitecturally specialised brain modules are arranged so that simple configural codes (e.g. that underpin non-structural memory representations in the perirhinal cortex) are critically required for underpinning more complex representations in upstream brain regions (e.g. structural memory codes in the hippocampus). The behavioural findings of the present investigation challenge this assumption in one important respect. As expected, response times to the more demanding structural configurations were longer than that of non-structural configurations. However, a Bayesian analysis revealed that this difference did not vary as a function of memory strength. In the lowest memory strength (Str1), processes controlling the retrieval of configural information should be minimally engaged as there is little information to actually retrieve. Consequently, reaction time differences that emerge between trial types in Str1 should be primarily driven by differences in visual processing. However, if configural memory codes are represented hierarchically, the processing latencies between trial types should increase with memory strength reflecting the emergence of more complex memory codes from higher level processing modules. The observation that reaction time differences between trial types remained constant across Str levels is inconsistent with hierarchically organised models of configural information coding. In contrast, the observed pattern is wholly consistent with the view that configural contingencies are represented by rule-like semantic representations.

Our suggestion that configural information is encoded by the semantic system does not exclude the possibility that the MTL are critical for initially processing configural information. To address this, we carried out an MVPA on regions within the MTL for data recorded at different memory strengths. This indicated that a number of MTL regions (namely the hippocampal, parahippocampal, perirhinal and entorhinal cortices) did exhibit distinct BOLD patterns to structural and non-structural stimuli both before and after high levels of learning had taken place. Based on this result we cannot say whether each region is coding for either structural-, or non-structural-information, or indeed both. However, it does suggest that these regions do code for some form of configural information online, even before that information has been fully learned. Moreover, the finding that the strength of this information was predictive of subsequent performance shows that it is functionally relevant to the learning process. These findings do therefore support the notion that the MTL processes configural information even if such information is subsequently encoded into brain regions associated with the semantic system. Accordingly, the MTL are often viewed as an extension to the visual ventral stream specialised for perceptually processing high-level visual representations (e.g. Saksida & Bussey, 2010; Lee, Yeung, Barense, 2012). Damage to hippocampus and other MTL structures has been observed to result in perceptual impairments for complex stimuli (e.g. Lee et al., 2005; Barense, Gaffan, Graham, 2007).

Another hypothesis that was tested as part of the current study concerned whether the hippocampus is involved in generalising between learned configurations. The term generalisation can refer to any processes requiring the transfer, integration or flexible expression of previously learned information in the support of untrained behaviour. As such, different forms of mnemonic generalisation exist and not all are critically dependent on the hippocampus (see Kumaran, 2012 for a review). One form of generalisation that is thought to be hippocampally dependent is inference. This has been previously studied using the paired associates inference (PAI) paradigm (Bunsey & Eichenbaum, 1996; Preston, Shrager, Dudukovic & Gabrieli, 2004; Zeithamova & Preston, 2010), acquired equivalence paradigm (Shohamy & Wagner, 2008) and transitive inference discriminations (DeVito, Kanter & Eichenbaum, 2010; Zalesak & Heckers, 2009; Heckers, Zalesak, Weiss, Ditman & Titone, 2004; Greene, Gross, Elsinger & Rao, 2006; Van der Jeugd et al., 2009). All of these tasks share the central feature that they require the integration of two or more previously learned associative relationships that were initially formed at different times.

Early evidence emerged that while not necessarily critical for acquiring simple stimulus-stimulus associations, the hippocampus is critical for integrating such associations in support of mnemonic inference (Bunsey and Eichenbaum, 1996; Dusek & Eichenbaum, 1997). Given this, Eichenbaum (1999) posited that a primary role of the hippocampus is in underpinning the systematic organisation and flexible expression of memory to support behaviours that were never explicitly

trained. Classically, there are two classes of models that can account for the role of the hippocampus in generalisation; encoding based models (e.g. the temporal context model, Howard & Kahana, 2002; Polyn & Kahana, 2007; Howard, Fotedar, Datey & Hasselmo, 2005), and retrieval based models (e.g. REMERGE, Kumaran & McClelland, 2012). Encoding models propose that individual study episodes sharing common features are linked in memory at the point of encoding by the formation of unitary or overlapping memory representations. Consequently, activating one representation can result in the activation of another and this supports the integration of information across training episodes as required for inference. On the other hand, retrieval models pose that the overlap between related study events is not explicitly encoded at the time of study but can be inferred at the point of retrieval via the implementation of reciprocal connections between representational layers (e.g. Kumaran and McClelland, 2012).

While both encoding and retrieval models implicate the hippocampus, they make different predictions regarding at what stage the hippocampus is involved. Encoding models predict that hippocampal activity at the time of study should uniquely contribute to (and therefore correlate with) subsequent inference performance (even after controlling for the trace memory strength of the directly learned associations). In contrast, retrieval models suggest that any hippocampal involvement at the time of encoding should purely reflect encoding operations for the directly learned associations - on this view, memory integration processes are only ever invoked at the point of inferential test. Initial investigations directly testing these differential predictions produced conflicting results. Animal studies have shown that hippocampal damage acquired after initial associative training both does (DeVito, Kanter & Eichenbaum, 2010) and does not (Van der Jeugd et al., 2009) impair inference performance. Results from human neuroimaging studies are equally ambiguous. Some investigations have shown hippocampal involvement at the point of inferential retrieval alone (Preston, Shrager, Dudukovic & Gabrieli, 2004; Heckers, Zalesak, Weiss, Ditman & Titone, 2004), while other report inference-related operations to occur at encoding (Greene, Spellman, Elsinger & Rao, 2006; Shohamy & Wagner, 2008).

In view of these conflicting data, a subtler view has emerged positing that encoding and retrieval models are not mutually exclusive (see Zeithamova, Schlichting & Preston, 2012). Specifically, it can be hypothesised that the hippocampus contributes to both encoding- and retrieval-based generalisation via the same fundamental pattern completion mechanism (see Rolls, 2013), and that the dominant route to generalisation depends on how well learned the directly trained configurations are. Initially, associations with overlapping features may be encoded as distinct, pattern separated representations. As such, when it comes to integrate these representations at inferential test, the hippocampus may be recruited to pattern complete and retrieve the overlapping representations to support ‘on-the-fly’ inference (e.g. Kumaran & McClelland, 2012). However,

when an association is encoded by the hippocampus, automatic retrieval processes have been observed to activate previously encoded and overlapping representations (Zeithamova, Dominick & Preston, 2014). Given this, after a sufficient number of learning instances, it is likely that the representations of overlapping events will become fully integrated into a unitary memory code; so-called 'retrieval-mediated learning'. In support of this hypothesis, one neuroimaging study using a single-trial learning procedure observed hippocampal and parahippocampal involvement in generalisation both at encoding and test (Zeithamova & Preston, 2010). Furthermore, it is noteworthy that previously discussed reports highlighting no hippocampal involvement at inferential test tended to train directly learned associations to ceiling (93% mean accuracy in the case of Shohamy & Wagner, 2008).

In the present study, we showed that right-lateralized posterior hippocampal activity at the time of inferential test was strongly related to transitive performance. In examining this region's activity during initial configural acquisition, much weaker correlations between learning-related activity and subsequent transitive performance were detected, even at the very lowest trace-memory strength (Str1; i.e. before the configural representations had been fully formed). As such, these data do lend support to a mixed retrieval/encoding-based hypothesis of hippocampal inference. Nonetheless, it is noteworthy that the hippocampal region did not exhibit any BOLD modulations across memory strengths, even after controlling for individual differences in transitive performance. Given this, it is unlikely that the hippocampus was functionally representing an integrated representation formed via 'retrieval-mediated learning'. Instead, we suggest that hippocampal involvement in transitive inference primarily took place at test and involved integrating well learned, rule-like configural contingencies that had been encoded by the semantic system.

In summary, the findings reported here support the role of MTL structures in representing visual configurations online. While these online representations do appear to be relevant to learning, we suggest that well learned configural memory codes may be underpinned by the semantic memory system. Nonetheless, even when represented in this way, we have demonstrated that the hippocampus is still used to integrate between configural memory codes when generalising across them.

Chapter 3

Applying the temporal context model to cross-situational learning

3.1 Abstract

Cross-situational learning (xSL) has been implicated as a primary route to semantic memory formation in infants. It allows for the concurrent acquisition of multiple word-object associations by integrating information across a series of ambiguous study events. Current models suggest that all semantic information initially depends on the episodic memory system. In line with this, we hypothesised that word-object bindings in xSL are underpinned by overlapping contextual representations as described by the temporal context model. This hypothesis makes the specific prediction that errors in naming stimuli after xSL are influenced by the temporal arrangement of those stimuli during study. This prediction was tested in a standard xSL experiment involving 32 healthy adults. The results revealed no evidence that xSL is subserved by contextual learning mechanisms and a Bayesian analysis weighted the null effect as more probable than the predicted effect. As such, we suggest that xSL is not subserved by the development overlapping contextual representations yet further research will be required to establish this.

3.2 Introduction

Since Tulving (1972) made the distinction between episodic and semantic memory, there has been much debate regarding how these types of memory interact. Primary language acquisition by infants is one form of learning that exhibits both episodic and semantic characteristics. In particular, language acquisition occurs rapidly (Schafer & Plunkett, 1998) and is subject to mnemonic generalisations (e.g. overextensions; Rescorla, 1980) - traits indicative of episodic memory. At the same time, language is retained throughout life with great stability (Cohen, 1979) - a quality more associated with the semantic system. Dominant theories account for this mix of features by suggesting that all learned information initially depends on the episodic system before being consolidated (McClelland, McNaughton, & O'Reilly, 1995) or transformed (Winocur & Moscovitch, 2011) to become reliant on the semantic system. As such, these theories predict that language learning mechanisms are fundamentally underpinned by episodic memory functions.

Importantly, models of how infants acquire new nouns (i.e. word-object associations) must accommodate the observation that such learning can take place when word-object associations are never explicitly communicated. Specifically, given a series of ambiguous study episodes, each presenting multiple unknown words and objects, learners can still acquire the underlying associations by keeping track of word-object co-occurrences across time. For example, if a learner hears the words *fork* and *sink* whilst simultaneously viewing each of their referents, it may be ambiguous which word refers to which object. However, if that learner subsequently studied the words *fork* and *plate* alongside their associated objects, enough information has been supplied to infer the word-object mappings across all three pairs. This is termed cross-situational learning (xSL) and has been demonstrated experimentally in both infants and adults (Yu & Smith, 2007; Smith & Yu, 2008).

To date, two broad types of model for describing xSL mechanisms have been proposed. On one account, word-referent mappings are acquired by associative means where all word-object co-occurrences are traced simultaneously (Kachergis, Yu, & Shiffrin, 2012a; McMurray, Horst, & Samuelson, 2012). In contrast, Medina, Snedeker, Trueswell and Gleitman (2011) have suggested that xSL is facilitated by the generation of a single hypothesised referent for each word that is retained across learning trials unless the hypothesis is falsified (i.e. unless a word is absent in a scene where its hypothesised referent is present or vice versa). Few studies have directly tested the differential predictions of these two types of models. Nonetheless, better support for an associative account has come from comparing computational implementations of learning via associations versus via single hypotheses. In particular, associative accounts are thought to more readily reproduce empirical data of xSL in humans (Kachergis, Yu, & Shiffrin, 2012b), especially when referential ambiguity is high (Smith, Smith & Blythe, 2011). Despite this, it remains unclear

exactly what information learners draw on when engaging in xSL and how this information is integrated across situations. One hypothesis might be that the word-object associations are tracked by an effortful working memory process that roughly counts the number of stimulus co-occurrences. However, this seems unlikely. XSL can occur incidentally, without a conscious intention to learn (Kachergis, Yu, & Shiffrin, 2010a). Also, the limited capacity of working memory means that its use in xSL appears unreasonable (Medina et al., 2011), especially in the context of language acquisition by infants. Here we propose that an existing model of episodic and associative learning, the Temporal Context Model (TCM; Howard & Kahana 2002; Howard, Fotedar, Datey, & Hasselmo, 2005; Howard, 2004), may be able to accommodate xSL.

The TCM was initially formulated to account recency and contiguity effects observed in free recall paradigms but has also been shown to readily account for the emergence of incidental associative learning, such as during the paired-associates inference paradigm (see Kumaran, 2012 for a review). Recency refers to the phenomenon where items that are encountered towards the end of a study list are better remembered than those that are encountered earlier. Contiguity refers to the effect where study items that are encountered closer together in time tend to be recalled adjacently as well. The TCM explains these effects by specifying the presence of two representational layers which are interconnected and interact with each other during learning; 1) a feature layer representing individual study items (e.g. objects and words) and, 2) a contextual layer representing the encoding context for each item. Content in the contextual layer changes gradually over time and is influenced by information in the feature layer (i.e. the study memoranda). This therefore acts as a slowly changing frame of reference against which memories are formed. During learning, connections between the feature and context layers are updated such that items presented close together in time are bound to similar contextual representations. Because of this, the recall of any one item has the ability to cue its associated encoding context. Likewise, when an encoding context is reactivated, it can cue feature layer representations that were encountered around the same time. Given this, recency occurs because the state of temporal context at the time of recall is most similar to the encoding context of later list items thereby facilitating their retrieval. Similarly, contiguity occurs because when recalled, each item activates its associated encoding context which then goes on to cue other items encountered around the same time.

Mathematically, the feature and context layers of the TCM correspond to high dimensional vectors where F is the feature space and T is the context space (see figure 3-1). The state of these two vectors at time i is denoted as f_i and t_i respectively. Inputs from the feature layer to the context layer (${t_i}^{IN}$) result from the product of feature-to-context connections defined in the matrix ${M_i}^{FT}$:

$${t_i}^{IN} = {M_i}^{FT} \times f_i \qquad \textit{(Eq. 1)}$$

With this input, content in the context layer evolves gradually over time as a weighted sum of the input ($t_i{}^{IN}$) and the previous state of the context layer (t_{i-1}):

$$t_i = (\rho_i \times t_{i-1}) + (\beta \times t_i{}^{IN}) \quad \textit{(Eq. 2)}$$

Here, β is a free parameter reflecting the relative influence of new inputs to the context layer. The parameter ρ_i defines the rate of contextual drift and is chosen at each time-point as a value between 0 and 1 such that the absolute magnitude of t_i is unity. During learning, feature-to-context connections (i.e. $M_i{}^{FT}$) are updated via a Hebbian learning rule so that featural representations can cue their associated encoding context. The TCM further suggests that context-to-feature connections defined in the matrix $M_i{}^{TF}$ provide inputs to the feature layer ($f_i{}^{IN}$):

$$f_i{}^{IN} = M_i{}^{TF} \times t_i \quad \textit{(Eq. 3)}$$

Connections in $M_i{}^{TF}$ are also updated during learning thereby enabling contextual states to activate their associated feature states. As such, if a given item was encoded at time i and then its associated context was later reactivated at time r, inputs to the feature layer will drive an activation pattern for the item. This activation pattern (a_i) can be represented as the dot product of $f_r{}^{IN}$ and the feature state at the time of encoding (f_i):

$$a_i = f_r{}^{IN} \times f_i \quad \textit{(Eq. 4)}$$

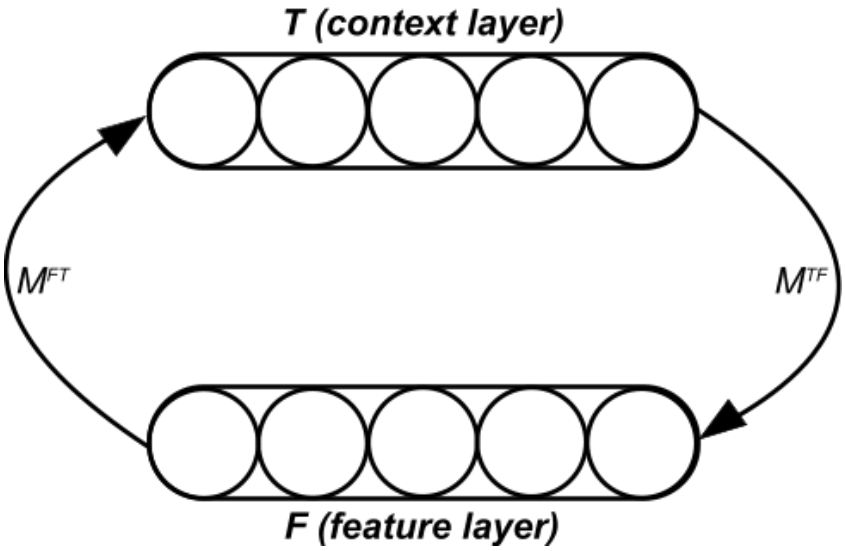

Figure 3-1. *A graphical illustration of the temporal context model.*

These properties of the TCM powerfully afford item-to-item associative learning. For instance, if two items are simultaneously presented at study, the shared feature state they result in will drive a common contextual representation. Learning in the matrices M^{FT} and M^{TF} will enable this feature state to cue the context state and vice versa. Subsequently, if one of the items is later represented in isolation, the contextual state that results may go on to cue featural representations of the non-presented item. Notably, this effect will also occur for items that are presented sequentially instead of simultaneously because the context state evolves gradually (c.f. Eq. 2). Considering these associative mechanisms, it is easy to see how the TCM may account for xSL. On this view, word-object associations are acquired because the context layer input at each study instance for a word always contain information derived from its associated object. After a sufficient number of instances, updates in feature-to-context connections will mean the contextual information evoked by that word contains more information about its corresponding object than any non-corresponding stimulus. Likewise, updates in context-to-feature connections will mean that this overlapping contextual information will have a strong ability to cue the associated object.

It is noteworthy that one existing adaptation of the TCM, the predictive TCM, has suggested that new word learning and the formation of semantic associations can take place when an unknown word is used in a context which predicts the occurrence of a known word (Howard, Karthik, Shankar, & Jagadisan, 2011). For example, if a learner encountered the sentence, “The baker reached into the oven and pulled out a taftoon.”, the words “bread” and “taftoon” may become associated even if “taftoon” is unfamiliar. This is because contextual cues within the sentence predict and activate “bread”. As such, the encoding context for “taftoon” now contains information derived from the word “bread”. To date, this model has not been empirically tested. However, support for the TCM more generally has come from neuroimaging studies demonstrating that the recall of an item reinstates the pattern of brain activity that was present during its encoding (Polyn, Natu, Cohen, & Norman, 2005; Sederberg et al., 2007; Johnson & Rugg, 2007). In one of these studies, multivariate pattern analysis of fMRI data showed that brain activity specific to the encoding of three classes of pictorial stimuli (famous faces, landmarks and objects) was reinstated at least 5.4 seconds prior to the recall of an item (Polyn et al., 2005). Additionally, intracranial electroencephalography (EEG) has highlighted that gamma band oscillatory activity originating from the hippocampus predicts the successful encoding of items and is reinstated during recall (Sederberg et al., 2007).

Importantly, the hypothesis that xSL is underpinned by temporal context coding mechanisms leads to a specific prediction not made by any other model. If word-object associations are trained via xSL and then tested using an alternative-forced-choice (AFC) paradigm, the TCM predicts that erroneous pairings made between non-corresponding stimuli should, at least in part, be influenced

by the temporal arrangement of those stimuli during study. Specifically, the closer together in time that any two non-corresponding stimuli are presented, the higher the likelihood they will be erroneously matched at test - this can be viewed as a form of contiguity effect for word-object associations. Importantly, other models of xSL (e.g. the single hypothesis account) may predict that non-corresponding stimuli presented on the same study trial have a higher likelihood of being erroneously matched at test. However, because temporal context evolves gradually, only the TCM predicts that sequential presentations of stimuli also increase the likelihood that those stimuli will be erroneously matched.

In the present investigation we set out to test this prediction. Healthy adult participants learned associations between 9 novel objects and 9 pseudowords. Throughout study, the trained associations were intermittently tested on 9-AFC test trials. We examined whether the number of times that a pair of stimuli were presented on successive study trials predicted why some stimuli were erroneously matched over others.

3.3 Methods

3.3.1 Subjects

Thirty-nine native English speaking students were recruited from the University of Sussex, UK. All gave written informed consent to take part. To ensure that all subjects entered into the analysis were effectively learning via xSL, we only included data when at least half of the trained associations had been acquired by the end of the task. Given this threshold, data from 7 subjects were discarded owing to insufficient levels of learning. This left a final sample of 32 subjects (15 female) with a mean age of 23.72 years (*SD* = 5.14). The study was approved by a local ethics committee (C-REC, University of Sussex).

3.3.2 Stimuli

9 colour photographs of obscure objects (e.g. rocket air blower) and 9 four-letter pseudowords (e.g. "Ospi") were selected from the NOUN Database (Horst, 2009). Prior to each experimental session, these stimuli were randomly paired together to form the trained word-object associations. During the task, both the pseudowords (140 x 240 pixels) and obscure objects (black text; 240 x 240 pixels) were presented on a computer monitor (1280 x 1024 pixels; 38.60 x 28.96 cm) positioned approximately 60 cm in front of the subject.

3.3.3 Procedure

The xSL task consisted of 8 blocks of study trials each followed by a block of test trials. On each study trial, 3 of the 9 word-object pairs were randomly selected for presentation such that corresponding stimuli were consistently presented together whereas non-corresponding co-occurrences occurred randomly. Of the 3 selected pairs, objects were presented at random positions to the left of the display and words were presented at random positions to the right (see figure 3-2A). There was no indication of which object went with which word. Study trial presentations lasted for 6 seconds and were followed by a 2 second inter-trial interval. There were 12 study trials to a block and across these trials all 9 word-object pairs were presented 4 times (32 presentations per pair within the entire experiment).

Test blocks consisted of 9 trials, one for each of the trained associations. On these trials, a single object was cued by being presented to the left of the display (see figure 3-2B). Alongside this image, a 3x3 grid of all 9 words was shown with a red cursor being randomly positioned around one of them. Using a standard computer keyboard, participants could move the cursor around the grid in order to select the word associated with the cued object (i.e. a 9-AFC test). Tests occurred in a random order and were entirely self-paced. Blocks of study and test were separated from one another by a 6 second inter-block interval. Before taking part, subjects were fully informed of the

task procedure and told that they would be learning one-to-one correspondences between 9 objects-word pairs.

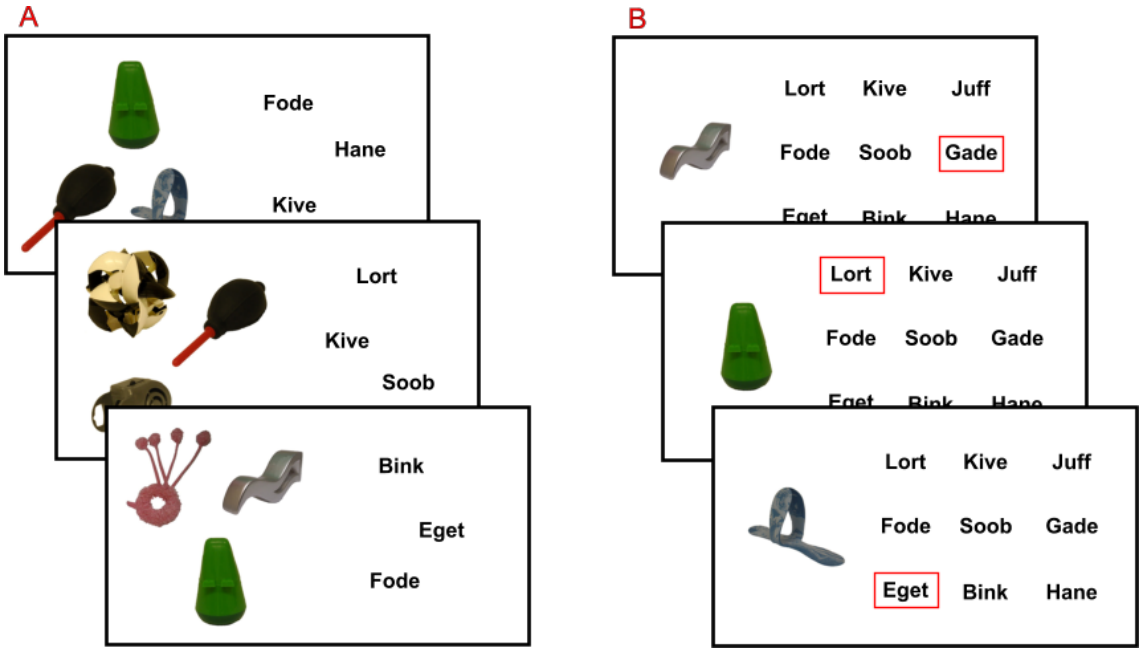

Figure 3-2. *Example trials at study (**A**) and at test (**B**).*

3.4 Results

All analyses were implemented in MATLAB (Mathworks) using the statistics toolbox. The primary behavioural outputs were binary correct vs incorrect statistics relating to accuracy on each 9-AFC test trial. Correct responses were coded as 1's and incorrect responses were coded as 0's. In order to confirm that xSL was actually taking place, we first computed a subject-specific block-wise measure of word-object matching accuracy. To do this, the binary performance statistics were independently averaged within blocks and the result was taken as a block-wise trajectory of performance. Figure 3-3 displays the sample average performance trajectory showing significant above chance performance in all 8 blocks, minimum $t(31) = 6.836$, $p < .001$. Furthermore, there was a significant change in performance across blocks, $F(17,217) = 55.26$, $p < .001$, with both linear ($F = 151.01$) and quadratic ($F = 18.88$) trends. The mean number of errors made by each subject was 18.72 ($SD = 12.84$).

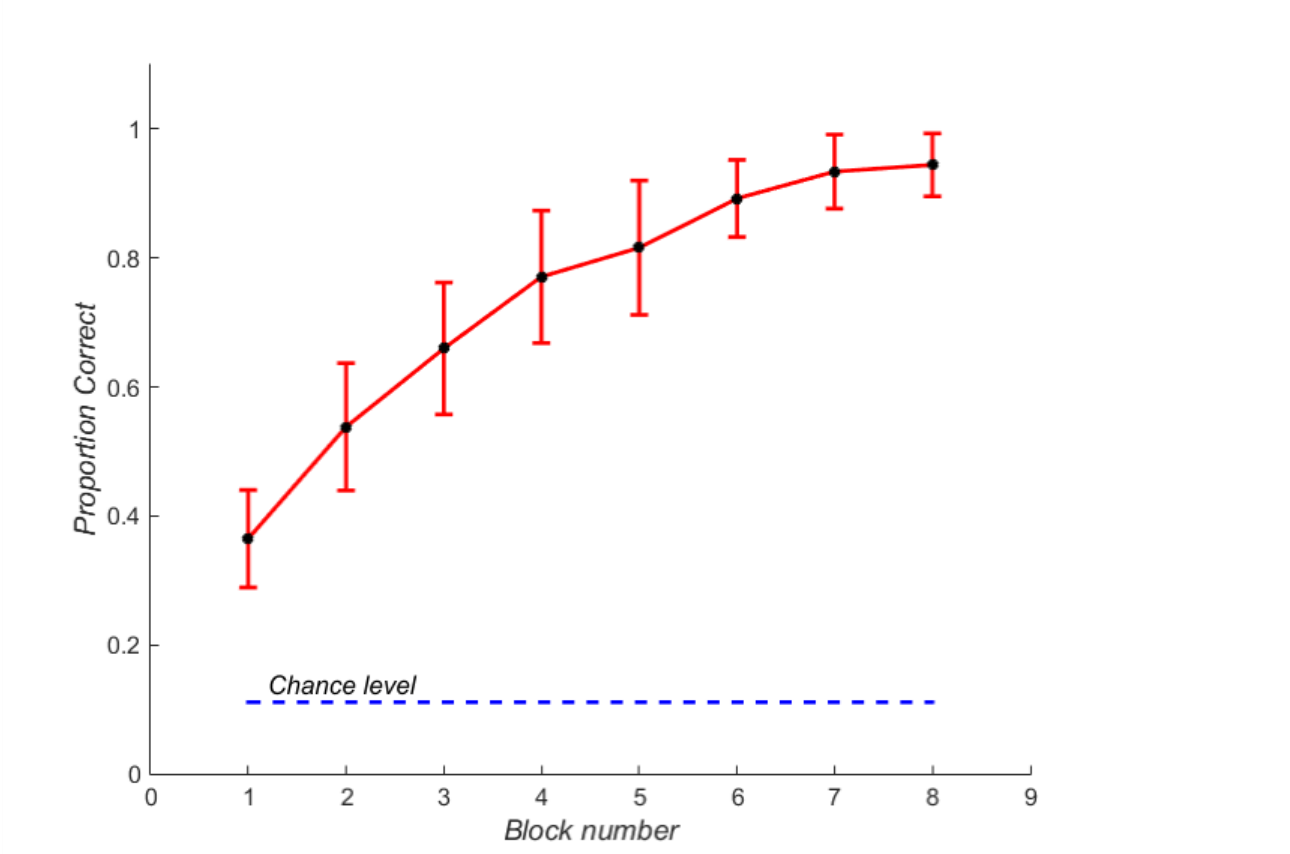

Figure 3-3. *Sample average performance trajectory. Error bars indicate 95% confidence intervals corrected for the within subject-error term.*

In order to test our principal hypothesis, we counted the number of times that erroneously matched objects and words were presented on the same trial (same-trial occurrences), and successive trials (successive-trial occurrences) during the preceding study block (see figure 3-4). Along with these frequency statistics for errors that had actually been made (actual errors), we also computed equivalent statistics for erroneous matches that could have been made in place of the actual error (hypothetical errors). Histograms plotting the distribution of these statistics across all subjects are shown in figure 3-5. A mixed effects logistic regression model was then specified which attempted to differentiate actual errors from hypothetical errors using the number of same-trial and successive-trial occurrences. Data from all subjects were included in the model together. The outcome variable was error type (i.e. actual vs hypothetical) with actual errors being coded as 1's and hypothetical errors being coded as 0's. Fixed effects predictor variables included the constant term, the number of same-trial occurrences and the number of successive-trial occurrences. Additionally, due to statistical dependencies relating to repeated measurements from subjects and individual test trials, random intercepts for subjects and trials were included as random effects predictors. The model utilised a logit link function and was estimated via maximum likelihood estimation.

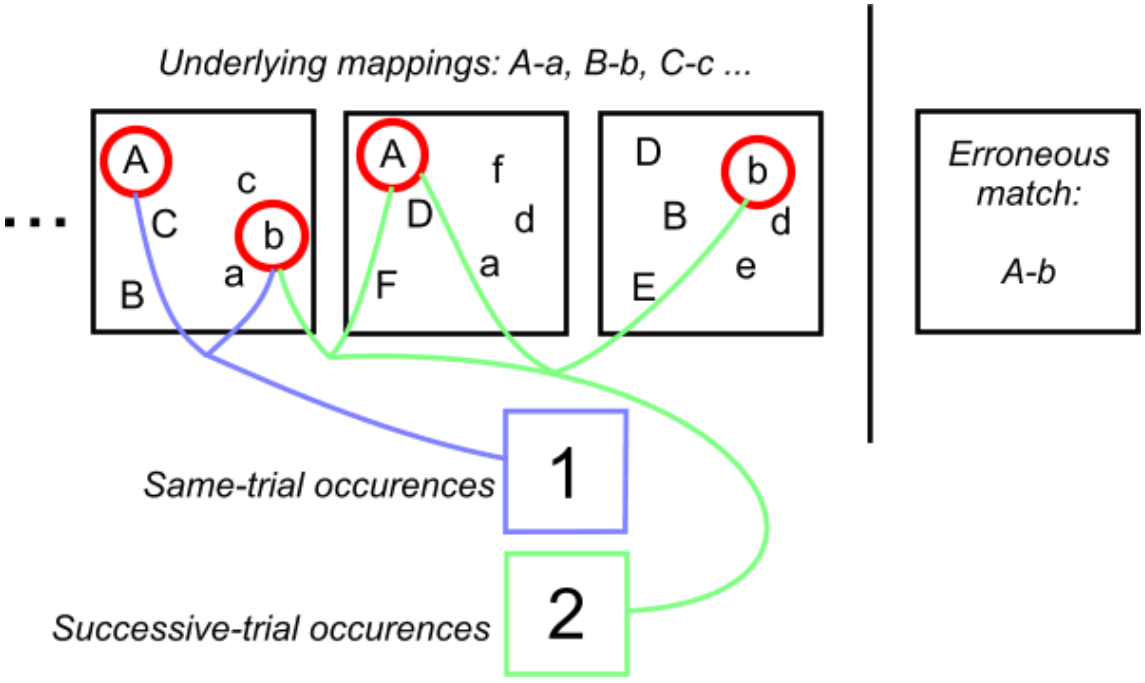

Figure 3-4. *Illustration of how same-trial and successive-trial occurrence statistics were calculated for an actual error. Upper-case letters denote objects; lower-case letters denote words. At test, object "A" was erroneously matched to word "b". Over the preceding study block, the number of times that "A" and "b" were presented on the same/successive trials is counted. The same procedure was also carried out for "hypothetical errors", i.e. A-c, A-d, etc.*

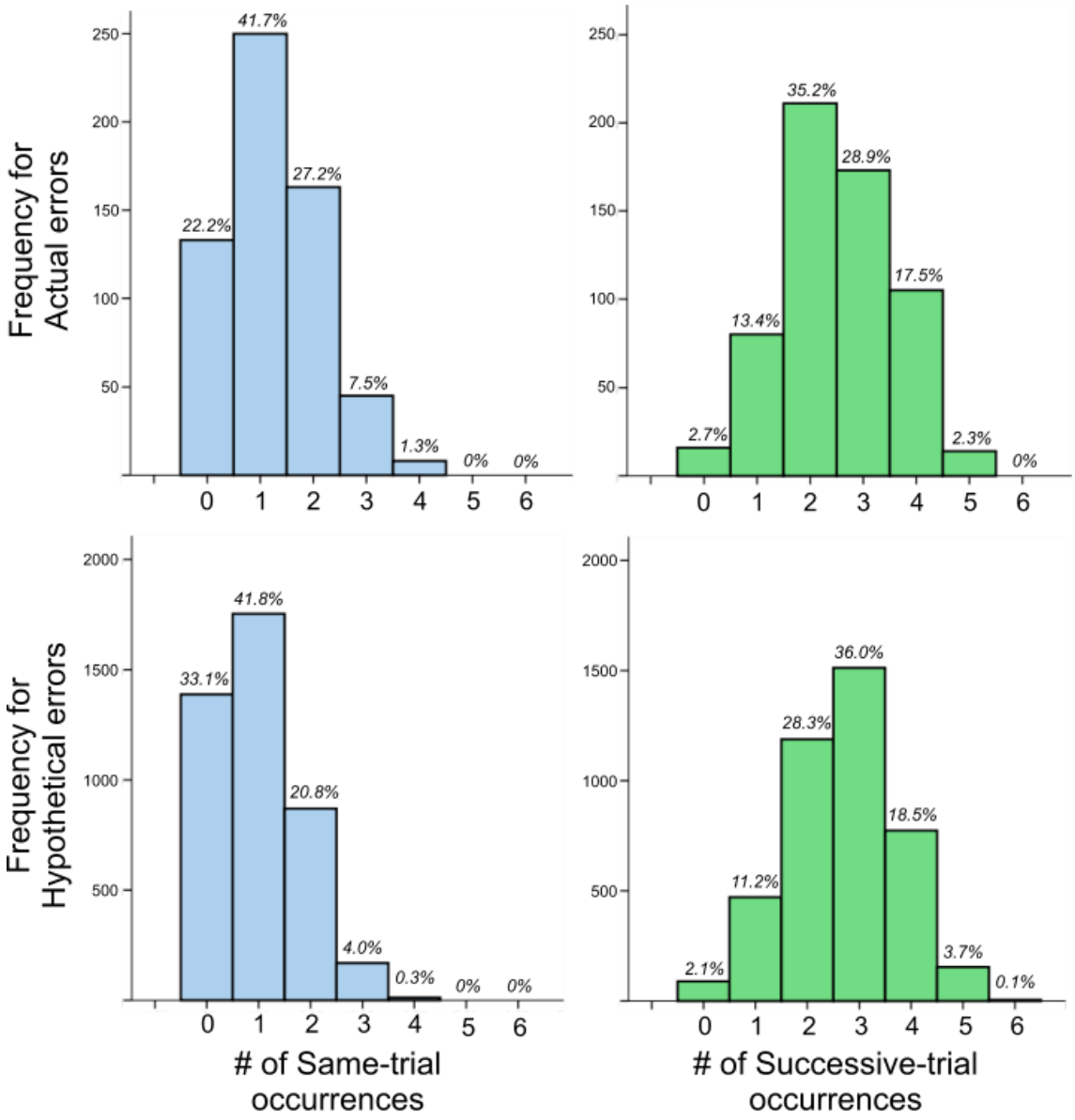

Figure 3-5. *Histograms plotting the frequencies of same-trial occurrences (blue bars) and successive-trial occurrences (green bars) for actual and hypothetical errors (top and bottom rows respectively).*

Along with their associated significance values, estimates for each fixed effects term are listed in table 3-1. Critically, while this shows that same-trial occurrences did predict the incidence of errors, the estimate for successive-trial occurrences was not significant. We therefore wished to examine whether there was more evidence in favour of the null hypothesis for this model term. To do this, a Bayesian analysis was run as described by Dienes (2011). Here, the strength of evidence in favour of the null (H_0) is compared to that of the alternative hypothesis (H_1). Our prior for H_1, (i.e. the range of plausible effect size assuming H_1 to be true) was set as a uniform distribution between 0 and 0.2854 (that is, ranging from no effect to the same effect size returned for same-trial

occurrences). Based on this prior, a Bayes factor in favour of H_0 was return as 3.57 [$p(H_0|Data)$ = .781] which suggests that there was over 3.5 times more evidence in favour of H_0 compared to H_1. This value represents substantial evidence for of the null hypothesis (see Jeffreys, 1961).

Table 3-1. *Outputs from the mixed effects logistic regression.*

Model term	*Estimate*	*Standard error*	*t-Statistic*	*Degrees of freedom*	*p-Value*	*95% Confidence Interval*
Intercept	-1.9814	0.045	-44.0232	4788	$p < 10^{-37}$	[-2.0697 : -1.8932]
Same-trial occurrences	0.2854	0.0651	4.384	4788	1.19×10^{-5}	[+0.1578 : +0.413]
Successive-trial occurrences	-0.0108	0.0723	-0.1497	4788	0.881	[-0.1525 : +0.1309]

3.5 Discussion

We hypothesised that xSL is subserved by the acquisition of overlapping contextual representations as described by the TCM (Howard & Kahana, 2002). This predicts that erroneous pairing made during xSL should be more frequent for non-corresponding stimuli that have been studied closer together in time. Using data from a xSL experiment, we tested this prediction by examining whether presentations of stimuli on successive trials was associated with an increased incidence of mispairing errors for those stimuli. The results suggested this not to be the case. Successive trial presentations did not significantly influence subsequent errors and a Bayesian analysis revealed greater evidence a null effect in our data.

In light of this result, it is possible that xSL is underpinned by mechanisms other than learning to a gradually changing contextual representation. This leaves open the possibility that propositional logic and inference play a major role in xSL as described by the single hypothesis account (Medina et al., 2011). However, given our highly specific prediction, the current study is unable to provide any evidence that would corroborate or falsify this theory. Nonetheless, there are notable reasons why learning via temporal context may be unsuitable for xSL. For instance, if the rate of contextual drift was too slow (i.e. the parameter ρ_i in Eq. 2 was too large), then the encoding context at each study event may have contained too much of information about non-corresponding stimuli for contextual states to adequately activate unique feature representations. This may therefore render context learning mechanism inadequate over the time-scales at which xSL takes place meaning that other learning mechanisms are recruited.

Importantly however, there are also some extreme circumstances in which our prediction of increased error incidences would not have borne out despite the use of temporal context learning mechanisms. With further reference to Eq. 2, it is noteworthy that the drift rate parameter (ρ_i) is dependent on the magnitude of context inputs (${t_i}^{IN}$). As mentioned above, this parameter is selected so that the magnitude of the resultant context state does not exceed 1 (Howard & Kahana, 2002). Consequently, if the magnitude of the context inputs was sufficiently large, it is possible that the contextual state on any one trial would have been entirely driven by the current state of the feature layer. In this case, while contextual information would be utilised for binding stimuli presented concurrently, it does not act to associate stimuli presented on concurrent trials since contextual information does not leak from one trial to the next. This possibility limits the conclusions that can be drawn here and so further investigations will be required to examine the role of contextual learning in xSL. One potential avenue of future investigation could examine neuroanatomical predictions of the TCM. As noted in the introduction, context reinstatement effects have been observed in the brain during free recall (Polyn, Natu, Cohen, & Norman, 2005), source memory judgments (Sederberg et al., 2007), and episodic retrieval (Johnson & Rugg, 2007). As

such, if temporal context plays a role in xSL, it may be possible to observe such effects during study. Furthermore, neuroanatomical models of temporal context learning unequivocally suggest that feature and context layer representations are bound together by the hippocampus (Polyn & Kahana, 2008; Howard, Fotedar, Datey, & Hasselmo, 2005). Given this, further evidence for or against a role of contextual learning in xSL may be provided by neuroimaging studies examining hippocampal activity during noun acquisition.

In summary, we tested the hypothesis that xSL is underpinned by learning associations between featural representations and slowly changing contextual states. No evidence of this was found and so we suggest that temporal context learning mechanisms are unlikely to be employed in xSL. However, further work will be required to fully establish this.

Chapter 4

The brain systems underpinning Cross-Situational learning

4.1 Abstract

Prominent models suggest that all associations between novel stimuli are initially encoded by the hippocampal system before being consolidated or transformed to depend on the neocortex. However, some evidence suggests that amnestic patients with hippocampal damage may be able to gradually learn new associative information. Additionally, infants are able to rapidly acquire new word-object associations (i.e. nouns) despite having an underdeveloped declarative memory system. Here we hypothesised that a method of statistical learning implicated in primary language development (cross-situational learning; xSL) may be principally dependent on neocortical learning mechanisms rather than the hippocampus. During event-related fMRI, nineteen right handed participants learnt a set novel word-object associations as trained via xSL. At the same time, a different set of word-object associations were passively viewed having been pre-learned via a standard explicit encoding procedure. During periods of xSL, cortical areas associated with semantic processing, attention, and reasoning exhibited increases in activity that scaled proportionally with the amount of learning taking place. Furthermore, at the same stages of acquisition, a PPI analysis highlighted that BA22 (implicated in speech processing) showed increased functional connectivity with the left temporal pole. In contrast, the hippocampus showed greater in activity when processing the pre-learned associations (relative to xSL) as well as enhanced connectivity with BA22 and the occipital cortex. These results suggest that the semantic memory system is directly engaged in xSL yet the hippocampus is more involved in processing explicitly trained associations. However, whilst we suggest that xSL may be hippocampally independent altogether, neuropsychological data will be required to properly test this.

4.2 Introduction

Long-standing models of declarative memory suggest that neocortical learning for novel semantic information is slow and gradual (McClelland, McNaughton, & O'Reilly, 1995; McClelland, 2013). Supposedly, this is because the rapid acquisition of new information would result in catastrophic interference – the destruction of previously established memory codes and the impaired formation of others (see McCloskey & Cohen, 1989). As such, the hippocampal system is thought to encode all novel information in the short term before repeated activations of hippocampal traces allow uptake by the neocortical system. This process has been characterised as system consolidation (McClelland et al., 1995), and memory transformation (Winocur & Moscovitch, 2011). In support of this, many reports suggest that patients with hippocampal amnesia retain crystallised semantic memories formed well before neuropsychological insult but appear unable to learn any new semantic information (e.g. Squire & Alvarez, 1995).

Despite these findings, it has been suggested that new semantic learning can occur independently of the hippocampal system. Patients with an amnestic syndrome from birth are able to acquire semantic knowledge sufficient to support good levels of language function (Martins, Guillery-Girard, Jambaqué, Dulac, & Eustache, 2006; Vargha-Khadem, Gadian, & Mishkin, 2001). Additionally, patients with acquired amnesia have been observed to learn new labels for unfamiliar shapes when the labels are decided on through collaborative discussion (Duff, Hengst, Tranel, & Cohen, 2006). Learning information that is related to previously established semantic knowledge (so-called schema-assisted learning) appears to be particularly spared in amnesia (O'Kane, Kensinger, & Corkin, 2004; Skotko et al., 2004).

At the very least, schema-assisted learning is known to speed up consolidation. Tse et al. (2007) observed that newly learned smell-location associations in rats can become hippocampally independent within 24-hours if learning takes place in a well-known environment. Moreover, these rapidly consolidated associations were attained within a single rewarded trial. This suggest that as well as accelerating consolidation, schema assisted learning can facilitate the formation of associative memories in the first place. In line with this, earlier studies have demonstrated higher rates of learning and retention for information that is presented within an appropriate contextual framework (Bransford & Johnson, 1972).

While the findings by Tse et al. appear inconsistent with consolidation theory, the model can accommodate accelerated neocortical learning for schema-consistent information. This is because rapid learning via schema modification may not result in catastrophic interference (McClelland, 2013). Complementary to this, the medial prefrontal cortex has been implicated in detecting schema-consistent information in aid of rapid neocortical acquisition (van Kesteren, Ruiter,

Fernandez, & Henson, 2010). However, consolidation theory remains unable to account for the aforementioned reports of learning by patients with developmental amnesia. Furthermore, Sharon, Moscovitch and Gilboa (2011) have suggested that encoding novel word-object associations is possible in acquired amnesia using a learning procedure called “fast mapping” (FM).

On each trial of the FM procedure, two objects or animals are simultaneously presented, only one of which is previously known (see figure 1-1A). Participants are then asked a simple yes/no question regarding the visual appearance of one of these items. If the question refers to the unknown item by name, participants must deduce the item-name association in order to respond. Sharon et al. observed that four amnestic patients with hippocampal system damage were capable of learning new word-object associations via FM and retaining them over the course of a week. At the same time, these patients were severely impaired at learning other word-object associations’ trained using standard associative learning instructions (referred to as explicit encoding; EE). This suggest that FM may provide a direct route to neocortical semantic learning that is independent of the hippocampus. In support of this, Sharon et al. further reported that two patients with damage to the left temporal pole were impaired at FM. Furthermore, 14 month old infants can learn via FM despite not having a fully developed hippocampal system (Friedrich & Friedrich, 2008; Bauer, 2008).

Despite this, consensus is still lacking as to whether FM is entirely independent of the hippocampus. At least two studies using a number of amnestic patients have failed to replicate the findings by Sharon et al. (Smith, Urgolites, Hopkins & Squire, 2014; Warren & Duff, 2014). Furthermore, Greve, Cooper and Henson (2014) highlighted that there was no evidence for a relative sparing of FM in a group of healthy adults with reduced hippocampal volume. Additionally, it remains unclear exactly what features of FM underlie it proposed ability to facilitate learning in amnesia. FM differs from traditional methods of paired-associate learning in three respects; 1) associative links are not explicitly conveyed but have to be actively deduced through syllogistic reasoning; 2) novel associations are presented within the context of a pre-learned and semantically relevant association; and 3) the learning of associations is not deliberate (Sharon et al., 2011).

Like FM, “cross-situational learning” (xSL) also involves acquiring associations that are not explicitly given but must be extracted by the learner (see Chapter 3 and Yu & Smith, 2007). As previously discussed, a number of unfamiliar word-object pairs (typically 3 or 4) are simultaneously presented. However, because each trial will tend to present pairs in the context of different non-corresponding stimuli, learners can extract the underlying associations by tracking the co-occurrences between objects and words. Investigations, have shown that adults (Yu & Smith, 2007) and 12 month old infants (Smith & Yu, 2008) can acquire word-referent associations via

cross-situational means given very few learning instances. Following 36 trials, Yu and Smith (2007) reported an average acquisition rate of 14 out of 18 associations when 3 word-object pairs were presented on each trial. Like FM, xSL has also been implicated as a primary route vocabulary acquisition during infancy. Again, giving the underdeveloped hippocampal system in infants, this raise the question of whether xSL is independent of the hippocampus.

Importantly, xSL differs from FM in several key ways. Firstly, as mentioned above, it involves a high degree of referential ambiguity with multiple to-be-learned associations being presented simultaneously. Because of this, each individual study event conveys a relatively small amount of information which may not be amenable to hippocampal encoding. Indeed, the experiment in chapter 3 of this thesis showed that xSL cannot be accounted for by a prominent model of hippocampal learning, the temporal context model. Instead, it is likely that word-referent mappings learned via xSL are acquired by approximately tracking stimulus co-occurrences in a statistical manner (Kachergis, Yu & Shiffrin, 2012b; Smith, Smith, & Blythe, 2011). Importantly, these studies found that statistical learning strategies appear to be used even when adult learners hold a conscious learning intention. Since the neocortical learning system is also thought to rely on the extraction of statistical regularities (Winocur & Moscovitch, 2011; McClelland et al., 1995), we hypothesised that xSL constitutes a pure form of semantic learning - that is, it should show heavy reliance on neocortical learning mechanisms and independence from the hippocampus. Aside from the high degree of referential ambiguity, two further differences between FM and xSL are notable; novel associations are not learned in the context of pre-established knowledge, and a specific learning intention is often in force (although not necessary for learning to take place; Kachergis, Yu & Shiffrin, 2010). These aspects of xSL are also characteristic of more traditional pair-associate learning via EE. As such, if xSL is indeed a direct route to neocortical learning, it may suggest that acquisition under a high degree of referential ambiguity is the key feature that functionally distinguishes the neocortical and hippocampal learning systems.

To date, no studies have directly investigated the brain mechanisms involved in xSL. Here we used event-related functional magnetic resonance imaging (fMRI) to test the hypothesis that xSL preferentially engages neocortical learning mechanisms rather than the hippocampus. Over the course of 6 in-scanner study blocks, participants used xSL to learn associative links underlying 9 unfamiliar word-object pairs (words were aurally presented and objects were visually presented). Between study blocks, test trials tapped knowledge for the word-object associations thereby yielding information regarding learning rate. To serve as a comparison condition, a matched set of 9 word-object associations had been pre-learned through EE and were also presented during training and test in the same manner. This paradigm thereby allowed us to examine BOLD effects indicative of xSL at study and activation differences corresponding to the retrieval of xSL- versus

EE-trained associations. Additionally, by modelling psychophysiological interactions (PPIs) during study (Friston et al., 1997), we explored whether the hippocampus and a neocortical region involved in speech processing (BA22) exhibited differential patterns of functional connectivity with other areas depending on how word-object associations were trained. BA22 was chosen as a neocortical seed due to its known involvement in the processing of auditory stimuli, particularly speech (DeWitt & Rauschecker, 2011; DeWitt & Rauschecker, 2013; Demonet et al., 1992), as well as the cross-modal integration of such information (e.g. Foxe et al., 2002).

Four key predictions were under test; 1) during periods of study and test, xSL-trained associations will activate regions of the neocortical semantic memory system (e.g. the anterior temporal lobes) but not the hippocampus, 2) during periods of study and test, the hippocampus will be activated when processing EE-trained associations but not when processing xSL-trained associations, 3) during periods of study, functional connectivity between BA22 and semantic association areas will be increased for xSL-trained associations relative to EE-trained associations, and finally, 4) during periods of study, the automatic retrieval of word-object mappings learned via EE will result in increases in functional connectivity between the hippocampus and cortical representations of words and objects.

4.3 Methods

4.3.1 Subjects

Twenty-three right-handed, native English speaking students were recruited from the University of Sussex by way of online advertisement. All gave written informed consent to take part and were compensated for their time. Subjects had either normal or corrected-to-normal vision and reported no history of neurological or psychiatric illness. Of those who took part, data from four participants could not be included in for analysis due to problems with fMRI data acquisition (1 subject), and a failure to fully learn all associations to ceiling (3 subjects). As such, analyses included data from 19 subjects (11 males) with a mean age of 25.42 (*SD* = 4.03). The study was approved by the Brighton and Sussex Medical School's Research Governance and Ethics Committee.

4.3.2 Stimuli

18 colour photographs of obscure objects (e.g. rocket air blower) and 18 four-letter pseudowords (e.g. "Ospi") were selected from the NOUN Database (Horst, 2009) to be used as stimuli during the in-scanner task. Prior to each testing session, these stimuli were randomly paired together to form the trained word-object associations. Each pair was then randomly allocated to one of two groups (a "pre-learned" set and a "to-be-learned" set) consisting of 9 word-object pairs each. Additionally, 9 other obscure objects and pseudowords were drawn from the NOUN database to be used as lure stimuli during a pre-scanner recognition memory task (described below). All images had a resolution of 240 x 240 pixels and were taken against a well-lit, white background. High quality, uncompressed recordings of each pseudoword spoken by the same, neutral female voice were produced and underwent digital processing to equate them for perceived loudness. Throughout training and test, these recordings were presented binaurally (using headphones).

4.3.3 Procedure

4.3.3.1 Pre-scanner training

Prior to scanning, word-object associations for pairs in the pre-learned stimulus set were trained using an explicit encoding paradigm; following a 2 second inter-trial interval, a single object was centrally presented for 6 seconds and during this time, the object's corresponding pseudoword was played (figure 4-1A). There were 5 such study trials for each of the 9 word-object pairs in the pre-learned set (i.e. 45 in total) and these progressed in a random order. Subsequently, participants were tested on the trained associations with a single 9-alternative forced choice (9-AFC) test trial for each pair; on each of these, a 3x3 grid of all the pre-learned objects was displayed and after being cued with a single pre-learned pseudoword, a randomly positioned red cursor appeared

around an object in the grid (see figure 4-1B). Using a computer keyboard, participants could then move the cursor around the grid in order to select the cued object.

To equate the level of familiarity between pre-learned and to-be-learned stimuli, participants also engaged in a simple familiarisation phase for the to-be-learned objects and words. This took the form of a recognition memory test which ran in a similar way to the explicit encoding procedure described above with the key difference that each study trial only presented one type of stimulus (i.e. either a pseudoword or an object but not both simultaneously; figure 4-1C). There were 5 study trials for each of the 18 to-be-learned stimuli (i.e. 90 in total) and these progressed in a random order. A two-alternative forced choice recognition test then followed where a single to-be-learned stimulus (the target) was presented alongside a same-modality, unstudied lure. For pseudoword test trials, the target and lure words were serially presented in a random order before the text strings "First" and "Last" were displayed on screen with a red cursor placed randomly around one of them (figure 4-1D). Using the computer keyboard, participants were tasked with selecting the text strings that indicated whether the target was heard before or after the lure. During object test trials, the target and lure images were themselves displayed on screen and made selectable with the red cursor. There was a single test trial for each of the 18 to-be-learned stimuli and these were sequenced at random.

The order of the above pre-scanner tasks was counterbalanced between participants and each was fully described to participants prior to being run.

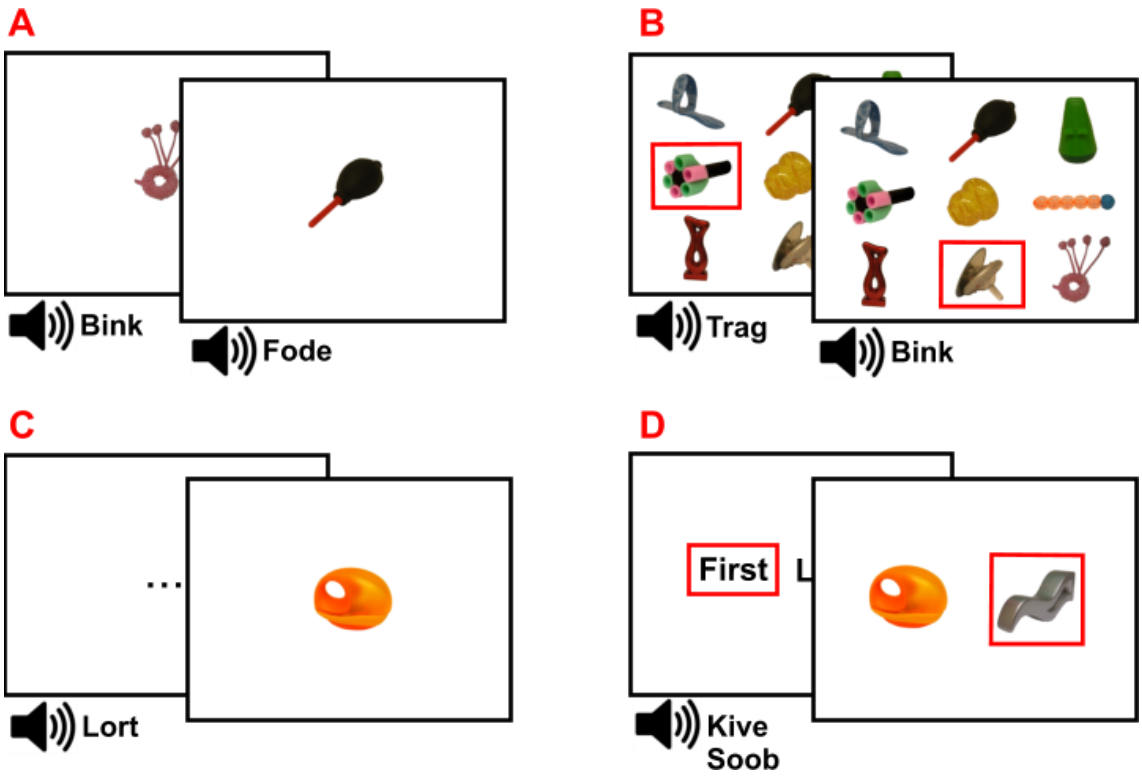

Figure 4-1. *Pre-scanning procedure.* ***A:*** *Explicit encoding trials for pre-learned stimuli.* ***B:*** *9-AFC test trials.* ***C:*** *Familiarisation phase for to-be-learned stimuli.* ***D:*** *Recognition memory test for to-be-learned stimuli.*

4.3.3.2 In-scanner task

The in-scanner task consisted of 6 blocks of study trials each followed by a block of test trials. After a variable (uniformly distributed) inter-trial interval of between 3 and 7 seconds, individual study trials followed lasting for 6 seconds in total. During this time, 3 objects randomly sampled from either the pre-learned or to-be-learned stimulus sets were displayed simultaneously (that is, each of the 3 objects in any one trial originated from the same stimulus set; figure 4-2). The objects were positioned randomly in one of three on-screen locations and within the 6 second presentation window, their corresponding pseudowords were aurally presented, one after another, in a random order. There was no indication of which object went with which word. Both pre-learned and to-be-learned trials occurred in a random, intermixed order and trials were constructed so that no stimulus was presented on consecutive trials as to limit the use of working memory (e.g. Kachergis, Yu, & Shiffrin, 2012b). Given that previous studies have successfully trained up to 18 word-objects pairs via xSL (e.g. Yu & Smith, 2007), we do not expect that the addition of pre-learned trials had a significant effect on performance. Within study blocks, each pair from the pre-learned and to-be-learned sets was repeated 3 times meaning that there were 18 trials per study block.

Each test block consisted of 18 trials, one for each of the pre-learned and to-be-learned pairs. Individual test trials occurred in a similar way to the aforementioned 9-AFC tests performed during pre-scanner training; on trials testing a to-be-learned association, a 3x3 grid of all the to-be-learned objects was displayed. After being aurally cued with a single to-be-learned pseudoword, a randomly positioned red cursor appeared around an object in the grid (as in figure 4-2B). 1100 ms post-pseudoword onset, participants could move the cursor around the grid and select the cued object with an MRI compatible button box. Pre-learned test trials ran identically with the exception that the 3x3 grid was composed of pre-learned objects. All test trials occurred in a random order and were spaced with a variable (uniformly distributed) inter-trial interval of between 2 and 4 seconds. Study and test blocks were separated from one another with an inter-block interval of 6 seconds.

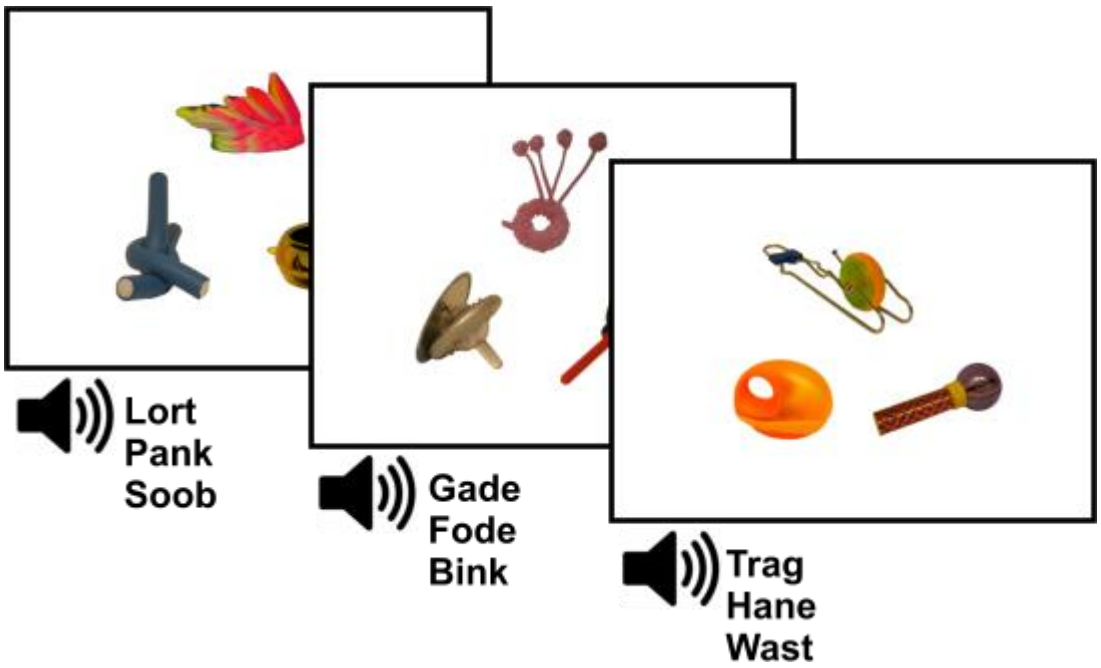

Figure 4-2. *Illustration of xSL procedure.*

4.3.4 MRI Acquisition

All images were acquired in a 1.5 Tesla Siemens Avanto scanner equipped with a 32-channel phased array head coil. First, while the main task was under-way, gradient-echo T2*-weighted scans were acquired using echo-planar imaging (EPI) recording 34 contiguous axial slices (approximately 30° to AC-PC line; ascending interleaved) and the following parameters; repetition time (TR) = 2520 ms, echo time (TE) = 43 ms, flip angle (FA) = 90°, slice thickness = 3.6 mm, in-plane resolution = 3 x 3 mm, acquisition matrix = 64 x 64, & Field of View (FoV) = 192 x 192 mm. To allow for T1 equilibrium, the first 5 EPI volumes were acquired before the task started and then discarded. Subsequently, a field map was captured to allow the correction of geometric distortions caused by field inhomogeneity (see the Image Preprocessing section below). Finally, for purposes of co-registration and image normalisation, a standard whole-brain T1-weighted structural scan was captured with a $1mm^3$ resolution using a magnetization-prepared rapid gradient echo (MP-RAGE) pulse sequence.

4.3.5 Image Preprocessing

All image preprocessing and statistical analyses were performed in SPM8 (www.fil.ion.ucl.ac.uk/spm). First, each subject's EPI volumes were corrected for inter-slice acquisition delay. Images were then spatially realigned to the first image in the time series while simultaneously correcting for inhomogeneity-based geometric distortions (as well as the interaction between motion and such distortions) using the Realign and Unwarp algorithms in SPM (Anderson et al. 2001; Hutton et al. 2002). Following this, the EPI volumes were coregistered to the relevant structural scan which was then used to calculate a set of native-space to MNI-space transformation parameters. These parameters were subsequently applied to the functional images in order to normalise them to MNI-space using the DARTEL toolbox (Ashburner, 2007). Finally, the resultant EPI volumes were spatially smoothed with an isotropic 8 mm full-width at half-maximum Gaussian kernel prior to statistical analysis. In order to visualise statistical data, the structural scans were themselves normalised with the DARTEL toolbox and a mean T1 image was computed to serve as an anatomical underlay for group level statistics.

4.3.6 Data Analysis

4.3.6.1 Behavioural data

The primary behavioural outputs from the in-scanner task were binary correct vs incorrect statistics relating to accuracy on each of the 9-AFC test trials. Correct responses were coded as 1's and incorrect responses were coded as 0's. To inform the imaging analyses, we wished to compute a subject-specific block-wise measure of word-object matching accuracy for both pre-learned and to-be-learned associations individually. To do this, the binary performance statistics relating to each

trial type were independently averaged within blocks thereby generating proportion correct values. This values were taken as a block-wise trajectory of performance (hereafter referred to as pre-learned and to-be-learned “Pc” values). In addition to this measure, we wished to quantify the degree of subject-specific learning (i.e. an individual's change in performance) that was occurring within study blocks. As such, the first order derivatives (i.e. the rates of change) for pre-learned and to-be-learned Pc values were computed (hereafter referred to as “ΔPc” values), and taken as an index of the amount learnt within each study block.

4.3.6.2 Analysis of univariate BOLD activations

Following image preprocessing, a primary first-level general linear model (GLM) of the fMRI data was produced for each subject. Movement parameters derived from the image realignment procedure were included in each as nuisance regressors and a white matter signal indexing the normalised mean white matter intensity per volume was used to account for nuisance fluctuations such as scanner drift and aliased biorhythms. In total, the model included 15 event-related regressors of interest. Twelve of these specified study trial events as 6 second boxcar functions grouped according to trial type (pre-learned vs to-be-learned) and block (i.e. blocks 1 - 6). The remaining 3 regressors related to test trials which modelled 1) correctly answered to-be-learned tests, 2) incorrectly answered to-be-learned tests, and 3) correctly answered pre-learned test trials as separate event types. Where applicable, incorrectly answered pre-learned tests were also modelled yet, as few subjects made pre-learned errors (see behavioural results below), estimates of this regressor were not analysed in any way. All test events were specified as boxcar functions with an onset corresponding to that of the aurally presented cue and a length of 1100 ms (that is, the time between the cue and when the object selection cursor became visible). An additional regressor of no interest modelled periods of key pressing that followed each test trial. As there were many key presses per trial, these periods were specified as a single boxcar function for each test trial with its onset at the first key press and it’s offset as the final key press of the trial (roughly equivalent to modelling each key press with a unique delta function). All event-related regressors were convolved with SPM's canonical hemodynamic response function (HRF) before HRF amplitude estimates (β values), and temporal and dispersion derivatives, were calculated for each on a voxel-wise basis.

To examine group-wide BOLD differences in study trials a function of trial type, block and their interaction, a 2x6 (trial type x block) ANOVA model of the HRF amplitude estimates was specified at second-level. Along with the 12 (2x6) categorical predictors denoting trial type & block number, four continuous predictors were included in the model. These independently specified the correlation between HRF estimates and; 1) to-be-learned Pc values for to-be-learned trials, 2) to-be-learned Pc values for pre-learned trials, 3) to-be-learned ΔPc values for to-be-learned trials,

and 4) to-be-learned ΔPc values for pre-learned trials. Note, pre-learned Pc and ΔPc values were not included owing to no significant non-zero variance across these vectors. This model thereby allows the examination of BOLD correlations with to-be-learned Pc and ΔPc measures over and above any nonspecific BOLD effects not directly related to the to-be-learned trials (i.e. the interactions between Pc/ΔPc and trial type). Since the study had a repeated measures design, regressors coding for within-subject effects were included in the model and parameters were estimated with SPM8's nonsphericity modelling algorithms using restricted maximum likelihood estimation (Henson & Penny, 2003; Friston, Stephan, Lund, Morcom & Kiebel, 2005).

We also wished to examine group-wide BOLD difference across the three test trial events of interest; 1) correctly answered to-be-learned tests, 2) incorrectly answered to-be-learned tests, and 3) correctly answered pre-learned tests. To do this, the HRF amplitude estimates of these events were entered into a one-way repeated measure ANOVA which also included within-subject effects and was estimated using the same nonsphericity modelling algorithms mentioned above. Where fMRI activations are plotted graphically, percent signal change was calculated by scaling beta estimates with the corresponding GLM regressor heights, and normalising the resultant values with the constant term (as implemented in the MarsBaR toolbox; Brett, Anton, Valabregue & Poline, 2002).

4.3.6.3 Psychophysiological Interactions

Finally, we specified two PPI models to test our hypotheses that, during study events, the hippocampus and BA22 would show differential patterns of functional connectivity depending on trial type, word-object match accuracy (i.e. Pc) and the amount of learning taking place (i.e. ΔPc). Each seed region was defined with bilateral, anatomical masks in MNI-space as provided by the AAL Atlas for the hippocampus (Tzourio-Mazoyer et al., 2002) and the WFU Pick Atlas for BA22 (Maldjian, Laurienti, Kraft & Burdette, 2003). Then, the two first-level PPI models (one for each seed region) were produced using the Generalized PPI Toolbox (McLaren, Ries, Xu & Johnson, 2012). Both of these models included all the same event-related and nuisance regressors as specified in the primary first-level GLM described above. However, the PPI models included an additional 13 regressors; one coding the overall BOLD time course of the seed region, and the remaining 12 representing the interaction between this time course and each study event regressor of interest (i.e. all 2x6 study events). The BOLD time course of each seed was extracted as the first eigenvariate resulting from a principal component analysis (PCA) on voxels contained within the seed's mask. This time course was then deconvolved with the HRF, multiplied by each event-related regressor and then re-convolved with the HRF to compute the PPI interaction terms.

To examine psychophysiological interactions at the group level, we specified second-level models similar to that used in analysis of study-related BOLD activations (described above). For each seed region separately, estimates of the PPI interaction terms relating to the 12 study event regressors were entered into 2x6 (trial type x block) ANOVA model. As before, along with the 12 (2x6) categorical predictors denoting trial type & block number, four continuous predictors were included in the model. These independently specified the correlation between the PPI interaction terms and; 1) to-be-learned Pc values for to-be-learned trials, 2) to-be-learned Pc values for pre-learned trials, 3) to-be-learned ΔPc values for to-be-learned trials, and 4) to-be-learned ΔPc values for pre-learned trials. Again, the model included within-subject effects was estimated with SPM8's nonsphericity modelling algorithms using restricted maximum likelihood estimation.

4.3.6.4 Bayesian methods

Where statistical tests are non-significant and the absence of an effect is of theoretical interest, we report the results of follow-up a Bayesian analysis as described by Masson (2011). This tests the relative strength of evidence in favour of the null hypothesis (H_0) compared to the alternative hypothesis (H_1) by computing a Bayesian information criterion (BIC). The BIC statistic is calculated by contrasting the total variance in the data against the variance accounted for by the effect of interest. In comparison to other Bayesian methods (e.g. Dienes, 2011), this has the advantage that a prior expectation regarding the size of the effect need not be specified. Both H_0 and H_1 are assumed to be equally likely a priori.

4.3.6.5 Imaging thresholds

Across all imaging analyses, reported activations survive whole-brain, family wise error (FWE) corrected thresholds at either the peak- or cluster-level (cluster defining threshold: $p < .001$). Additionally, given our strong a priori hypotheses that effects of interest may be observed in the hippocampus, we report activations surviving a small volume correction for voxels falling within a bilateral hippocampal mask taken from the AAL Atlas (Tzourio-Mazoyer et al., 2002).

4.4 Results

4.4.1 Behavioural performance

Regarding the stimulus familiarisation and pre-learning phases administered prior to scanning, all participants correctly recognised each of the to-be-learned stimuli and all but one performed at ceiling on the 9-AFC tests of pre-learned associations. The participant who did not achieve perfect performance only made two errors across the nine pre-learned test trials and reached ceiling for these associations by the second block of the in-scanner task.

Figures 4-3A and 4-3B display mean Pc and ΔPc statistics (respectively) for both pre-learned and to-be-learned word-object pairs as tested across the 6 in-scanner block. All participants showed a high degree of learning on the to-be-learned associations as performance increased from a little over chance in test block 1, to ceiling in test block 5. In contrast, performance on the pre-learned associations varied very little across blocks with only seven of the nineteen participants failing to show perfect performance across all the test blocks. A 2x6 (trial type x block) repeated measures ANOVA on the Pc statistics revealed significant main effects of trial type, $F(1,90)$ = 44.785, $p < .001$, and block $F(5,90)$ = 59.924, $p < .001$ which were superseded by the interaction between these two factors, $F(5,90)$ = 59.712, $p < .001$. Importantly, a one-way ANOVA contrasting between block performance statistics for the pre-learned associations alone showed that Pc scores did not vary significantly across blocks, $F(5,90)$ = 1.487, p = .202. Additionally, a Bayesian analysis highlighted substantially greater evidence in favour of the null hypothesis for a between-block difference in pre-learned performance, $p(H_0|Data)$ = .999.

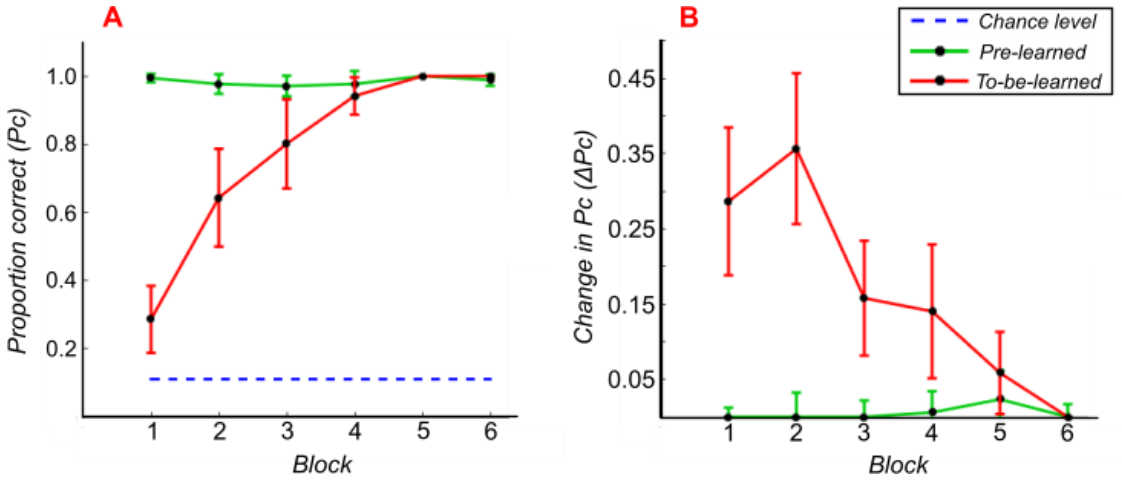

Figure 4-3. *For the in-scanner task, block-wise measures of performance (proportion correct: A), and learning (change in proportion correct: B) broken down 'trial type'. Error bars indicate 95% confidence intervals corrected for the within subject-error term.*

4.4.2 Study trials: Univariate BOLD activations

4.4.2.1 Main effect of trial type

The 2x6 ANOVA model on the study trial imaging data revealed a wide range of brain regions exhibiting a main effect trial type (see table 4-1). Most of these regions, showed greater activity when processing to-be-learned trials relative to pre-learned trials and so may be involved in the acquisition of new word-object associations. However, a network of nine regions displayed the opposite pattern; BOLD increases on pre-learned relative to the to-be-learned trials. These activations may be indicative of selective involvement in processing associations acquired via explicit encoding. Alternatively, because the pre-learned associations were likely to have a greater overall trace-memory strength than the to-be-learned associations, such effects could reflect the overall strength of word-object associations. To discriminate between these possibilities, we ran a follow up analysis examining whether each of these regions displayed between block differences in BOLD activity for the to-be-learned trials alone; i.e. a one-way repeated measures ANOVA with 6 levels. If a region exhibited significant BOLD modulations across to-be-learned study blocks (i.e. as trace-memory strength increased), the activation likely reflects the overall strength of word-object associations. In contrast, if there is more evidence in favour of no block-wise BOLD modulation (as revealed by the Bayesian information criterion), the data better support the interpretation that the region is selectively involved in processing explicitly encoded stimuli.

Table 4-1. *Regions showing a main effect of 'trial type' on study trials. Asterisks denote significance at p(peak-FWE) < .05. Daggers denote significance at p(cluster-FWE) < .05. Superscript characters indicate activations in the same cluster.*

Region label	Peak F	k	x	y	z
To-be-learned > Pre-learned					
Left Intraparietal Sulcus (hIP1, hIP3)	267.56 *	7822 † A	-30	-57	45
Right Intraparietal Sulcus (hIP1, hIP3)	203.96 *	A	36	-54	48
Left Fusiform Gyrus (FG2)	126.91 *	A	-42	-72	-9
Left & Right Precuneus (BA7)	109.68 *	A	6	-69	45
Left & Right Occipital Cortex (BA17, BA18)	75.71 *	A	-27	-90	6
Left Middle Temporal (BA21)	68.97 *	A	-63	-30	3
Right Middle Temporal (BA21)	45.07 *	A	60	-36	-9
Right Fusiform Gyrus (FG2)	44.66 *	A	33	-48	-18
Left Precentral Gyrus (BA8)	211.29 *	3473 † B	-42	6	36
Left Inferior Frontal Gyrus (p. Triangularis, BA45)	184.57 *	B	-45	27	27
Right Inferior Frontal Gyrus (p. Orbitalis, BA47)	127.99 *	B	33	24	0
Left Middle Frontal Gyrus (BA6)	98.42 *	B	-33	3	60
Left Anterior Prefrontal Cortex (Fp1, BA10)	67.58 *	B	-33	57	12
Left Inferior Frontal Gyrus (p. Orbitalis, BA47)	65.75 *	B	-30	24	0
Left Caudate	38.97 *	B	-15	9	9
Right Caudate	42.41 *	B	12	6	9
Left & Right Superior Medial Gyrus (BA8)	161.27 *	662 †	-3	21	48
Right Inferior Frontal Gyrus (p. Triangularis, BA45)	147.25 *	1800 † C	48	30	30
Right Middle Frontal Gyrus (BA6)	82.75 *	C	36	9	57
Right Inferior Frontal Gyrus (p. Opercularis, BA44)	64.82 *	C	39	9	30
Right Anterior Prefrontal Cortex (Fp1, BA10)	59.81 *	C	27	57	0
Pre-learned > To-be-learned					
Left Retrosplenial Cortex (BA29, BA30, BA23)	67.85 *	332 †	-9	-51	33
Left & Right Ventromedial Prefrontal Cortex (Fp2)	56.02 *	1307 †	-6	54	-3
Left & Right Posterior Cingulate Cortex (BA31)	49.65 *	425 †	-12	-30	42
Right Supramarginal Gyrus (PF, PFop, OP1, PFt)	39.62 *	318 †	57	-27	36
Left Supramarginal Gyrus (Pfop, OP1, PF)	34.31 *	87 †	-60	-33	27
Left Hippocampus & Parahippocampal Gyrus	32.05 *	47 †	-33	-45	-3
Right Lingual Gyrus (BA18)	29.16 *	77 †	12	-51	6
Right Rolandic Operculum	27.3 *	121 †	51	3	9

Of the nine regions showing greater activity on pre-learned trials, all but the ventromedial prefrontal cortex (vmPFC) and the left hippocampal region showed significant BOLD modulations across the 6 blocks of to-be-learned study trials; all *F*'s > 4.00, all *p*'s < .003. Additionally, between block changes in BOLD activity within the vmPFC were approaching significance; $F(5,90) = 2.253$, $p = .063$. These effects may therefore reflect the suppression of task irrelevant activity when rates of learning were at their highest (see Fox et al., 2005). Similarly, greater activity on pre-learned trials in the hippocampus may be indicative of greater default-mode deactivation during periods of learning. However, this appears less likely given the observation that the hippocampal cluster produced substantially more evidence in favour of the null hypothesis for a between-block difference in to-be-learned BOLD estimates; $F(5,90) = 0.4001$, $p = .8419$, $p(H_0|Data) > .999$ (see figure 4-4). This indicates that the left hippocampal cluster exhibited greater BOLD activity to pre-learned study events that was unmodulated during periods of xSL. It is possible, therefore, that the region is involved in processing explicitly encoded associations alone.

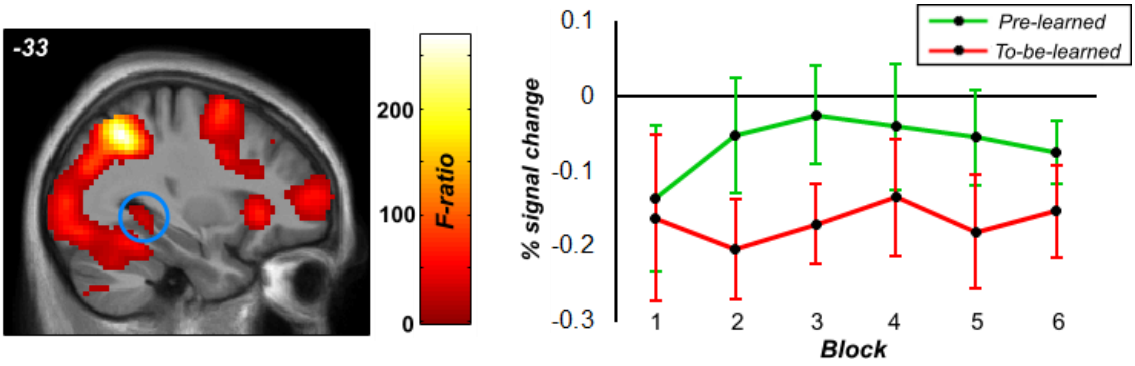

Figure 4-4. *Left hippocampal cluster exhibiting a main effect of 'trial type' on study trials. Error bars indicate 95% confidence intervals corrected for the within subject-error term.*

4.4.2.2 Main effect of block and correlations with to-be-learned "Pc"

No regions showed a significant main effect of block. Additionally, we tested for where to-be-learned Pc positively correlated with BOLD activity on to-be-learned study trials over and above the same correlation for pre-learned study trials; that is the one-sided interaction between Pc and trial type. This contrast also did not reveal any significant effects.

4.4.2.3 Trial type x block interaction and correlations with to-be-learned "ΔPc"

The interaction between trial type and block was significant in number of brain regions including; the inferior frontal gyrus (IFG) and the intraparietal sulcus (IPS) bilaterally (see table 4-2, and figure

4-5). On inspection of the parameter estimates from each of these regions, it is clear that all these effects reflect selective increases in to-be-learned BOLD activity during blocks where xSL was greatest (c.f. figure 4-3B). As such, these regions do appear to be involved in xSL. However, in order to test this more formally, we then looked for where to-be-learned ΔPc positively correlated with BOLD activity on to-be-learned study trials over and above the same correlation for pre-learned study trials; that is the one-sided interaction between ΔPc and trial type. This revealed a group of 9 regions demonstrating significant effects (see table 4-3, and figure 4-6); IFG bilaterally, IPS bilaterally, caudate bilaterally, left MFG, superior medial gyrus (SMG) bilaterally, and the left fusiform gyrus. It is notable that, with the exception of the left and right caudate, all of these regions were also highlighted by the "trial type x block" interaction test; mean peak voxel displacement: 8.91 mm. Instead, the left and right caudate nuclei were highlighted by the main effect of trial type; mean peak voxel displacement: 10.81 mm.

Table 4-2. *Regions showing a 'trial type' by 'block' interaction on study trials. Asterisks denote significance at p(peak-FWE) < .05. Daggers denote significance at p(cluster-FWE) < .05. Superscript characters indicate activations in the same cluster.*

Region label	Peak F	k	x	y	z
Left Inferior Frontal Gyrus (p. Triangularis, BA45)	14.48 *	705 † [A]	-42	24	30
Left Middle Frontal Gyrus (BA6)	9.59 *	[A]	-30	3	66
Left Precentral Gyrus (BA6)	9.24 *	[A]	-36	-3	54
Left Intraparietal Sulcus (hIP1, hIP3)	13.18 *	1322 † [B]	-30	-60	48
Left & Right Precuneus (BA7)	9.96 *	[B]	0	-66	48
Right Intraparietal Sulcus (hIP1, hIP3, hIP2)	8.69 *	[B]	39	-54	48
Left Fusiform Gyrus (FG2)	9.02 *	109 †	-42	-69	-12
Right Inferior Frontal Gyrus (p. Triangularis, BA45)	8.4 *	46 †	45	33	30
Left Anterior Prefrontal Cortex (Fp1, BA10)	8.21 *	158 †	-33	51	6
Left & Right Superior Medial Gyrus (BA8)	7.25	122 †	-3	15	48
Right Fusiform Gyrus (BA37)	7.00	150 †	33	-42	-21
Right Middle Frontal Gyrus (BA8)	6.32	73 †	33	12	48

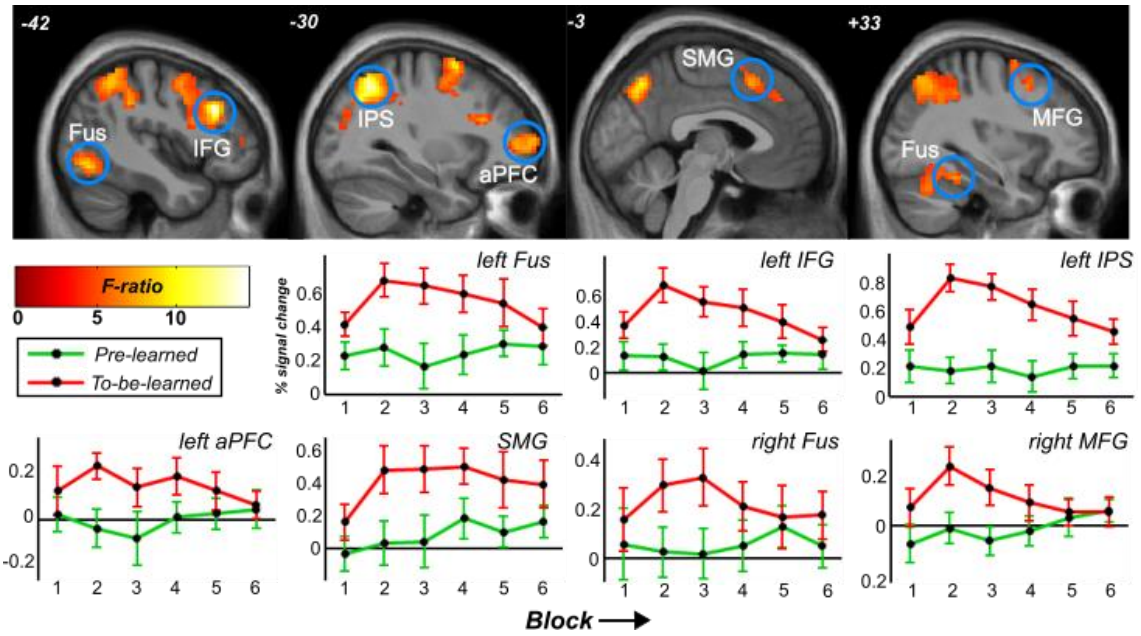

Figure 4-5. *Top: Clusters exhibiting a 'block' by 'trial type' on study trials. Bottom: % signal change estimates for these effects. Error bars indicate 95% confidence intervals. Abbreviations: Fus = fusiform gyrus, IFG = inferior frontal gyrus, IPS = intraparietal sulcus, aPFC = anterior prefrontal cortex, SMG = superior medial gyrus, MFG = middle frontal gyrus. Error bars indicate 95% confidence intervals corrected for the within subject-error term.*

Table 4-3. *Regions showing a one-sided interaction between 'ΔPc' and 'trial type'. Asterisks denote significance at p(peak-FWE) < .05. Daggers denote significance at p(cluster-FWE) < .05. Superscript characters indicate activations in the same cluster.*

Region label	T statistic	k	x	y	z
Left Inferior Frontal Gyrus (p. Triangularis, BA45)	6.23 *	363 †	-45	24	27
Right Intraparietal Sulcus (hIP1, hIP3)	5.72 *	261 †	24	-63	48
Left Intraparietal Sulcus (hIP1, hIP3)	5.15 *	429 †	-30	-51	42
Left Caudate Nucleus	5.05 *	122 †	-9	15	3
Left Middle Frontal Gyrus (BA6)	4.86 *	403 † [A]	-27	6	63
Left & Right Superior Medial Gyrus (BA8)	4.58	[A]	-6	12	63
Right Inferior Frontal Gyrus (BA45)	4.56	64 †	45	33	27
Left Fusiform Gyrus (FG2)	4.48	174 †	-51	-60	-12
Right Caudate Nucleus	4.43	93 †	9	12	0

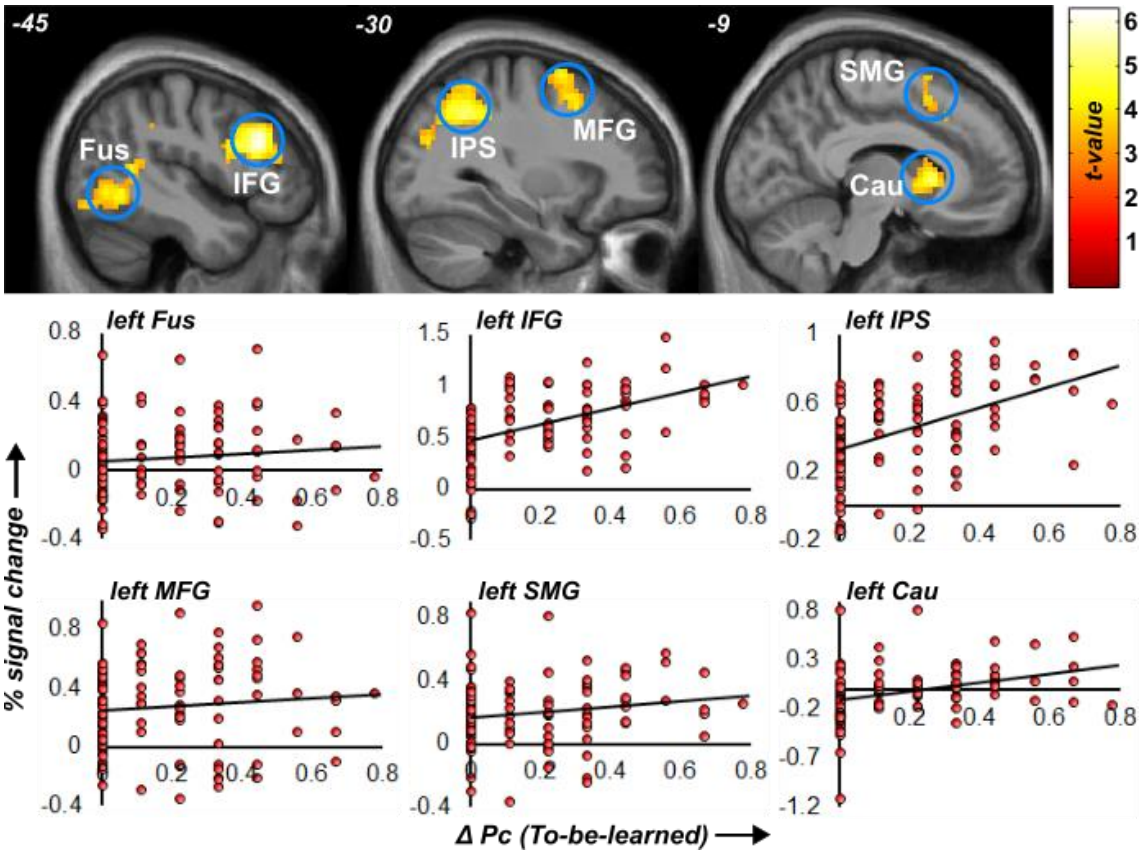

Figure 4-6. *Top: Clusters exhibiting a one-sided interaction between 'ΔPc' and 'trial type'. Bottom: Plots displaying % signal change estimates on to-be-learned study trials against ΔPc statistics. Abbreviations: Fus = fusiform gyrus, IFG = inferior frontal gyrus, IPS = intraparietal sulcus, MFG = middle frontal gyrus, SMG = superior medial gyrus, Cau = caudate.*

4.4.3 Test trials: Univariate BOLD activations

The one-way ANOVA model contrasting to-be-learned test trials (correct vs incorrect) along with correctly-answered pre-learned tests revealed a set of brain regions showing some form of BOLD difference across the 3 event types (see table 4-4). All these effects were then classified by their activation pattern based on planned follow-up contrasts; 1) "correct > incorrect" (collapsed across trial types), 2) "to-be-learned > pre-learned" (regardless of accuracy), and 3) "pre-learned > to-be-learned" (regardless of accuracy).

4.4.3.1 Correct > incorrect

Six regions showed greater activity to on correct relative to incorrect test trials. Of these, a conjunction analysis revealed that the left hippocampal cluster partially overlapped with the hippocampal/parahippocampal region showing a “pre-learned > to-be-learned” study trial effect (discussed above, peak voxel displacement: 15.588 mm). On the test trials, this region showed significantly greater BOLD signals on both types of correctly answered tests (to-be-learned and pre-learned) relative to incorrectly answered tests; minimum $t(18)$ = 5.452, maximum $p < .001$. There was no significant difference between to-be-learned (correct) and pre-learned (correct) trials with substantial evidence in favour of the null hypothesis for this effect; $t(18)$ = 0.758, p = .458, $p(H_0|Data)$ = .764. Of the remaining activations highlighted by the test trial analysis, all but the right inferior temporal gyrus (ITG) showed significant BOLD differences between all 3 test events such that; “pre-learned (correct) > to-be-learned (correct) > to-be-learned (incorrect)”, minimum $t(18)$ = 2.155, maximum p = .045. Effects such as these may reflect the activation strength of a word-object trace since the memory associations for pre-learned pairs were most likely stronger than those of to-be-learned pairs (owing to the greater number of learning instances). While the right ITG also demonstrated BOLD effects following this same pattern, the difference between pre-learned and correctly-answered to-be-learned trials was not significant; $t(18)$ = 1.573, p = .133. Despite this, a Bayesian analysis proved insensitive when comparing the strength of evidence in favour of the null vs the alternative hypothesis; $p(H_0|Data)$ = .564.

4.4.3.2 To-be-learned > pre-learned

Nine regions showed greater activity to on to-be-learned relative to pre-learned test trials. Of these, a conjunction analysis revealed that clusters, all occurring bilaterally, in the inferior parietal lobule (IPL), IFG, SMG and anterior prefrontal cortex (aPFC), overlapped with previously reported effects implicating their involvement in xSL during periods of study (c.f. tables 4-1, 4-2 and 4-3). With the exception of the right MFG, each cluster displayed significantly greater BOLD responses on both correct and incorrect to-be-learned test trials relative to pre-learned test trials (minimum $t(18)$ = 4.397, maximum $p < .001$). Additionally, again with the exception of the right MFG, BOLD responses in each cluster did not significantly differ between correct vs incorrect to-be-learned tests (maximum $t(18)$ = 1.723, maximum p = .102). Moreover, a Bayesian analysis revealed substantially greater evidence in favour of the null hypothesis for this difference in the left IPL, right IPL, and left aPFC; $p(H0|Data)$ = .783, .791, .813 for each region respectively. In contrast, the right MFG activation showed a significant “incorrect > correct” BOLD difference for both to-be-learned [$t(18)$ = 3.731, p = .002] and pre-learned [$t(18)$ = 8.106, $p < .001$] test trials. There was no significant difference between correct to-be-learned and pre-learned test trials; $t(18)$ = 1.449, p = .165, $p(H_0|Data)$ = .604.

4.4.3.3 Pre-learned > to-be-learned

Only the left vmPFC exhibited increased BOLD activity on pre-learned test trials relative to to-be-learned test trials. Importantly, this region showed no significant BOLD difference between correct vs incorrect to-be-learned test trials; $t(18)$ = 0.634, p = .534, and a Bayesian analysis revealed substantially more evidence in favour of the null for this effect; $p(H_0|Data)$ = .779 (see figure 4-7). Furthermore, in the previously reported analysis of study trial BOLD activations, this region demonstrated a main effect of trial type producing greater BOLD estimates on pre-learned study trials relative to to-be-learned study trials, peak voxel displacement: 8.49 mm.

Table 4-4. *Regions identified in the analysis of test trial. Asterisks denote significance at p(peak-FWE) < .05. Daggers denote significance at p(cluster-FWE) < .05. Superscript characters indicate activations in the same cluster.*

Region label	Peak F	k	x	y	z
Correct > Incorrect					
Left Inferior Parietal Lobule (PFt, PF,PFcm)	39.23 *	4357 † [A]	-57	-39	27
Left & Right Middle Cingulate Cortex (BA24)	28.09 *	[A]	6	-6	48
Right Inferior Parietal Lobule (Pft, PF,PFcm)	25.49 *	[A]	60	-30	33
Right Inferior Temporal Gyrus (BA20)	26.39 *	21 †	45	12	-42
Left Hippocampus (Subiculum)	22.28 *	19 †	-24	-36	-12
Left Putamen	17.66	120 †	-27	9	9
To-be-leaned > Pre-learned					
Left Inferior Parietal Lobule (hIP1)	26.93 *	[A]	-36	-57	45
Right Inferior Parietal Lobule (hIP1)	31.05 *	168 †	42	-54	48
Left & Right Precuneus (BA7)	26.24 *	295 †	9	-69	42
Left Inferior Frontal Gyrus (p. Triangularis, BA45)	23.64 *	212 †	-45	15	36
Left & Right Superior Medial Gyrus (BA8)	23.55 *	153 †	0	33	42
Right Inferior/Middle Frontal Gyrus (BA9)	21.43 *	80 †	45	30	33
Left Anterior Prefrontal Cortex (Fp1, BA10)	18.75	196 †	-33	54	3
Right Middle Frontal Gyrus (BA8)	18.7	144 †	39	21	57
Right Anterior Prefrontal Cortex (Fp1, BA10)	18.64	56 †	27	63	-3
Pre-learned > To-be-leaned					
Left Ventromedial Prefrontal Cortex (Fp2)	15.79	152 †	-6	57	3

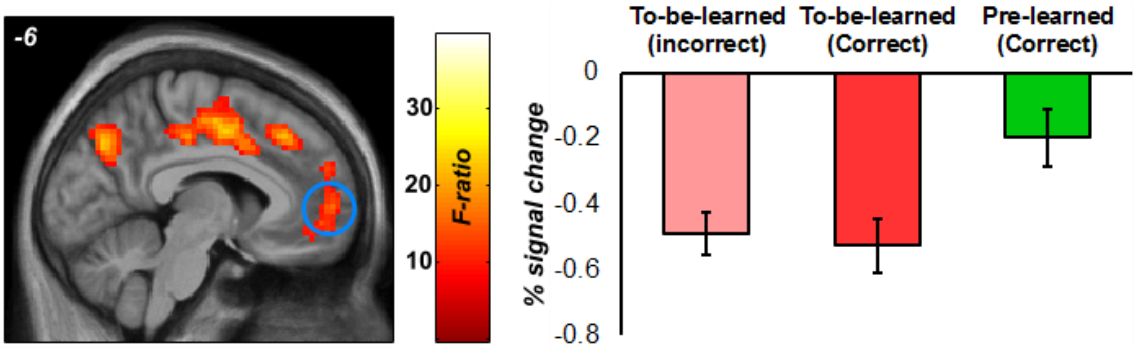

Figure 4-7. *The vmPFC exhibiting a main effect of 'pre-learned > to-be-learned' on test trials. Error bars indicate 95% confidence intervals corrected for the within subject-error term.*

4.4.4 Study trials: PPI analyses

Similar to the study trial analysis reported above, the 2x6 ANOVA models on psychophysiological interaction estimates examined changes in seed-to-voxel connectivity during study trials as a function of; 1) the "main effect of trial type", 2) the "main effect of block", 3) the "trial type x block" interaction, 4) the "Pc x trial type" interaction, and 5) the "ΔPc x trial type" interaction. For both seed regions, neither Pc or ΔPc interactions with trial type yielded significant effects. However, for completeness, we further tested the simple correlations between Pc/ΔPc statistics and connectivity estimates on to-be-learned trials alone. These did produce significant effects and so are reported below along with results for each of the other model terms.

4.4.4.1 Hippocampal seed

For the hippocampal PPI, a main effect of trial type was detected in the right middle occipital gyrus such that connectivity between this region and the seed was greater overall on pre-learned relative to to-be-learned study trials (see figure 4-8); $F(1,212)$ = 18.72, $p(cluster\text{-}FWE)$ = .010, k = 78, *MNI* = [+30, -96 +06]. While this effect may be indicative of increased levels of hippocampal connectivity on the pre-learned trials per se, it may instead reflect higher levels hippocampal connectivity when processing associations with a greater overall trace-memory strength (which pre-learned pairs were likely to have). In order to discriminate between these possibilities, we ran a follow up analysis examining whether connectivity estimates differed between blocks for the to-be-learned trials alone; i.e. a one-way repeated measures ANOVA with 6 levels. This revealed no such modulation, $F(5,90)$ = 1.100, p = .365, and a Bayesian analysis revealed substantially more evidence in favour of the null hypothesis for this effect; $p(H_0|Data)$ > .999. Of all remaining model terms, no other significant effects were detected.

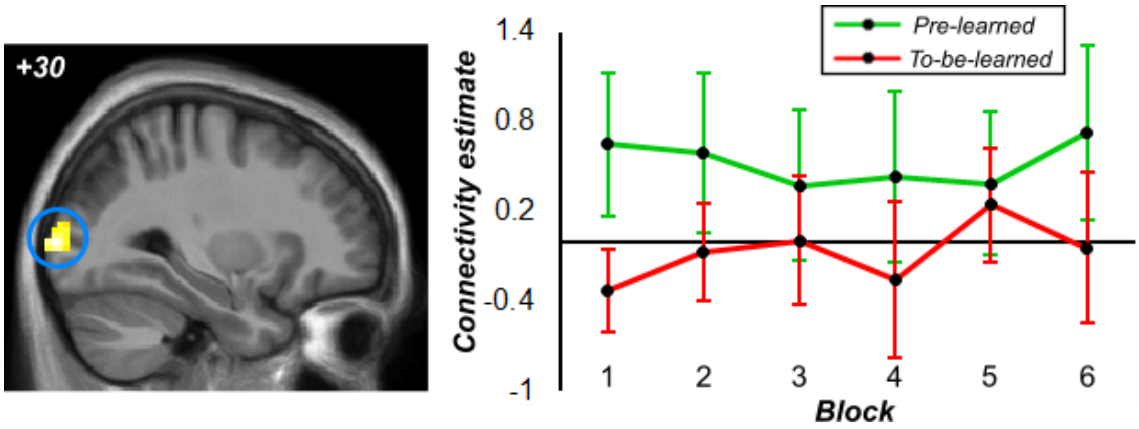

Figure 4-8. *Results of hippocampal PPI. Right middle occipital gyrus showing increased connectivity with the hippocampus on pre-learned study trials. Error bars indicate 95% confidence intervals corrected for the within subject-error term.*

4.4.4.2 BA22 seed

For the BA22 PPI, a main effect of trial type was also detected in the right middle occipital gyrus such that connectivity between this region and the seed was greater overall on pre-learned relativity to to-be-learned study trials (see figure 4-9A); *F(1,212)* = 18.78, *p(cluster-FWE)* = .004, *k* = 95, *MNI* = [+33, -90, +15]. This cluster extensively overlapped with the equivalent effect identified by the hippocampal PPI reported above (peak voxel displacement = 11.225 mm). As before, we ran a one-way ANOVA on the to-be-learned connectivity estimates to determine whether these increased levels of seed connectivity reflected an effect of the pre-learned trials per se or differences in trace-memory strength between trial types. This returned a non-significant effect, *F(5,90)* = 0.916, *p* = .468, and a Bayesian analysis revealed substantially more evidence in favour of the null hypothesis; $p(H_0|Data)$ > .999. Of all remaining model terms, only two other significant effects were detected. Both of these reflected a correlation between connectivity estimates on to-be-learned trials and to-be-learned ΔPc statistics. The left temporal pole showed a positive correlation, *t(212)* = 4.39, *p(cluster-FWE)* = .015, *k* = 71, *MNI* = [-39, +06, -24], while a cluster in the left hippocampus showed a negative correlation, *t(212)* = 3.85, *p(peak-FWE)* = .028 (corrected within the hippocampal ROI), *k* = 5, *MNI* = [-36, -21, -18], see figure 4-9B & 4-9C. The hippocampal cluster extensively overlapped with the analogous effect revealed by the hippocampal PPI reported above (peak voxel displacement = 3 mm).

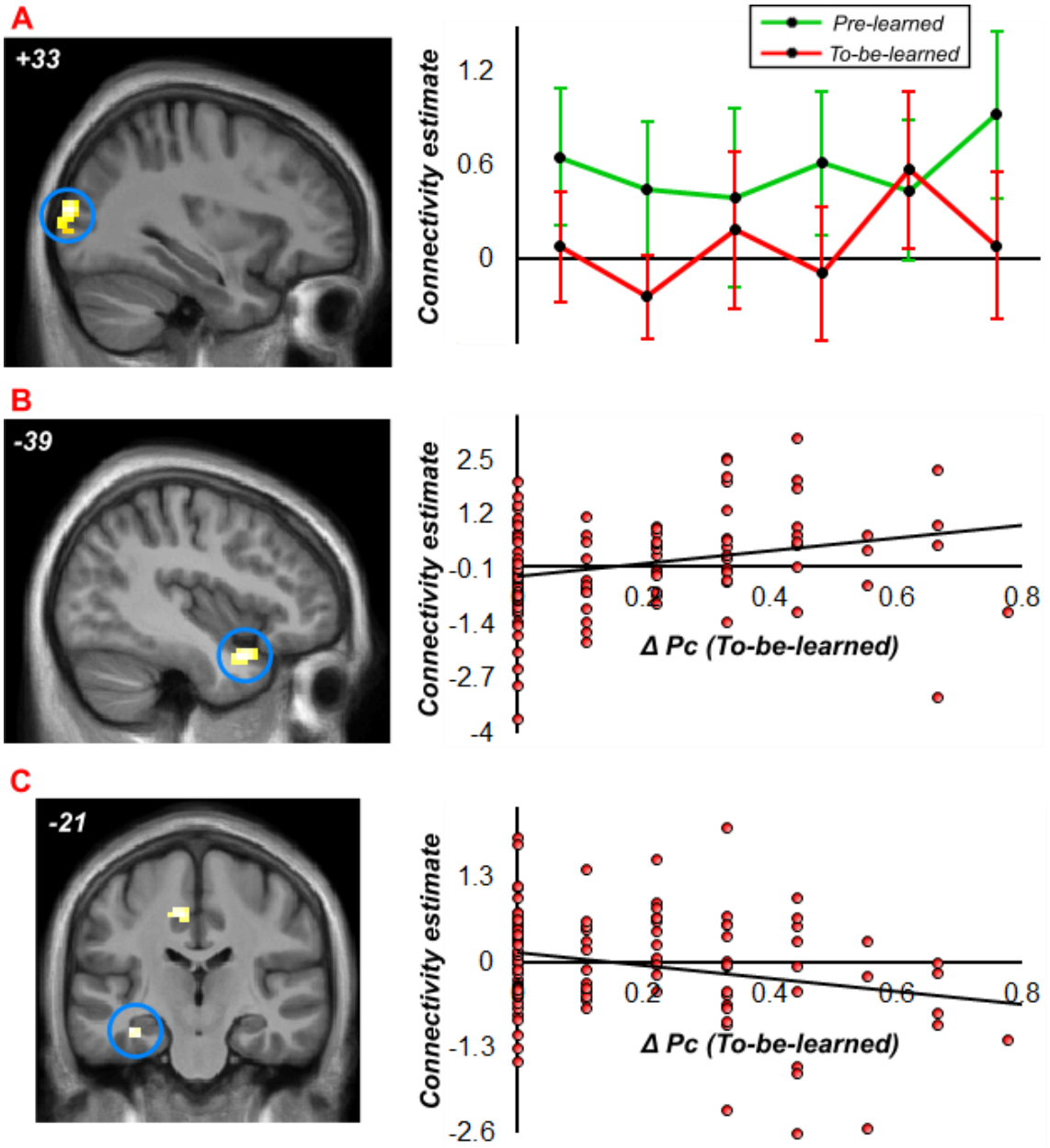

Figure 4-9. *Results of BA22 PPI.* ***A:*** *Right middle occipital gyrus showing increased connectivity with BA22 on pre-learned study trials.* ***B:*** *Left temporal pole cluster showing increased connectivity with the hippocampus as a function of ΔPc.* ***C:*** *Left hippocampal cluster showing reduced connectivity with BA22 as a function of ΔPc. Error bars indicate 95% confidence intervals corrected for the within subject-error term.*

4.5 Discussion

We investigated the brain regions involved in xSL which requires the abstraction of statistical regularities across a series of ambiguous events. During periods of acquisition, increases in activity were observed within the IFG, IPS, caudate, SMG (all bilaterally), and the left MFG. Each of these activations scaled proportionally with amount of information encoding actually taking place. Furthermore, a subset of these areas also exhibited increased activation when accessing xSL associations at test. In contrast, the hippocampal formation only showed greater study-related activity when processing associations that had been previously learned via EE; that is, where word-object mappings were explicitly given rather than having to be inferred. Notably however, the correct retrieval of both xSL- and EE-trained associations elicited equally high levels of hippocampal activity.

Models of memory consolidation predict that the hippocampal system is involved in rapidly learning all novel associations, including via xSL. This is inconsistent with our finding that the left hippocampus showed greater study-related activity on pre-learned trials yet no effects related to the acquisition of xSL-trained associations. Furthermore, our results leave open the possibility that xSL is facilitated by neocortical learning mechanisms alone. Consistent with this, acquisition via xSL was associated with decreases in functional connectivity between BA22 (implicated in speech processing) and the hippocampus, yet increases in connectivity between BA22 and the left temporal pole. This latter finding is significant since the temporal poles are known to be a key part of the semantic system (Binder, Desai, Graves & Conant, 2009) and contribute to the long-term storage of category-specific semantic knowledge (Warrington, 1975; Warrington & Shallice, 1984; Lambon Ralph, Lowe & Rogers, 2007; Noppeney et al., 2007). In contrast, the right occipital cortex demonstrated increased functional connectivity with both the hippocampus and BA22 when processing pre-learned associations. This mirrors similar findings suggesting that increased connectivity in these regions (and a range of other cortical areas) is a signature of episodic recollection (King, de Chastelaine, Elward, Wang & Rugg, 2015).

The observation that the hippocampus was equally activated in response to retrieving both pre-learned and to-be-learned associations may suggest that it was involved in the storage of each. This is a possibility that we cannot rule out. Nonetheless, it is noteworthy that correctly retrieving any word-object association at test is very similar to an EE-encoding instance for the tested pair. As such, the test-related increases in hippocampal activity may be indicative of hippocampal (re-) encoding processes rather than the activation of a pre-established memory trace. This principle of hippocampal re-encoding is a central tenant of multiple trace theory (MTT) which states that each time an episodic memory is activated, a new trace of that memory is added to the hippocampal ensemble (Nadel & Moscovitch, 1997).

As noted, we suggest that xSL is a direct route to neocortical semantic learning that is independent of the hippocampus, perhaps because of the way in which information is gradually acquired from a series of ambiguous events. In particular, xSL involves repeated presentations of multiple to-be-learned associations that are interleaved with one another; precisely the conditions in which the neocortical system is thought to encode information (McClelland et al., 1995). As to why the hippocampus shows a lack of involvement in xSL altogether, it is notable that a high degree of referential ambiguity is key feature of this learning method. Each individual study event conveys a relatively small amount of referential information which may not be amenable to encoding by the hippocampal system. Instead, it is possible that the hippocampus can only encode associations when relational mappings are explicitly known and unambiguous from the outset (as is in the case for EE). In line with this, xSL share features common to other types of hippocampally independent learning, e.g. non-declarative skill acquisition (Cohen & Squire, 1980). During such learning, associations between visual inputs, motor commands, lexical representations, etc. are gradually accumulated and refined by feedback-related information provided across multiple study events. Since the hippocampus is known to be involved in cross-episode binding when associations are explicitly given (e.g. Zeithamova, Schlichting & Preston, 2012; Staresina & Davachi, 2009), we hypothesise that the degree of referential ambiguity during information integration is the one feature that principally determines whether or not learning is hippocampally dependent.

Our suggestion that neocortical regions are principally responsible for xSL leads to the question of which particular brain areas are involved. As mentioned, the left temporal pole may be involved in semantic storage yet our data strongly suggest that other regions also play a role. With the exception of the caudate nucleus these regions have been implicated in the so-called “task-positive network”. Nodes within this network exhibit a high level of functional integration and are commonly activated in tasks requiring top-down attention and working memory (Fox et al., 2005; Corbetta & Schulman, 2002). Nonetheless, the potential contribution of each specific region to xSL is discussed in context of previous evidence.

4.5.1 Inferior frontal gyrus

Neuroimaging studies have implicated the IFG, particularly the left IFG (lIFG), in a wide range of language related functions. These include; phonological processing (Strand et al., 2008; Costafreda et al., 2006), syntactic operations (Tettamanti et al., 2009; Bahlmann, Schubotz & Friederici, 2008; Musso et al., 2003; Maess, Koelsch, Gunter & Friederici, 2001), and semantic processing (Obleser et al., 2007; Binder, Desai, Graves & Conant, 2009). In light of this, the lIFG has been proposed to act as a unification space integrating linguistic information across the phonological, semantic, and syntactic domains (Hagoort, 2005). Evidence for this has come from an fMRI study examining the learning of phonological to semantic mappings (Eisner, McGettigan,

Faulkner, Rosen, & Scott, 2010). Eisner et al., trained participants to understand spoken sentences distorted to match the sensory output of a cochlear implants. In a procedure not dissimilar to that of the current study, this form of perceptual learning was tracked across a series of test blocks. The lIFG showed activations at both study and test when processing to-be-learned stimuli - a finding that mirrors the effect reported here. Furthermore, BOLD increases in the region positively correlated with performance increases during learning, and participants working memory scores. Together with the results presented above, these finding suggest that lIFG supports a working memory process that acts to map between perceptual and semantic representations while learning is ongoing.

4.5.2 Intraparietal sulcus and Inferior parietal lobule

The IPS/IPL are part of the dorsal parietal cortex which has implicated in top-down attentional control (Corbetta & Shulman, 2002; Beauchamp, Petit, Ellmore, Ingeholm & Haxby, 2001; Nobre, Gitelman, Dias & Mesulan, 2000). Moreover, the attentional functions subserved here have been implicated in supporting a variety of perceptual functions including perceptual organisation, cross-modal integration and auditory stream selection (Calvert, 2001; Shafritz, Gore & Marois, 2002; Donner et al., 2002; Wardak, Olivier & Duhamel, 2002; Cusack, 2005). Given this, it is possible that the IPS/IPL activations reported here simply reflect the attentional selection of perceptual inputs in aid of learning/retrieval. Recently however, the role of the dorsal parietal cortex has been extended to cover attention to memory processes (Cabeza, Ciaramelli, Olson & Moscovitch, 2008; also see: Cabeza, 2008; Ciaramelli, Grady & Moscovitch, 2008). Specifically, this region is proposed to maintain goal-based information online in order to guide the retrieval of memory traces in a top-down manner. Based on this, IPS/IPL involvement in xSL at both study and test could be indicative of memory retrieval mechanisms.

4.5.3 Caudate

Caudate activations are commonly reported in learning tasks with probabilistic reinforcement contingencies or when such contingencies change over time (e.g. Aron et al., 2004; Poldrack, Prabhakaran, Seger & Gabrieli, 1999; Poldrack et al., 2001; Cools, Clark, Owen & Robbins, 2004; Rogers, Andrews, Grasby, Brooks & Robbins, 2000). The caudate has also been implicated in learning more generally, as long as performance can be made reliant a single error-related signal informed by feedback (Doeller, King, & Burgess, 2008). Additionally, Seger and Cincotta (2005) showed that activity in the head of the caudate (at the same site reported above) mainly reflected the receipt of positive feedback and increased when feedback was most critical to learning. In line with this, the caudate is known to receive input from dopaminergic cells in the midbrain and to form a corticostriatal loop with other regions involved in feedback-informed learning (Swanson, 1982; Fiorillo, Tobler & Schultz, 2003; Middleton & Strick, 1996; Hornak et al., 2004). While the xSL task

used here did not provide explicit feedback, it is likely that feedback related signals were generated endogenously when word-object mappings became unambiguous. As such, caudate involvement in xSL may reflect the relay of these feedback signals to the cortex.

4.5.4 Superior medial gyrus

Anatomically, the SMG lies anterior to the supplementary motor area (SMA) and so is often denoted as pre-SMA. However, much evidence has accumulated to suggest that this region is both structurally and functionally interconnected with the prefrontal cortex to a much larger extent than the SMA itself (Luppino, Matelli, Camarda & Rizzolatti, 1993; Lu, Preston & Strick, 1994; Zhang, Ide & Li, 2012). Activations in the SMG have been reported when engaging in deductive reasoning operations such as logical transformations (e.g. negation), displacing variables, and logical connectives (e.g. conjunctions; Monti, Osherson, Martinez & Parsons, 2007; Monti, Parsons, & Osherson, 2009; Rodriguez, Moreno & Hirsch, 2009). It is noteworthy that deductive reasoning has been proposed to play a central role in xSL (Medina, Snedeker, Trueswell & Gleitman, 2011; Trueswell, Medina, Hafri, & Gleitman, 2013). On one account, xSL is facilitated by the generation of a single hypothesised referent for each word and retaining it across learning trials unless the hypothesis is falsified. As such, deductive reasoning operations underpinned by the SMG may support xSL by acting to test hypothesised associations. However, while hypothesis testing may indeed play a role in xSL, it is clear that associative mechanisms involved in tracking co-occurrences more generally are also used, especially when referential ambiguity is high (Smith, Smith, & Blythe, 2011; Kachergis, Yu, & Shiffrin, 2012b).

In summary, we report evidence that xSL provides a means by which the neocortical memory system can rapidly acquire novel associative information independent of the hippocampus. Neuropsychological studies testing xSL in hippocampally amnesic patients will be required to fully support this or falsify this hypothesis, yet to date, no such studies have been carried out. Nonetheless, the results of our fMRI experiment do suggests that xSL principally relies on a network of brain regions implicated in semantic processing, attention, and reasoning.

Chapter 5

The effect of minocycline on hippocampal and non-hippocampal memory systems

5.1 Abstract

Neuronal-microglial interactions in the medial temporal lobe (MTL) are believed to regulate learning and memory processes such as LTP and neurogenesis. Minocycline (a tetracycline antibiotic) crosses the blood-brain barrier and is known to inhibit microglial activity via mechanisms distinct from its antimicrobial action. Aberrant microglial over-activity has been implicated in various neurodegenerative conditions (e.g. Alzheimer's disease) and minocycline is currently being investigated for its therapeutic potential. However, models of immune influences in the brain predict that microglial inhibition by the drug will also affect healthy cognitive functions yet this has not been examined. We used fMRI to test if minocycline can modulate healthy memory processes, and whether such effects are principally mediated by MTL memory systems. 20 healthy male subjects (mean age = 24.2) were recruited into a 2x2 repeated measures design; factor 1, minocycline vs placebo (100mg twice daily for 3 days prior to testing); factor 2, hippocampal dependent vs non-hippocampal dependent memory. Two in-scanner tasks were used; a virtual reality (VR) task constructed to simultaneously tap hippocampal- (boundary) and striatal- (landmark) based spatial learning/navigation, and a source memory (SM) task designed to assess item recognition (hippocampally independent) and source-memory (hippocampus dependent). While no modulations of memory performance were observed in the SM task, VR task performance indicated that minocycline biased subjects towards using hippocampally mediated navigation strategies which resulted in an impairment when learning to landmark. During periods of memory encoding, this corresponded to inappropriate activation increases in the right parahippocampal gyrus when on minocycline. This finding lends support to models implicating microglial function in learning and memory processes but suggest that the precise functional contributions of these cells remain poorly understood.

5.2 Introduction

The immune system plays a central role in cognition, particularly with regards to memory functions subserved by the medial temporal lobes (MTL). Numerous studies have demonstrated that peripheral inflammation impairs hippocampal function (e.g. Harrison, Doeller, Voon, Burgess, & Critchley, 2014; Bilbo et al., 2005). Furthermore, several lines of evidence suggest that some neurodegenerative conditions (e.g. Alzheimer's disease, AD) have their aetiologies based in aberrant inflammatory activity (Perry, Cunningham & Holmes, 2007). Microglia are immune cells within the brain that underpin many immune influences on cognition and the over-activity of these cells may contribute to neurodegeneration in AD (Domercq & Matute, 2004). Classically microglia are thought to be in one of two states at any one time; a quiescent (resting) state, or an activated state resulting from systemic inflammation or tissue damage (Stence, Waite & Dailey, 2001). In the healthy brain, resting microglia are highly branched (ramified), produce motile projections and partake immune surveillance and the clearance of cell debris (Nimmerjahn, Kirchhoff & Helmchen, 2005; Kreutzberg, 1996). In contrast, activated microglia become deramified, develop an amoeboid shape and are phagocytic towards damaged neurons (Stence, Waite & Dailey, 2001; Raivich et al., 1999).

To date, a number of studies have attempted to alleviate damaging microglial activity in neurodegenerative conditions by attenuating microglial activation. Minocycline is a tetracycline antibiotic that is known to inhibit the function of microglia via mechanisms distinct from its antimicrobial action (Hinwood et al., 2012; He, Appel, & Le, 2001; Sriram, Miller, & O'Callaghan, 2006). In non-humans this drug has been seen to provide neuroprotection against ischemia (Yrjänheikki, Keinänen, Pellikka, Hökfelt, & Koistinaho, 1998), glutamate excitotoxicity (Tikka & Koistinaho, 2001; Tikka, Fiebich, Goldsteins, Keinanen, & Koistinaho, 2001), and methamphetamine induced neurotoxicity (Hashimoto et al, 2007). However, while it is clear that minocycline does attenuate microglial activity in humans (Dodel et al., 2010), other studies have failed to find any neuroprotective benefit of the drug (Diguet, Goss, Tison, & Bezard, 2004; Sriram, Miller, & O'Callaghan, 2006). As such, consensus is lacking regarding the clinical efficacy of minocycline but despite this, the drug is currently being trialled as a neuroprotective agent for the treatment of AD (Minocycline in Alzheimer's Disease Efficacy trial, UKCRN, 2014).

Aside from the potential neuroprotective properties of minocycline, it is also known to inhibit the function of resting microglia (Hinwood et al., 2012). Because of this, models of immune influences in the brain predict that microglial inhibition by minocycline should modulate healthy MTL memory functions, even in the absence of neurodegeneration or inflammation. Specifically, these models suggest that resting microglia play a central role in hippocampally mediated learning through the regulation of long term potentiation (LTP) neural plasticity, and neurogenesis (Yirmiya & Goshen,

2011). In support of this, various investigations have shown that microglial derived cytokines (immunological signalling proteins) directly modulate neuronal activity in the hippocampus. Interleukin 1β (IL-1β) is a cytokine expressed by microglia that aids LTP by increasing neuronal spiking through NMDA receptor agonism (Viviani et al., 2003; Avital et al., 2003). Memory functions of the MTL are thought to be particularly sensitive to this since the region exhibits especially high densities of both IL-1 receptors and microglia (Ericsson, Liu, Hart, & Sawchenko, 1995; Lawson, Perry, Dri & Gordon, 1990). Furthermore, Tumour Necrosis Factor-α (TNFα), another cytokine expressed by microglia, has been observed to continually maintain synaptic strength in hippocampal neurons by adjusting the number of AMPA (α-amino-3-hydroxy-5-methyl-4-isoxazole propionic acid) receptors (Beattie et al., 2002). Finally, one study showed that hippocampal LTP in mice can be disrupted by minocycline-induced microglial inhibition (Zhong et al., 2010).

Microglia may also promote adult neurogenesis (Ekdahl et al. 2009) - a process which is thought to only occur within the olfactory bulb and the dentate gyrus of the hippocampus (Rakic, 2002; Alvarez-Buylla & Garcia-Verdugo, 2002). When healthy rats are subject to environmental enrichment, increased hippocampal neurogenesis is associated with microglial proliferation (Ziv et al., 2006). In contrast, inflamed rats show attenuated levels of neurogenesis (Ekdahl et al., 2003; Monje, Toda, & Palmer, 2003). These effects may be mediated by altered microglial expression of insulin growth factor-1 (IGF-1) and transforming growth factor β1 (TGF-β1) - hormones responsible for inducing neuronal stem cell differentiation (Battista et al., 2006). Microglial-mediated neurogenesis is significant to cognition as it has been functionally implicated in learning and memory (Deng et al., 2010; Leuner & Gould, 2010; Kempermann, Wiskott & Gage, 2004; Lledo, Alonso & Grubb, 2006). Newly formed neurons exhibit hyperexcitability and an increased propensity for LTP which aids plasticity (Ge, Yang, Hsu, Ming, & Song, 2007; Schmidt-Hieber et al., 2004; Deisseroth et al., 2004). Consistent with this, mice demonstrating enhanced hippocampal neurogenesis performed better on spatial tasks such as the Morris water maze and contextual fear conditioning (Saxe et al., 2006; van Praag, Shubert, Zhao, & Gage, 2005). As such, it would be expected that microglial inhibition by minocycline would adversely affect learning.

Despite the above findings, the hypothesis suggesting that minocycline selectively modulates hippocampal memory functions has yet to be tested. Here we explicitly examined this. Healthy adult participants received a 3-day course of both minocycline and a placebo at two time points (counterbalanced order, double-blind). Following each administration period, participants were scanned as they engaged in two memory tasks; a spatial navigation task implemented in virtual reality (VR; as used by Doeller, King, & Burgess, 2008) and a source memory task (e.g. Gaffan, 1994). Each of these allowed for the concurrent assessment of hippocampal and non-hippocampal memory performance. It was predicted that relative to the placebo, minocycline would selectively

modulate hippocampally dependent memory function in each task. Given that effects of microglia are commonly reported in the parahippocampal cortex and MTL more generally (e.g. Harrison et al., 2014), we additionally hypothesised that effects of minocycline would also be observed in these regions.

5.3 Methods

5.3.1 Subjects

Twenty non-smoking, unmedicated, right-handed students were recruited from the University of Sussex (UK) by way of online advertisement. All were male owing to the potential teratogenic effects of minocycline (Joint Formulary Committee & Royal Pharmaceutical Society of Great Britain, 2012). Each gave written informed consent to take part and all were compensated for their time. Subjects had either normal or corrected-to-normal vision and reported no history of neurological, psychiatric or inflammatory illness. Of those who participated, VR task data obtained from 2 subjects was discarded due to technical problems. As such, the VR analyses reported below include data from 18 subjects with a mean age of 24.55 years (*SD* = 5.03). All data obtained for the SM task was used in the SM analyses giving a sample with a mean age of 24.75 years (*SD* = 4.80). The study was approved by the Brighton and Sussex Medical School's Research Governance and Ethics Committee.

5.3.2 Design

A double-blind, repeated measures design was used in which all subjects were tested twice; once following a course of minocycline, and once following a placebo. Minocycline (100mg twice daily) and the placebo (identical protocol & appearance) were administered 3 days prior to their respective study sessions (spaced by at least 14 days). The order of minocycline vs placebo administration was counterbalanced between subjects.

5.3.3 Virtual Reality Task

The VR task (modified from Doeller, King, & Burgess, 2008) was designed to simultaneously tap two learning systems supporting spatial navigation; one coding spatial locations relative to environmental boundaries and another coding spatial locations relative to a single landmark. Previous work with the task has shown learning associated with each navigation cue is differentially reliant on the hippocampus and dorsal striatum respectively (Doeller et al., 2008). The virtual reality environment (figure 5-1A) was constructed in Unreal Engine 2 (Epic Games). It consisted of a circular grassy plain (arena) surrounded by a steep bank (boundary) and a traffic cone placed non-centrally (landmark). A backdrop of mountains, clouds and the sun was visible outside of the arena being projected to infinity - this served as an orientation cue without providing any location information that could be inferred by proximity or parallax. Conversely, both the boundary and landmark were rotationally symmetric as not to provide orientation information.

Using trial-and-error, the goal of the task was to learn the location of four everyday objects (e.g. clock, top hat) that appeared within the arena. Subjects were initially familiarised with the location

of these object across a series four “initial collection” trials. Here participants entered the arena with the relevant object already in place and collected it by walking over it. After this, spatial learning took place within 3 blocks of trials. Each block consisted of 16 trials (4 per object) progressing in a pseudorandom order. An illustration of the task procedure is displayed in figure 5-1B. Trials started with an object being cued by its presentation against a grey background (cue phase; fixed at 2 seconds). Next, the object was removed and the grey background remained over a variable delay period (2 - 6 seconds, uniformly distributed). Subsequently, subjects were placed into the VR environment at a random location - no objects were visible at this time. Subjects were then required to indicate the location of the cued object by walking up to that position and pressing a button (replace phase). Immediately following this, the true location of the object was revealed and participants re-collected the object by walking over it (feedback phase). This period of feedback allowed subjects to refine their memory regarding the location of that object for use in future trials.

In order to experimentally manipulate the use of different navigation strategies (i.e. boundary vs landmark based navigation), two objects were assigned to a “boundary-related” condition (B-related), and the remaining two were assigned to a “landmark-related” condition (L-related). Unbeknownst to participants, the landmark shifted its position at two time points during training; first at the start of block 2 (middle of northwest quadrant to middle of southwest quadrant), and second at the start of block 3 (middle of southwest quadrant to middle of southeast quadrant). Given this landmark shift, B-related objects maintained a fixed position relative to the boundary whereas L-related objects maintained a fixed position relative to the landmark (that is, their location shifted in line with the landmark, see figure 5-1C). Consequently, the boundary and landmark became differentially informative when learning the locations of B-related and L-related objects during feedback. Object assignments to navigation conditions and the order of landmark shifts was counterbalanced across participants. As subjects completed the VR task on two occasions, different objects, backdrops, and trained locations were used in each testing session thereby limiting carryover effects. The task ran identically to that reported by Doeller et al. (2008) with the exception that the original study involved 4 learning blocks rather than the three used here.

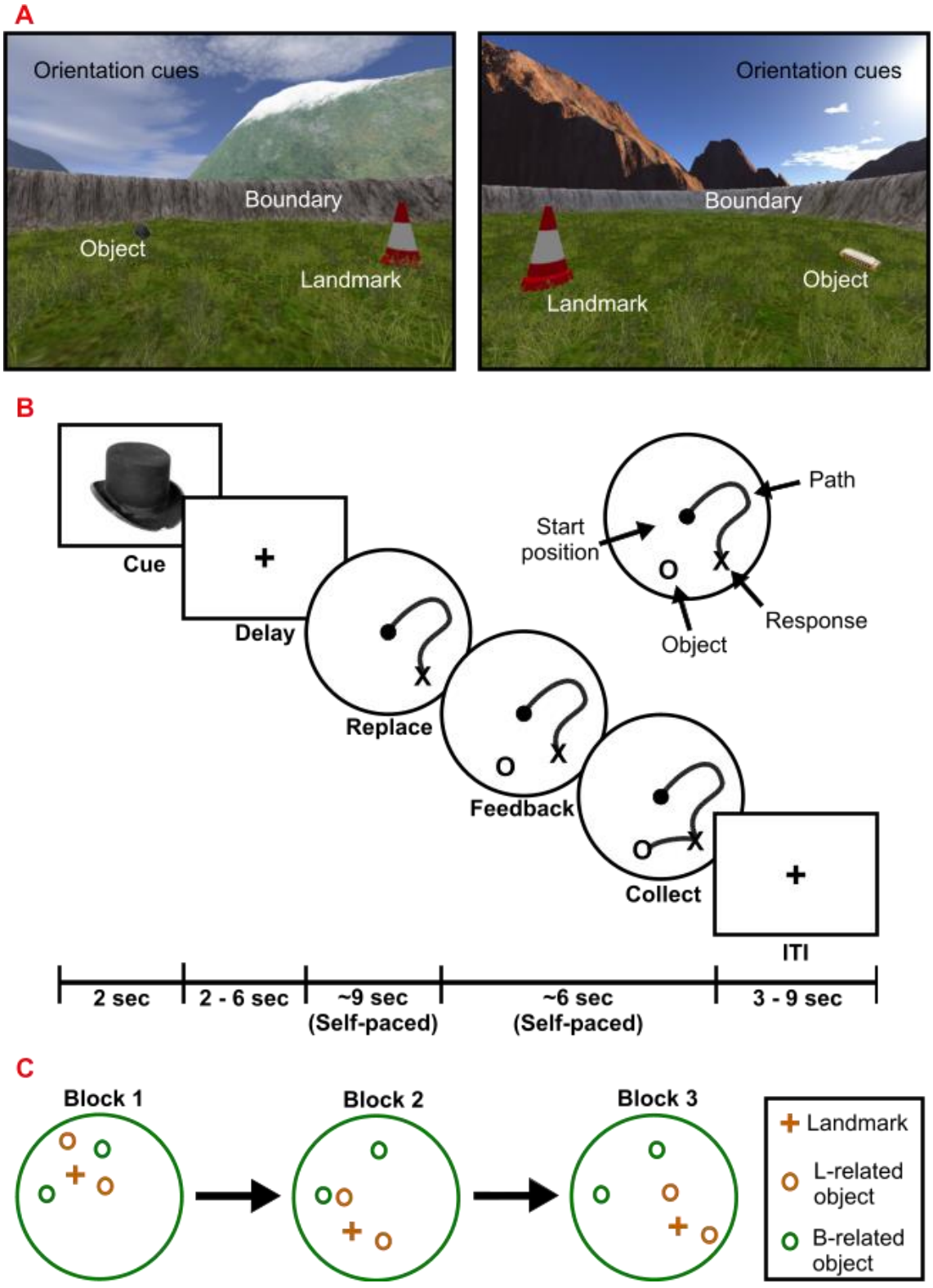

Figure 5-1. *Virtual reality task.* ***A:*** *Examples of the VR environments.* ***B:*** *A schematic illustration of the task procedure.* ***C:*** *Examples of the how the landmark, boundary and their associated objects moved relative to each other over the course of 3 blocks in order to train landmark vs boundary based navigation. Within each block, there were four learning trials for each object.*

5.3.4 Source Memory Task

The SM task sought to examine differences in brain activation at the time of memory encoding that corresponded to later remembering vs. forgetting (so-called subsequent memory effects). Subjects were scanned as they passively attended to a series of 100 trials, each presenting one object (source: Hemera Photo Objects, Focus Multimedia Ltd) superimposed onto a background image (e.g. sandy beach; retrieved from www.gettyimages.co.uk). In each study session, four background images were used and these were display behind an equal number of objects. Trials started with a presentation of the background image alone (500 ms), followed by the object on top of the background (2500 ms), and then the background alone once again (500 ms). Finally, a variable inter-trial interval (ITI) occurred for between 2 and 8 seconds (uniformly distributed, see figure 5-2A). Prior to scanning, subjects were asked to remember the background scene for each object as they would be tested on them later.

Approximately 20 minutes after study, subjects underwent the source memory test phase outside of the scanner. Here, the 100 study object (targets) had to be discriminated against 100 novel object that had not been seen before (lures). On each trial, a single object was presented in isolation (against a white background) and a visual analogue scale (VAS) was displayed underneath. On the VAS, subjects were asked to rate their confidence regarding whether or not they had seen the object before (item judgment phase). Extreme left and right ends of the VAS represented the highest confidence level for target and lure judgments respectively (see figure 5-2B). If subjects responded over half way towards the left end of the scale (i.e. more confidence that the item is a lure), the screen blanked and the next test trial advanced. Otherwise, a second display showed the test object surrounded by each of the four background images and subject were required to select the background against which the object appeared, i.e. a four-alternative forced choice test (4-AFC; source judgment phase). Following this, a final screen displayed the chosen background image above another VAS scale where subjects were required to indicate their confidence in the background choice; not at all confident to most confident (source confidence phase). The test procedure was entirely self-paced with all responses being made via a computer mouse cursor/button. Test object progressed in a pseudorandom order and since the task was to be completed on two occasions, different object and background images were used in each session.

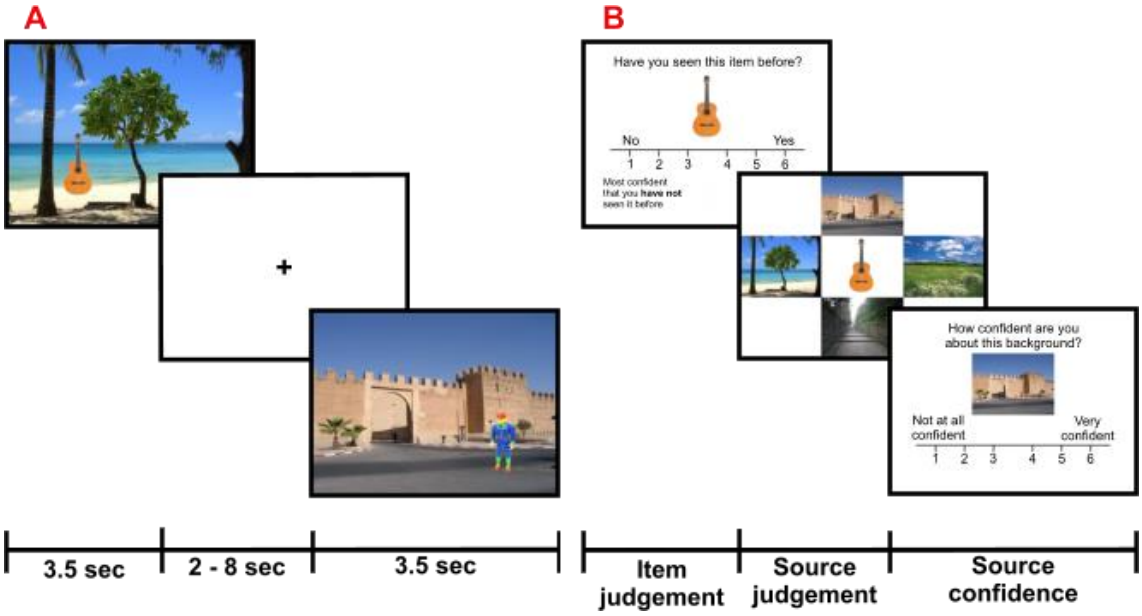

Figure 5-2. *Source memory task.* ***A:*** *Examples of 2 in-scanner study trials separated by an inter-trial interval.* ***B:*** *Source memory test procedure that took place outside of the scanner.*

5.3.5 MRI Acquisition

All images were acquired in a 1.5 Tesla Siemens Avanto scanner equipped with a 32-channel phased array head coil. During both VR and SM tasks, gradient-echo T2*-weighted scans were acquired using echo-planar imaging (EPI) recording 34 axial slices (approximately 30° to AC-PC line; ascending interleaved) and the following parameters; TR = 2520 ms, TE = 43 ms, flip angle (FA) = 90°, slice thickness = 3 mm, inter-slice gap = 0.6 mm in-plane resolution = 3 x 3 mm & acquisition matrix = 64 x 64. To allow for T1 equilibrium, the first 5 EPI volumes were acquired before the start of each task and then discarded. Finally, for purposes of coregistration and image normalisation, a whole-brain T1-weighted structural scan was acquired with a 1mm^3 resolution using an MP-RAGE pulse sequence.

5.3.6 Image Preprocessing

Image preprocessing was carried out identically for each task and performed in SPM8 (www.fil.ion.ucl.ac.uk/spm). Initially, each subject's EPI volumes were spatially realigned to the first image in the time series. Following this, EPI time series data were warped to MNI space with transformation parameters derived from the structural scans (using the DARTEL toolbox; Ashburner, 2007). Subsequently, the EPI volumes were spatially smoothed with an isotropic 8mm FWHM Gaussian kernel prior to GLM analysis.

5.3.7 Data Analysis

5.3.7.1 Virtual reality task

5.3.7.1.1 Behavioural data

Behavioural outputs on the VR task were Cartesian coordinates denoting location estimations made on each trial of the replace phase (so-called "replaced locations"). We first computed "drop error" statistics (in virtual meters) corresponding to the distance between replaced locations and the correct locations as revealed during feedback. Additionally, as has been done in previous studies (Doeller et al., 2008), we wished to generate a metric ("LB-influence") quantifying the relative influence of each navigation cue (boundary vs landmark) on replacement performance. To do this, we first calculated the distance between each replaced location and object location as predicted by both the boundary (dB) and the landmark (dL). For example, for an L-related object, dL was simply the drop error and dB was the distance between the replaced location and the B-related location that would have been correct prior to the most recent landmark shift. Given these distances, we then calculated LB-influence as the ratio of dL to the sum of dB and dL: $dL \div (dB + dL)$. The resultant metric varies between 0 and 1 with low values (i.e. close to 0) indicating a reliance on the landmark, and high values (close to 1) indicating reliance on the boundary. Note: LB-influence score could not be computed for trials blocks 1 since the distinction between B- and L-related objects was only instantiated at the start of block 2.

5.3.7.1.2 Imaging data

In the imaging analyses, we wished to examine memory encoding processes when differentially learning to landmark vs boundary. To do this, we quantified the level of memory encoding taking place on each replace phase by calculating the change in drop error ("Δ drop error") occurring from one trial to the next for each particular object. Thus, Δ drop error reflects the improvement in object replacement with high and low values indicating a high and low level of learning respectively. These statistics were then dichotomised by median split to divide both L-related and B-related trials into two categories; low versus high learning level.

First level general linear models of the fMRI time series data were specified. These included a single regressor for all object cue events, and separate regressors for the replace and collect phases in block 1. Replace phases in blocks 2 and 3 were modelled as a single event type parametrically modulated by LB-influence scores. The collect phases in blocks 2 and 3 were modelled with 4 separate regressors; 1) low learning level for L-related objects, 2) low learning level for B-related objects, 3) high learning level for L-related objects, and 4) high learning level for B-related objects. As well as HRF amplitude estimates, temporal and dispersion derivatives pertaining to all these periods of interest were modelled. Motion parameters were modelled as

nuisance regressors and the data were subject to a high-pass filter (cut-off = 1/128 Hz). This imaging analysis is highly similar to that reported by Doeller et al. (2008), the principal difference being that we split Δ drop error into 2 categories (low vs high) rather than 4. Since our task involved one block fewer than that reported by Doeller et al., this analysis difference ensured comparable numbers of trials were used when estimating BOLD signals at each level of learning.

5.3.7.2 Source memory task

5.3.7.2.1 Behavioural data

At test, behavioural outputs were VAS ratings ranging from -400 (confidently a lure) to +400 (confidently a target). When VAS ratings were above zero, responses to the 4-AFC test were recorded as either correct (1's) or incorrect (0's) along with a VAS rating reflecting confidence in the background choice (ranging from -400 to +400). As well as evaluating differences in confidence level, we wished to examine whether minocycline had differential effects on item versus source memory accuracy. To do this, we first dichotomised item VAS ratings as either "old" (rating > 0), or "new" (rating ≤ 0). Given this, we then classified each response into one of 5 categories and recorded their frequencies; 1) correctly recognised targets with a correct background response ["Hit+"], 2) correctly recognised targets with an incorrect background response ["Hit-"], 3) missed targets ["Miss"], 4) falsely recognised lures ["false alarm"], and correctly rejected lures ["correct rejection"]. It is noteworthy that the category frequencies relating to source memory accuracy (i.e. "Hit+" versus "Hit-") are dependent on item responses. Additionally, as they were tested via 4-AFC, correct background selections should occur 25% of the time by chance alone. In order to account for these issues when estimating memory performance, joint-multinomial process tree (JMPT) modelling was used to analyse the category frequency data (see Batchelder & Riefer, 1999). This approach is consistent with previous studies that have tested a similar source memory task (Simons, Verfaellie, Galton, Miller, Hodges & Graham, 2002).

Here, two tree structures (one for targets, the other for lures) modelled the psychological processes underlying item and source memory judgments (see figure 5-3). The tree for target stimuli contained 3 free parameters; the probability that a studied item will be correctly recognised (parameter A), the conditional probability that a recognised item will have its background retrieved (parameter B), the probability that an unrecognised target will be accepted as old (i.e. the bias for responding old, parameter C). Parameter C was also present in the second tree which categorised lures as either false alarms or correct rejections. These parameters were estimated for each subject and session individually via an expectation maximisation (EM) algorithm running in multiTree v0.45 (Moshagen, 2010).

Previous studies have shown that while source memory performance (i.e. parameter B) is heavily depended on hippocampal memory function, item memory performance (parameter A) is not (Davachi, Mitchell & Wagner, 2003; Cansino, Maquet, Dolan & Rugg, 2002; Bachevalier & Nemanic, 2008; Barker & Warburton, 2011). Given this, when evaluating the effect of minocycline, we took source and item memory performance to be indices of hippocampal and non-hippocampal memory function respectively. However, it is noteworthy that JMPT models assume the retrieval of both item and source memories to be a high-threshold process - that is, retrieval results in an 'all-or-nothing' memory signal that is not graded by memory strength (see Wixted, 2007). While this assumption is often thought to hold for source memory judgments, item memory judgments may be made on the basis of a combination of two distinct processes; 1) a graded familiarity signal that is produced independently of the hippocampus, and 2) a high-threshold recollective process that is hippocampally dependent, a (Aggleton & Brown, 1999, 2006; Yonelinas, 1999).

Considering this, in addition to using the JMPT models, we estimated item memory performance via the analysis of receiver operating characteristics (ROC) in the context of the dual-process signal detection model (see Yonelinas, Boddins, Szymanski, Dhaliwal & King, 1999). Here, hit rate (i.e. the probability of responding 'old' to a target item) is plotted against false alarm rate (the probability of responding 'old' to a lure item) as a function of response confidence (i.e. VAS ratings binned into 6 levels). This results in an ROC curve (see figure 5-4) which is decomposed into two recognition components; recollection (parameterised by the statistic R_0), and familiarity (parameterised by the statistic *d'*). R_0 corresponds to the y-axis intercept on the ROC curve and models the high-threshold process, principally indicative for high-confidence hits. *D'* corresponds to the degree of ROC curvature and models the continuous difference in memory strength between a Gaussian distribution for targets and Gaussian distribution for lures. The values of *Ro* and *d'* are estimated together via a Gauss-Newton algorithm that minimises the sum of squares error between the observed data and the fitted ROC curve.

5.3.7.2.2 Imaging data

For the source memory study phase, first level general linear models of the fMRI time series data were specified. These included separate regressors for study events that were subsequently classified as; Hit+, Hit-, and Misses. As well as HRF amplitude estimates, temporal and dispersion derivatives pertaining to these periods of interest were modelled. Motion parameters were modelled as nuisance regressors and the data were subject to a high-pass filter (cut-off = 1/128 Hz). Where fMRI activations are plotted graphically, percent signal change was calculated by scaling beta estimates with the corresponding GLM regressor heights, and normalising the resultant values with the constant term (as implemented in the MarsBaR toolbox; Brett, Anton, Valabregue & Poline, 2002).

5.3.7.3 Imaging thresholds

Given our a priori hypotheses that effects of interest would be observed in the MTL (for both the VR and source memory task) and the dorsal striatum (for the VR task alone), two regions of interest (ROIs) were generated using the automated anatomical labelling atlas (Tzourio-Mazoyer et al., 2002). The MTL ROI included both hippocampal and parahippocampal cortices (bilaterally), and the striatal ROI included the caudate and putamen (bilaterally). Within this ROI, reported activations survive an uncorrected height threshold of $p < .001$ and a spatial extent threshold of 5 contiguous voxels (135 mm^3). We also report activations that survive a map-wide height threshold of $p < .001$ (uncorrected) and a spatial extent threshold of 30 contiguous voxels (810 mm^3).

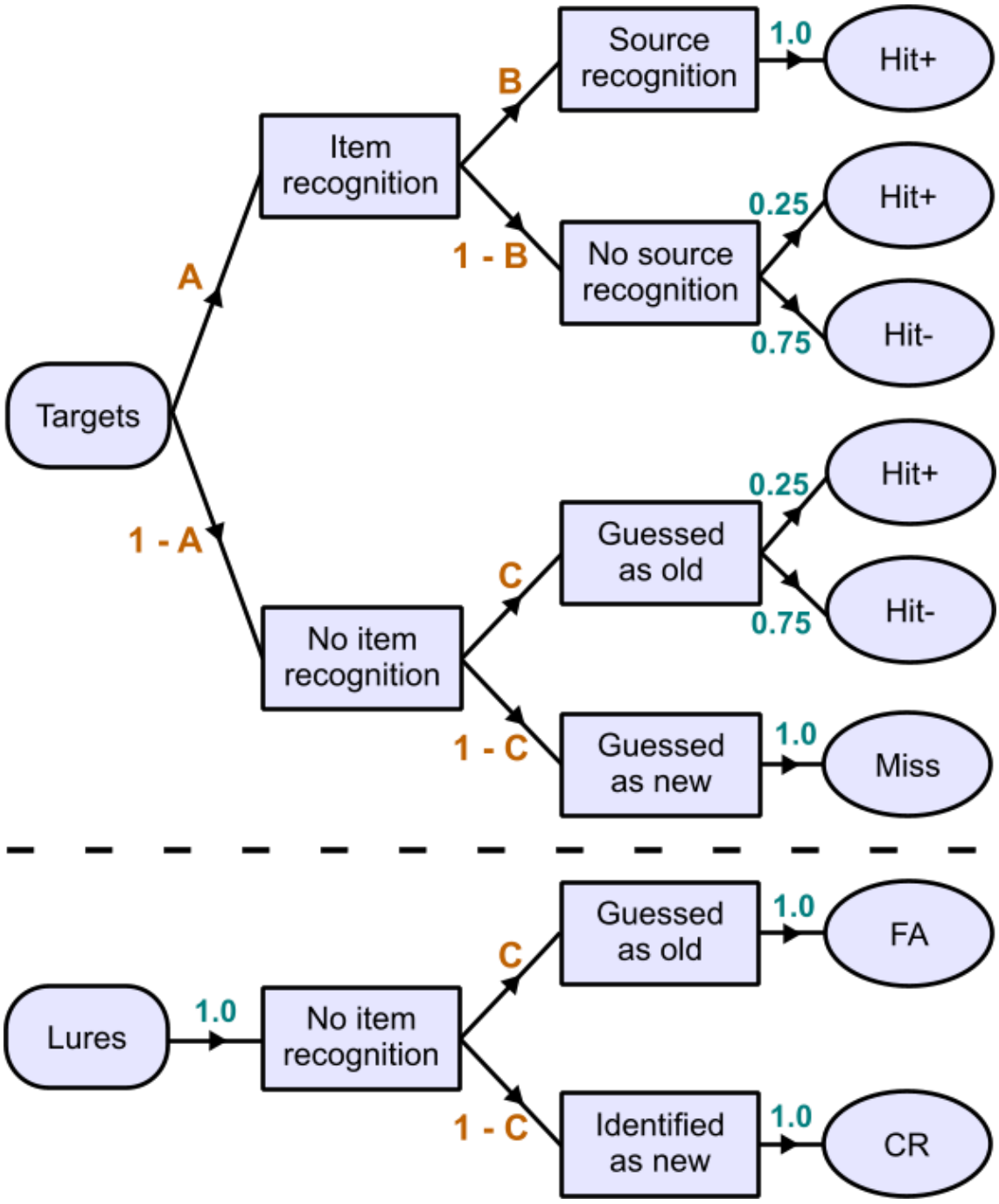

Figure 5-3. *Joint-multinomial process tree model used to analyse behavioural data from the source memory task. The model consists of two trees (top and bottom). The top tree specifies the proportion of target stimuli that are either remembered with their background (Hit+), remembered without their background (Hit-), or missed (Miss). The bottom tree specifies the proportion of lure stimuli are classified as old (i.e. false alarm, FA), or correctly rejected (CR). Category frequencies (i.e. numbers of Hit+'s, Hit-'s, etc.) are calculated from behavioural outputs. While, some branch probabilities can be assumed (blue digits), the branch probabilities corresponding to memory performance (orange digits) must be estimated, typically via EM (see Batchelder & Riefer, 1999).*

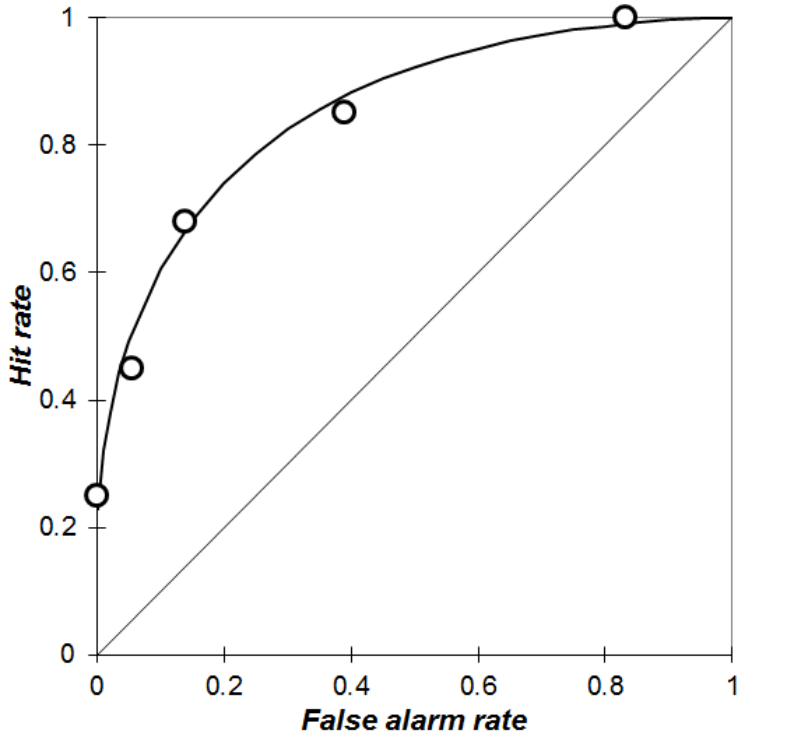

Figure 5-4. *Example ROC curve used to model item memory performance in the source memory task. The ROC plots hit rate (y-axis) against false alarm rate (x-axis) as a function of response confidence (individual points). The recollection parameter (R_0) corresponds to the y-axis intercept and reflects a high-threshold memory process. The familiarity parameter (d') corresponds to the degree of ROC curvature and reflects a continuous level of trace memory strength. Both parameters are estimated via a Gauss-Newton algorithm that minimises the sum of squares error between the observed data and the fitted ROC curve.*

5.4 Results

5.4.1 Virtual reality task

5.4.1.1 Behavioural data

Both LB-influence and drop error statistics were split by navigation condition (i.e. B-related vs L-related), and trial (4 per block) before being averaged across blocks 2 and 3. Note: data from block 1 could not be included as the distinction between B- and L-related objects was only instantiated at the start of block 2. These metrics were then entered into two separate 2x2x4 repeated measures ANOVA; factor 1 = drug (minocycline vs placebo), factor 2 = navigation condition (B-related vs L-related objects), factor 3 = trial number.

LB-influence scores are displayed in figure 5-5A. The ANOVA output showed a main effect of navigation condition indicating that LB-influence score were significantly higher for B-related objects overall; $F(1,17) = 193.761$, $p < .001$. Furthermore, there was a significant navigation condition by trial interaction such that as trials progressed, LB-influence scores increased for B-related objects but decreased for L-related objects; $F(3,51) = 42.129$, $p < .001$. Note: the difference in LB-influence scores on trial 1 are to be expected given that the analysis only included trials that occurred after object locations were differentially trained. Finally, there was a significant main effect of drug indicating that LB-influences scores were overall higher when on minocycline; $F(1,17) = 5.325$, $p = .034$. This indicated that when on the drug, minocycline may have biased participants towards using a boundary based strategy. No remaining model terms were significant.

Drop error statistics are displayed in figure 5-5B. The ANOVA output showed a main effect of trial such that as trials progressed drop error scores across both L-related and B-related objects decreased; $F(3,51) = 41.646$, $p < .001$. Furthermore, there was a significant drug by navigation condition interaction indicating that minocycline increased drop errors for L-related objects, but not B-related objects; $F(1,17) = 6.413$, $p = .021$. This effect demonstrates that the increased LB-influence score observed when on minocycline (reported above) corresponded to an impoverished or attenuated use of landmark based information during navigation. No other model terms in the drop error ANOVA were significant.

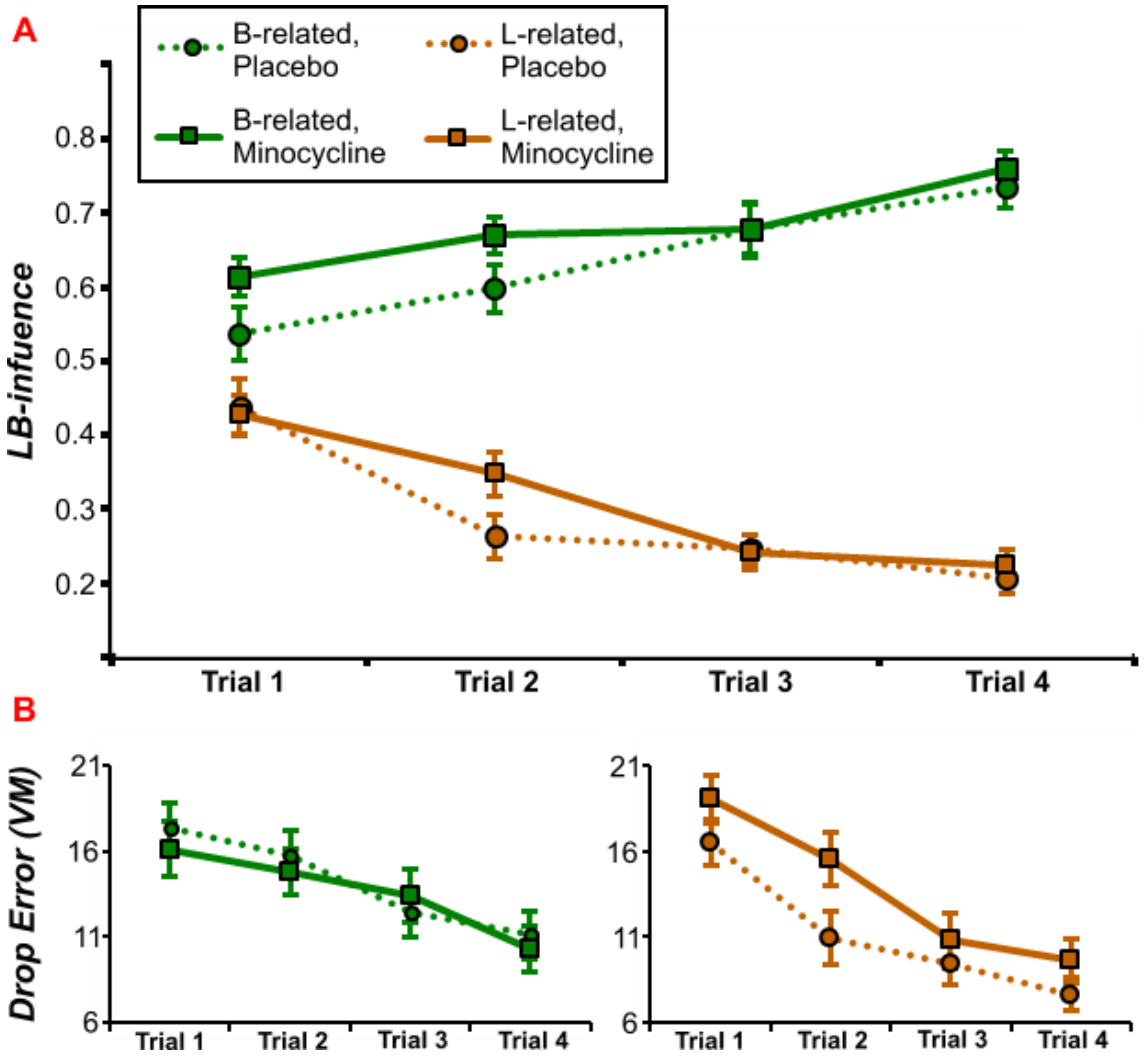

Figure 5-5. *Behavioural performance on the VR task. LB-influence scores (**A**) and drop error statistics (**B**) broken down by drug, navigation condition, and trial number. Error bars represent +/-1 standard error corrected for the within subject-error term. Abbreviation: VM = virtual meters.*

5.4.1.2 Imaging data

5.4.1.2.1 LB-Influence

Initially, beta estimates for the parametric modulation of BOLD amplitude by LB-influence during the replace phase were averaged across placebo and minocycline sessions for each subject. The resultant estimates were then entered into a group-wide one-sample t-test against zero thereby testing for significant correlations between LB-influence and BOLD. This revealed three regions showing positive correlations above threshold (i.e. activity increases with greater boundary reliance) as listed in table 5-1. We next examined whether any regions showed significant differences in the LB-influence correction between placebo and minocycline sessions by

contrasting the beta estimates in a paired samples t-test (i.e. a drug by LB-influence interaction). This revealed no suprathreshold effects.

Table 5-1. *Regions showing positive BOLD correlations with LB-influence during the replace phase. Dagger denotes significance at p(cluster-FWE) < .05.*

Region label	Peak t	k	x	y	z
Left medial frontal gyrus (BA8)	5.57	40	-6	18	51
Left inferior frontal gyrus (BA45)	5.5	71 †	-54	21	30
Left intraparietal lobule (Pft)	4.81	38	-51	-36	45

5.4.1.2.2 Effect of minocycline on learning to boundary vs landmark

To examine BOLD activity indicative of learning to boundary vs landmark, and whether such effects are modulated by minocycline, a three factor model was specified at second-level. Here, HRF amplitude estimates relating to the collect phase were grouped by drug (placebo vs minocycline), navigation condition (boundary vs landmark) and learning level (high vs low) and entered into a 2x2x2 repeated measures ANOVA. All suprathreshold activations for this analysis are listed in table 5-2. A region in the left hippocampus showed a main effect of navigation condition such that BOLD activity was overall greater on B-related trials compared to L-related trials (see figure 5-6). Despite this, it is noteworthy that activity in the hippocampal cluster was not modulated by learning level. Three regions (the putamen, fusiform gyrus, and anterior middle frontal gyrus, all on the left side) exhibited a drug by learning level interaction. On the placebo, these clusters produced a BOLD pattern indicative of increased activity when learning to both boundary and landmark, but the reverse pattern when on minocycline (see figure 5-7). Finally, four regions showed a three-way interaction between drug, navigation condition and learning level; the left superior frontal gyrus, left anterior insula, right superior temporal gyrus, and right parahippocampal gyrus. On the placebo, BOLD patterns in each of these areas indicates increased activity when learning to boundary but not when learning to landmark. However, when on minocycline this pattern appears disrupted (see figure 5-8).

Table 5-2. *Regions identified in the 2x2x2 ANOVA examining the effect of drug on learning to landmark vs boundary. Asterisks denote significance at p(peak-FWE) < .05. Daggers denote significance at p(cluster-FWE) < .05. § denotes p(peak-FWE) < .05 corrected within a priori anatomical ROIs.*

Region label	Peak F	k	x	y	z
Main effect of navigation condition					
Left hippocampus	19.58 §	14	-33	-30	-12
Drug x Learning level					
Left fusiform gyrus	27.3 *	122 †	-39	-48	-21
Left putamen	20.54 §	17	-27	6	9
Left anterior middle frontal gyrus	16.33	43	-36	42	6
Drug x navigation condition x learning level					
Left superior frontal gyrus	41.5 *	34 †	-18	30	36
Left anterior insula	30.49 *	49 †	-27	18	3
Right superior temporal gyrus	19.18	35	69	-30	12
Right parahippocampal gyrus	17.34 §	47	15	-39	-6

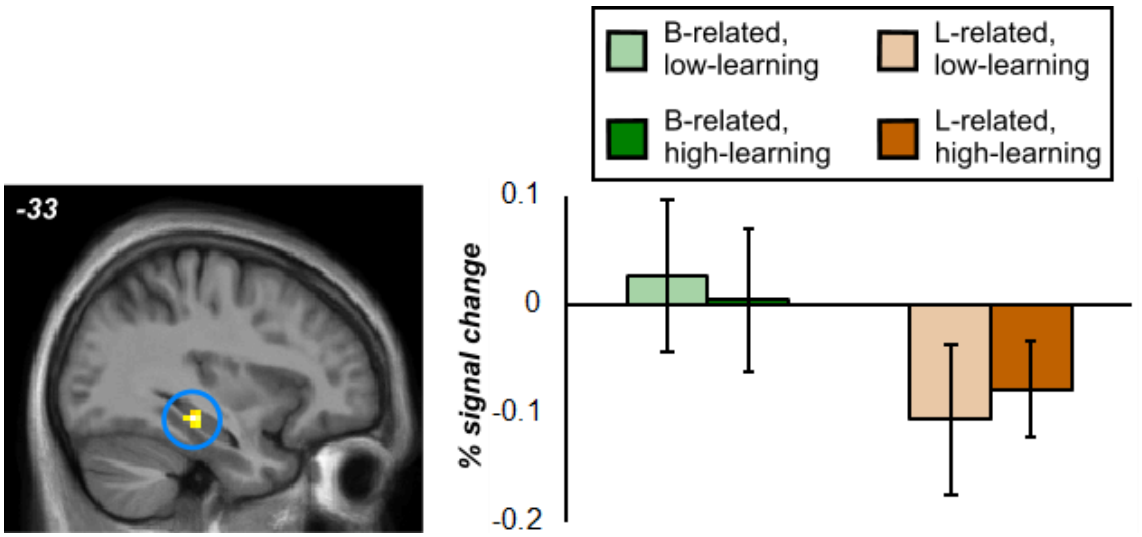

Figure 5-6. *A cluster in the left hippocampus exhibiting a main effect of navigation condition during the collect phase; "boundary > landmark". Error bars indicated 95% confidence intervals corrected for the within subject-error term.*

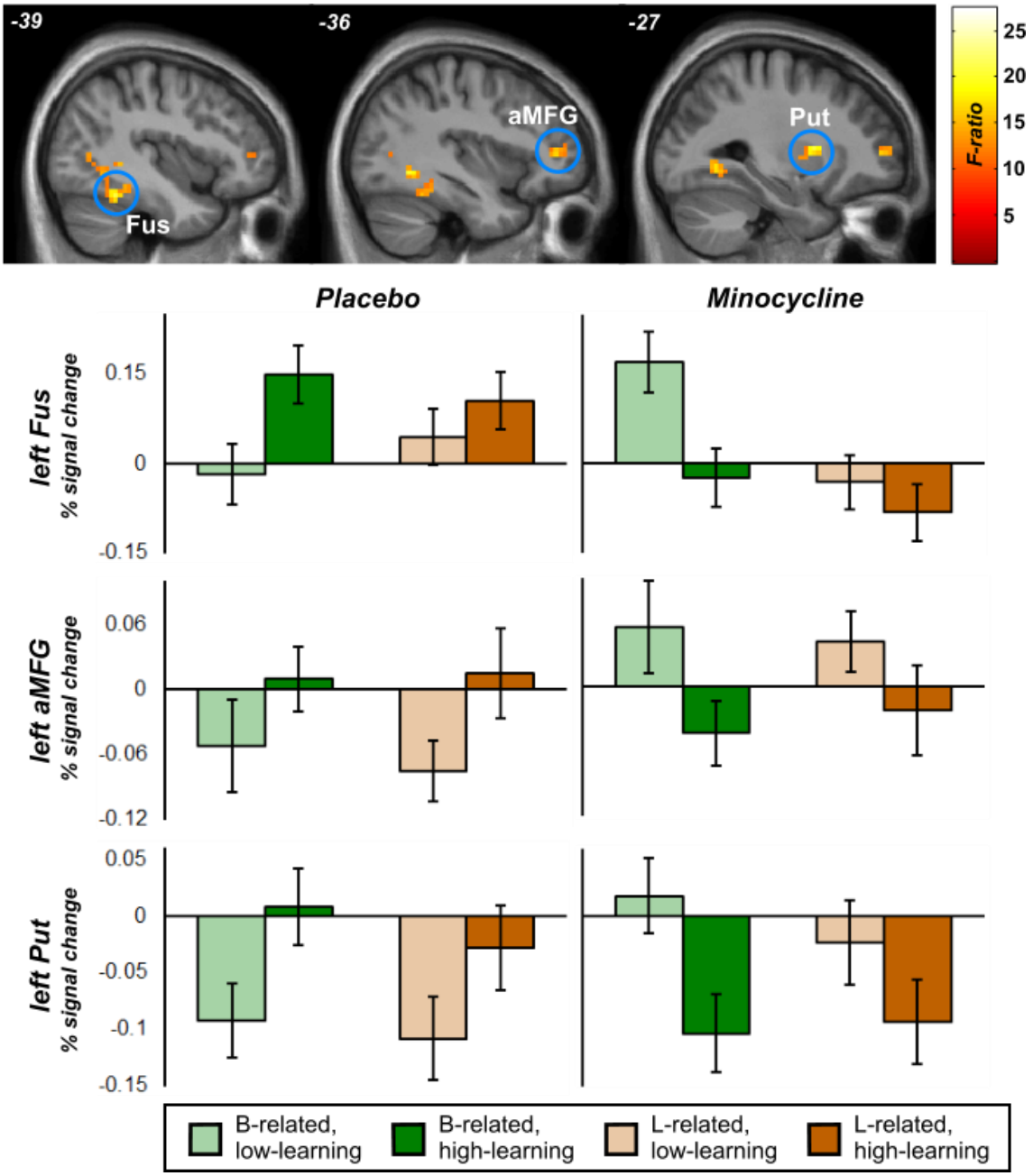

Figure 5-7. *Clusters showing a 'drug' by 'learning level' interaction during the collect phase. Error bars indicated 95% confidence intervals corrected for the within subject-error term. Abbreviations: Fus = fusiform gyrus, aMFG = anterior middle frontal gyrus, Put = putamen.*

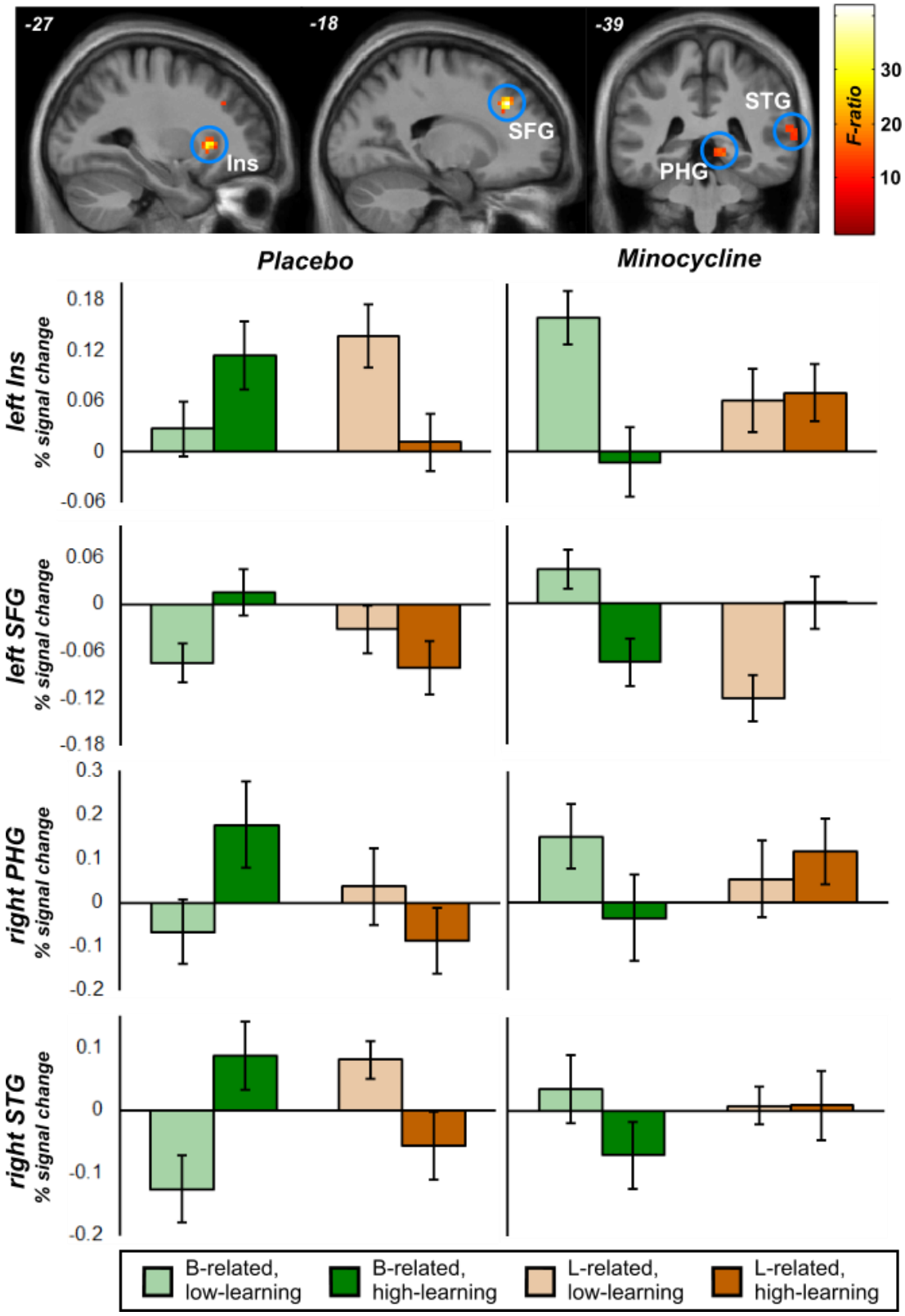

Figure 5-8. *Clusters showing a three-way interaction between 'drug', 'navigation condition', and 'learning level' during the collect phase. Error bars indicated 95% confidence intervals corrected for the within subject-error term. Abbreviations: Ins = insular cortex, SFG = superior frontal gyrus, PHG = parahippocampal gyrus, STG = superior temporal gyrus.*

5.4.2 Source memory task

5.4.2.1 Behavioural data

We first examined whether the JMPT model parameters relating to item and source memory performance were differentially affected by minocycline. The JMPT model showed that both the item memory (A), and source memory (B) parameters were significantly non-zero for all subjects and sessions. These were then entered into a 2x2 repeated measure ANOVA model; factor 1 = drug, factor 2 = parameter (A vs B). This revealed a significant main effect of parameter such that the probability of positively recognising a target was higher than the probability of correctly retrieving an item's background image; $F(1,19)$ = 11.675, $p < .003$. Aside from this, there was neither a significant main effect of drug or a significant drug by parameter interaction; $F(1,19)$ = 0.454 and 0.302 respectively. Given outputs of the dual-process signal detection model, we also tested whether item familiarity (*d'*) and recollection (R_0) differed between placebo and minocycline conditions. Paired samples t-tests indicated no significant differences; $t(18)$ = 0.915, 0.637 for *d'* and R_0 respectively.

Next we examined whether minocycline affected subjective confidence ratings for either item or source memory decisions. To do this for item confidence, VAS ratings made on Hit+, Hit-, Miss, False alarm and Correct rejection trials were entered into separate paired samples t-tests (placebo vs minocycline). These revealed no effect of minocycline across all response categories; $t(19)$'s < 0.614, p's > .547. For source memory confidence, VAS ratings made on Hit+, Hit-, and False alarm trials were also entered into separate paired sample t-test (placebo vs minocycline). Again, this revealed no effect of minocycline across each response category; $t(19)$'s < 1.447, p's > .164.

5.4.2.2 Imaging data

To examine group-wide BOLD differences in item/source memory encoding, and whether such effects were modulated by minocycline, HFR amplitude estimates for Hit+, Hit-, and Miss trials were entered into a 2x3 repeated measures ANOVA (factor 1: drug, factor 2: trial type). This revealed a set of 17 suprathreshold clusters which were then classified by BOLD pattern into five groups based on post-hoc contrasts; 1) “Miss > Hit+/-”, 2) increases with encoding success [“Hit+ > Hit- > Miss”], 3) decreases with encoding success [“Miss > Hit- > Hit+”], 4) “Hit+/- > Miss”, and 5) “Hit+ > Hit-/Miss” (see table 5-3). No regions exhibiting a main effect of drug or a drug by trial type interaction were detected.

Table 5-3. *Regions exhibiting BOLD differences between source memory study trials grouped by subsequent accuracy. Asterisks denote significance at p(peak-FWE) < .05. Daggers denote significance at p(cluster-FWE) < .05.*

Region label	Peak F	k	x	y	z
Miss > Hit+/-					
Right angular gyrus	37.59 *	540 †	54	-54	33
Posterior cingulate cortex / precuneus	31.41 *	876 †	3	-54	33
Left angular gyrus	19.34 *	264 †	-48	-57	30
Right superior frontal gyrus	13.97	199 †	21	36	45
Left middle temporal gyrus	11.88	35	66	-12	-12
Left postcentral gyrus	9.26	35	-66	-21	33
Hit+ > Hit- > Miss					
Left intraparietal sulcus	19.03 *	276 †	-24	-69	42
Left fusiform gyrus	17.5 *	384 †	-45	-60	-12
Right intraparietal sulcus	15.78 *	122 †	30	-66	30
Left inferior frontal gyrus (BA44)	14.11	99 †	-42	6	30
Posterior-medial frontal	12.63	39	-6	15	54
Left inferior frontal gyrus (BA45)	12.14	33	-51	30	15
Miss > Hit- > Hit+					
Right superior medial gyrus (Fp1)	14.97	324 †	6	63	6
Middle cingulate cortex	14.23	58	3	-24	39
Right middle temporal gyrus	11.26	55	66	-12	-12
Hit+/- > Miss					
Right inferior temporal/ fusiform gyrus	14.62	121 †	42	-60	-6
Hit+> Hit-/Miss					
Left precentral gyrus	11.91	48	-45	-6	33

5.5 Discussion

We investigated the functional consequences of minocycline, a microglial inhibitor, on human memory. While both on and off minocycline, participants learned the locations of objects in virtual reality (VR) relative to either a single landmark (reliant on striatal learning mechanisms) or an environmental boundary (reliant on the hippocampus). Additionally, a source memory (SM) task examined both item recognition (independent of the hippocampus), and object-scene bindings (hippocampally mediated). It was predicted that microglial inhibition via minocycline would result in modulations of hippocampal memory function alone.

No effects of the drug were detected in the SM task data. Nonetheless, behavioural outputs of the VR task showed that minocycline promoted reliance on boundary-based information for both landmark- and boundary-related objects. While this did not significantly affect errors when navigating to boundary, it selectively disrupted landmark-based navigation. Given that the hippocampal and striatal systems are known to compete with one another during learning (Doeller, King, & Burgess, 2008), this finding implies one of two possibilities; 1) minocycline selectively impairs landmark-related learning resulting in a greater influence of boundary-related information, or 2) minocycline directly increases the strength or weighting of boundary-related information thereby positively biasing its use and increasing errors when navigating to landmark. Our behavioural data cannot distinguish between these two possibilities alone.

Neuroimaging analyses highlighted that, when on the placebo, a region of the dorsal striatum (specifically the left putamen) exhibited increased activity during both landmark- and boundary-based learning, but the reverse pattern on minocycline. Because this interaction was not specific to either navigation condition (i.e. it occurred for both landmark- and boundary-related learning), the finding may reflect processes that are downstream of altered mnemonic functions (e.g. integration processes for combining hippocampal- and striatal- information). In contrast, the right parahippocampal cortex exhibited an activation pattern indicative of selective boundary-based encoding when on the placebo, but inappropriate over activity when learning to landmark on minocycline. Considering this, we tentatively suggest that minocycline modulates learning processes in the MTL, perhaps biasing their use relative to other learning systems.

While this interpretation requires further investigation, findings of the present study do lend support to models suggesting that microglia play a central role in underpinning healthy learning and memory functions (Yirmiya & Goshen, 2011). Nonetheless, it remains unclear exactly what contribution these cells make. As noted above, microglia are thought to aid LTP, synaptic scaling and neurogenesis by the expression of inflammatory cytokines and hormones (Viviani et al., 2003; Avital et al., 2003; Beattie et al., 2002; Ziv et al., 2006). Based on this, it may be expected that

resting microglial inhibition would result in impaired MTL memory function. Instead, our data suggest that MTL mediated processes were unimpaired but inappropriately active at times where other learning strategies were optimal. As such, it is possible that microglia may contribute to learning and memory functions in ways that are yet to be defined. One potential hint of this may come from the role of IL-6 which is another cytokine expressed by microglia (see Erta, Quintana, & Hidalgo, 2012). During spatial learning, IL-6 is expressed in the hippocampus of rats and has been observed to limit the duration of LTP - effectively acting as a potentiation stop signal (Balschun et al., 2004). In light of this, our suggestions of inappropriate MTL involvement in landmark-based navigation may be a consequence of LTP dysregulation within the MTL system. On a related note, hippocampal concentrations of IL-6 are known to increase with age (Ye & Johnson, 1999), and age-related changes in LTP are associated with microglial activation (Griffin et al., 2006). Since, LTP decreases are believed to contribute to neurodegeneration in AD (Koffie, Hyman, & Spires-Jones, 2011), the potential neuroprotective qualities of minocycline may be mediated by reductions in IL-6 expression by microglia.

Along with effects in the putamen and parahippocampal gyrus, the VR task also highlighted a number of other regions demonstrating modulations by learning and minocycline. Both the left fusiform gyrus and left anterior middle frontal gyrus showed activation patterns similar to that of the putamen (increased activity during both landmark- and boundary-based learning, but the reverse pattern on minocycline). As is suggested, these effects may reflect processes that are downstream of altered mnemonic functions. In line with this, each region is known to support process that are critical to learning the locations of objects. The fusiform gyrus is involved in visual processing and object recognition (e.g. Gauthier, Tarr, Anderson, Skudlarski, & Gore, 1999) and the anterior middle frontal gyrus has been implicated in the sustainment of items by working memory (Courtney, Ungerleider, & Keil, & Haxby, 1997). Showing effects mirroring that of the parahippocampal gyrus, three clusters in the left superior frontal gyrus, left anterior insula and right superior temporal gyrus were sensitive to minocycline in that they produced BOLD patterns indicative of over activity when learning to landmark. The superior frontal gyrus has been implicated in working memory processes (du Boisgueheneuc et al., 2006) whilst the anterior insula is associated with attentional control (Nelson et al., 2010), and the right superior temporal cortex with visual search (Gharabaghi, Berger, Tatagiba, & Karnath, 2006). As before, although the functional significances of these effects remains unclear, it is plausible that each are a consequence of altered memory function occurring in upstream brain regions.

Contrary to what has been reported by Doeller et al. (2008), the VR task did not highlight any caudate activations indicative of landmark based navigation or learning. Additionally, while a region in the left hippocampus did show greater BOLD activity on boundary-related trials, the

hippocampus was not significantly modulated by the level of boundary-related learning. This may be due to differences in statistical power and alternative methods of data modelling - while Doeller et al. principally examined behaviour-BOLD correlations, we were interested in absolute BOLD differences reflecting the behavioural effects of minocycline. Considering that we did not replicate many of the effects reported in the original study, further work will be required to fully evaluate the impact of the minocycline on the striatal and hippocampal systems. Also noteworthy is the failure to detect MTL activations in the SM task. Numerous fMRI and lesion studies have demonstrated that object-in-place bindings heavily involve the hippocampal and parahippocampal cortices (Davachi, Mitchell & Wagner, 2003; Cansino, Maquet, Dolan & Rugg, 2002; Bachevalier & Nemanic, 2008; Barker & Warburton, 2011). Given this, it is likely that the lack of effects in the current study reflect insufficient statistical power.

In summary, we suggest that microglial inhibition by minocycline leads to activation increases in the healthy MTL memory system thereby modulating mnemonic performance. This observation lends support to theories implicating microglia in learning and memory functions but suggests that the precise contribution of these cells is yet to be adequately characterised. Future studies probing the effects of minocycline on other hippocampally mediated processes (e.g. object perception; Lee & Rudebeck, 2010) will be required to support our findings. Furthermore, given that changes in microglial activation have been imaged in humans using [11C] (R)-PK11195 positron emission tomography (Dodel et al., 2010; Cagnin et al., 2001a/b), it should be possible to investigate whether the cognitive effects of minocycline directly correspond to microglial activity.

Chapter 6

General discussion

This thesis aimed to characterise the roles of hippocampal and neocortical subdivisions during the learning of different types of associative information. The following section summarises the findings of this thesis, discusses their theoretical implications, and puts forward novel hypotheses that require further examination.

Configural discriminations involve learning associations that are operationally defined to ensure that above chance performance cannot be supported by attending to single features (Sutherland & Rudy, 1989). As such, they necessarily require learning associative relationships between stimuli that have overlapping elements. Previous research has implicated different MTL subregions in the coding of configural contingencies with varying degrees of complexity. Configurations devoid of any intrinsic spatial structure are thought to depend on the perirhinal cortex (Saksida & Bussey, 2010). At the same time, lesion studies in rodents have implicated the hippocampus in underpinning configurations with a spatial element (Aggleton, Sanderson, & Pearce, 2007). In chapter 2, we investigated whether such dissociations occur in humans using fMRI. It was found that while a number of MTL subdivisions (including the perirhinal and hippocampal cortices) did process configural information throughout learning, they did not appear to represent this information once fully learned. Instead, the inferior temporal lobes (ITLs) and left angular gyrus (AG) exhibited BOLD patterns indicative of greater involvement as a function of configural memory strength. Both of these areas are key components of the semantic memory system (Binder, Desai, Graves, & Conant, 2009). Based on previous research, we proposed that the ITLs may store configural associations while the AG acts to selectively retrieve these representations at test (see Lambon Ralph, Lowe, Rogers, 2007; Ansari, 2008).

Prominent models suggest that all learned information for declarative material is initially encoded by the hippocampal system before being consolidated or transformed to depend on the neocortex (McClelland, McNaughton, & O'Reilly, 1995; Winocur & Moscovitch, 2011; Nadel & Moscovitch, 1997; McClelland, 2013). Contrary to this, the above result implies that humans can rapidly encode novel associations using their semantic system. Critically however, we do not suggest that the hippocampal system is never recruited to store configural associations in humans. Instead we propose that whether or not information is represented by the hippocampus depends on how information is presented at study. The experiment in chapter 2 required participants to learn multiple configural discriminations simultaneously - that is, at the outset of training, overlapping discriminations were interleaved with one another. This is not typical of the aforementioned animal

studies which train subjects to acquire configurations by progressively introducing the overlapping discriminations as each one is learned (e.g. Sanderson, Pearce, Kyd, & Aggleton, 2006). Consequently, the discrepancy between the rodent data and our fMRI data may be down to how discriminations are trained.

Classically, the hippocampus is thought critical for new learning because of its ability to pattern separate - i.e. form non-overlapping representations for similar events in order to avoid catastrophic interference (O'Reilly & McClelland, 1994; McClelland & Goddard, 1996). However, we suggest that if overlapping units of information are acquired across multiple "interleaved" episodes rather than being learned "progressively", pattern separation processes may be less effective at resolving hippocampal interference. This may be because, when interleaved, each to-be-learned unit has no pre-established hippocampal trace to be separated against. In such situations, we hypothesise that configural representations are encoded by the neocortical semantic system. At the same time, the hippocampal system may still contribute to the online processing of configural information in a manner that is functionally relevant to learning. Consistent with this, the hippocampus is often implicated in performing visual operations that occur online (Lee, Yeung, & Barense, 2012; Lee et al., 2005; Barense, Gaffan, & Graham, 2007). Yet in contrast to standard consolidation theory (SCT), our hypothesis implies that memory representations need not form in the hippocampal system before neocortical learning can take place. Additionally, while we agree that neocortical learning is more gradual than learning in the hippocampus, we suggest that it can take place more rapidly than previously thought.

The experiment in chapter 2 also showed that performance when transitively inferring across learned discriminations was strongly related to hippocampal activity at test and, to a lesser extent, during study. This provides some insight into the nature of the learned associative representations. Specifically, it highlights that the semantic encoding of configural information may not entail the formation of an integrated memory trace where all associations are coded in relation to each other. Instead, multiple overlapping configural contingencies in the semantic system may be represented separately and require extra processing to support inference performance. This contrasts with findings from other studies. When the directly trained associations are learned as well as they were in our study, transitive performance is most strongly related to hippocampal activity at encoding, not at test (e.g. Shohamy & Wagner, 2008). This has been taken to indicate that the hippocampus can represent an integrated trace of all associations which only needs to be activated at inference. Given this, we hypothesise that how transitive inference is subserved depends on whether information is encoded by the hippocampal or neocortical systems. As discussed above, this may in turn depend on how training takes place. If discriminative training progresses in an interleaved manner thereby resulting in semantic storage, the hippocampus may always be involved in

performing inference operations at test. However, if training occurs in a progressive manner resulting in hippocampal storage, the contingencies may be represented by a unitised trace which is not required to undergo any further inferential processing.

Since we suggest that neocortical learning for configural associations can take place in the absence of a pre-established hippocampal trace, it was next investigated whether the neocortical system can learn simpler, non-overlapping, associations independent of the hippocampus altogether. When learning concerns item-item associations that are repeated multiple times, this may be possible if the neocortical system draws on item-based information represented in sensory areas. Cross-situational learning (xSL) is a form of training which enables the acquisition of word-object associations through repeated presentations of word-object co-occurrences. Furthermore, associations between words and objects are never explicitly given in xSL because multiple unknown word-object pairs are presented simultaneously. This results in a high degree of "referential ambiguity" on any one trial and so learning mechanisms must acquire the associations by integrating information across trials. Behavioural studies have suggested that referential ambiguity in xSL may be addressed by gradually accumulating co-occurrence statistics in an associative manner (Kachergis, Yu, & Shiffrin, 2012b; Smith, Smith & Blythe, 2011). As the neocortex is often thought to extract statistical patterns in order to learn (Winocur & Moscovitch, 2011), we hypothesised that xSL may be principally supported by neocortical learning mechanisms rather than the hippocampus.

To test this, the experiment in chapter 3 first examined whether xSL is accounted for by hippocampally dependent contextual learning mechanisms as described by the temporal context model (TCM; Howard & Kahana 2002; Howard, Fotedar, Datey, & Hasselmo, 2005; Howard, 2004). The TCM states that associative learning can be facilitated when item representations are bound to a slowly changing representation of environmental context. Because of this, the model predicts that errors made when mismatching words and objects in xSL would depend on the temporal arrangement of stimuli at study. This prediction was not supported. We next examined xSL using fMRI with the hypothesis that neocortical learning mechanisms rather the hippocampal system would be principally involved in word-object acquisition (chapter 4). The results highlighted that periods of xSL corresponded to increased activity in a number of neocortical regions which have been implicated in semantic processing, attention and reasoning. Critically however, the hippocampus was more activated for associations that had been pre-learned via an explicit encoding procedure. This is consistent with the hypothesis that xSL draws on neocortical learning mechanisms, perhaps independently of the hippocampus.

Nonetheless, as alluded to in chapter 2, even if neocortical learning progresses quickly, information processing by the hippocampal system may still be functionally supportive. Considering this, it could very well be that hippocampal activity, while not detected in the experiment, is still required for xSL to take place. However, there is one important distinction between the word-object associations in xSL and the configural discriminations of the previous study. In particular, configural learning involves the simultaneous acquisition of overlapping memory codes while xSL involves one-to-one mappings between to-be-learned features. As such, it could be that the hippocampus is always critical when learning overlapping associations which, as suggested, may perform pattern separation operations. In contrast, the hippocampus may not be needed when associations are orthogonal with respect to one another thereby allowing neocortical learning to take place in the absence of hippocampal activity. This hypothesis will need to be tested in the context of hippocampal pathology that is sufficient to cause amnesia. However, if supported, it will force an adjustment of SCT stipulating that schema inconsistent information can be learned independently of the hippocampal system as long as to-be-learned associations are non-overlapping.

Chapter 5 explored the question of how the hippocampal system is specialised to underpin rapid learning. Models of immune influences in the brain have implicated a variety of immuno-controlled functions in supporting hippocampal learning mechanisms (Yirmiya & Goshen, 2011). In particular, hippocampal microglia are thought to regulate LTP and adult neurogenesis (Viviani et al., 2003; Avital et al., 2003; Ekdahl, Kokaia & Lindvall, 2009), both of which are thought to be important for rapid learning (e.g. Deng et al., 2010). Given this, we tested a prediction of these models by examining the effect of microglial inhibition induced by minocycline on two different navigation strategies: learning to landmark vs learning to boundary. With a virtual reality task similar to that used in chapter 5, Doeller and colleagues (Doeller & Burgess, 2008; Doeller, King, & Burgess, 2008) have demonstrated that learning spatial locations relative to an environmental boundary occurs incidentally and is reliant on the hippocampal system. In contrast, learning locations relative to a single landmark conforms to rules of associative reinforcement and is dependent on activity in the dorsal striatum. Based on the assumption that hippocampal learning mechanisms are contingent on microglial controlled processes, it was predicted that minocycline would selectively modulate learning to boundary. The results showed that minocycline did indeed modulate navigation performance but not in the way that was expected. Since microglia are thought to aid memory function, their inhibition should have caused an impairment when learning to boundary. Instead, we observed an over-recruitment of boundary-based strategies and a corresponding increase in hippocampal activity. This suggests that the precise functional roles of microglia in underpinning fast hippocampal learning mechanisms are not well understood. However, the study

does support the proposal that the immune system functionally contributes to hippocampal learning mechanisms.

To conclude, this thesis has provided evidence that the neocortical system in humans can encode novel information within shorter periods of time than previously thought. Additionally, we suggest that the learning of novel, non-overlapping associations may be hippocampally independent if that training requires the extraction of statistical regularities across a series of ambiguous events. Finally, we provide evidence that hippocampal learning mechanisms are dependent on immune functions within the brain which may account for why the hippocampal system is specialised for rapid incidental learning.

References

Aggleton, J. P., Albasser, M. M., Aggleton, D. J., Poirier, G. L., & Pearce, J. M. (2010). Lesions of the rat perirhinal cortex spare the acquisition of a complex configural visual discrimination yet impair object recognition. *Behavioral neuroscience*, *124*(1), 55.

Aggleton, J. P., & Brown, M. W. (1999). Episodic memory, amnesia, and the hippocampal–anterior thalamic axis. *Behavioral and brain sciences*, *22*(03), 425-444.

Aggleton, J. P., & Brown, M. W. (2006). Interleaving brain systems for episodic and recognition memory. *Trends in cognitive sciences*, *10*(10), 455-463.

Aggleton, J. P., Sanderson, D. J., & Pearce, J. M. (2007). Structural learning and the hippocampus. *Hippocampus*, *17*(9), 723-734.

Alvarado, M. C., & Rudy, J. W. (1995). Rats with damage to the hippocampal-formation are impaired on the transverse-patterning problem but not on elemental discriminations. *Behavioral neuroscience*, *109*(2), 204.

Alvarez-Buylla, A., & García-Verdugo, J. M. (2002). Neurogenesis in adult subventricular zone. *The Journal of neuroscience*, *22*(3), 629-634.

Andersson, J. L., Skare, S., & Ashburner, J. (2003). How to correct susceptibility distortions in spin-echo echo-planar images: application to diffusion tensor imaging. *NeuroImage*, *20*(2), 870-888.

Ansari, D. (2008). Effects of development and enculturation on number representation in the brain. *Nature Reviews Neuroscience*, *9*(4), 278-291.

Aron, A. R., Robbins, T. W., & Poldrack, R. A. (2004). Inhibition and the right inferior frontal cortex. *Trends in cognitive sciences*, *8*(4), 170-177.

Ashburner, J. (2007). A fast diffeomorphic image registration algorithm. *NeuroImage*, *38*(1), 95-113.

Avital, A., Goshen, I., Kamsler, A., Segal, M., Iverfeldt, K., Richter-Levin, G., & Yirmiya, R. (2003). Impaired interleukin-1 signaling is associated with deficits in hippocampal memory processes and neural plasticity. *Hippocampus*, *13*(7), 826-834.

Bachevalier, J., & Nemanic, S. (2008). Memory for spatial location and object-place associations are differently processed by the hippocampal formation, parahippocampal areas TH/TF and perirhinal cortex. *Hippocampus*, *18*(1), 64-80.

Bahlmann, J., Schubotz, R. I., & Friederici, A. D. (2008). Hierarchical artificial grammar processing engages Broca's area. *NeuroImage*, *42*(2), 525-534.

Balschun, D., Wetzel, W., Del Rey, A., Pitossi, F., Schneider, H., Zuschratter, W., & Besedovsky, H. O. (2004). Interleukin-6: a cytokine to forget. *The FASEB journal*, *18*(14), 1788-1790.

Barense, M. D., Bussey, T. J., Lee, A. C., Rogers, T. T., Davies, R. R., Saksida, L. M., ... & Graham, K. S. (2005). Functional specialization in the human medial temporal lobe. *The Journal of Neuroscience*, *25*(44), 10239-10246.

Barense, M. D., Gaffan, D., & Graham, K. S. (2007). The human medial temporal lobe processes online representations of complex objects. *Neuropsychologia*, *45*(13), 2963-2974.

Barker, G. R., & Warburton, E. C. (2011). When is the hippocampus involved in recognition memory?. *The Journal of Neuroscience*, *31*(29), 10721-10731.

Batchelder, W. H., & Riefer, D. M. (1999). Theoretical and empirical review of multinomial process tree modeling. *Psychonomic Bulletin & Review*, *6*(1), 57-86.

Battista, D., Ferrari, C. C., Gage, F. H., & Pitossi, F. J. (2006). Neurogenic niche modulation by activated microglia: transforming growth factor β increases neurogenesis in the adult dentate gyrus. *European Journal of Neuroscience*, *23*(1), 83-93.

Bauer, P. J. (2008). Toward a neuro-developmental account of the development of declarative memory. *Developmental psychobiology*, *50*(1), 19-31.

Beattie, E. C., Stellwagen, D., Morishita, W., Bresnahan, J. C., Ha, B. K., Von Zastrow, M., ... & Malenka, R. C. (2002). Control of synaptic strength by glial TNFα. *Science*, *295*(5563), 2282-2285.

Beauchamp, M. S., Petit, L., Ellmore, T. M., Ingeholm, J., & Haxby, J. V. (2001). A parametric fMRI study of overt and covert shifts of visuospatial attention. *NeuroImage*, *14*(2), 310- 321.

Bilbo, S. D., Biedenkapp, J. C., Der-Avakian, A., Watkins, L. R., Rudy, J. W., & Maier, S. F. (2005). Neonatal infection-induced memory impairment after lipopolysaccharide in adulthood is prevented via caspase-1 inhibition. *The Journal of neuroscience*, *25*(35), 8000-8009.

Binder, J. R., Desai, R. H., Graves, W. W., & Conant, L. L. (2009). Where is the semantic system? A critical review and meta-analysis of 120 functional neuroimaging studies. *Cerebral Cortex*, *19*(12), 2767-2796.

Bransford, J. D., & Johnson, M. K. (1972). Contextual prerequisites for understanding: Some investigations of comprehension and recall. *Journal of verbal learning and verbal behavior*, *11*(6), 717-726.

Brett, M., Anton, J. L., Valabregue, R., & Poline, J. B. (2002). Region of interest analysis using the MarsBar toolbox for SPM 99. *Neuroimage, 16*(2), S497.

Brodmann K. (1994/1909). *Localisation in the cerebral cortex*. London: Smith-Gordon.

Bunsey, M., & Eichenbaum, H. (1996). Conservation of hippocampal memory function in rats and humans. *Nature*, *379*(6562), 255-257.

Bussey, T. J., Saksida, L. M., & Murray, E. A. (2002). Perirhinal cortex resolves feature ambiguity in complex visual discriminations. *European Journal of Neuroscience*, *15*(2), 365-374.

Cabeza, R. (2008). Role of parietal regions in episodic memory retrieval: the dual attentional processes hypothesis. *Neuropsychologia*, *46*(7), 1813-1827.

Cabeza, R., Ciaramelli, E., Olson, I. R., & Moscovitch, M. (2008). The parietal cortex and episodic memory: an attentional account. *Nature Reviews Neuroscience*, *9*(8), 613-625.

Cagnin, A., Brooks, D. J., Kennedy, A. M., Gunn, R. N., Myers, R., Turkheimer, F. E., ... & Banati, R. B. (2001a). In-vivo measurement of activated microglia in dementia. *The Lancet*, *358*(9280), 461-467.

Cagnin, A., Myers, R., Gunn, R. N., Lawrence, A. D., Stevens, T., Kreutzberg, G. W., ... & Banati, R. B. (2001b). In vivo visualization of activated glia by [11C](R)-PK11195-PET following herpes encephalitis reveals projected neuronal damage beyond the primary focal lesion. *Brain*, *124*(10), 2014-2027.

Calvert, G. A. (2001). Crossmodal processing in the human brain: insights from functional neuroimaging studies. *Cerebral cortex*, *11*(12), 1110-1123.

Cansino, S., Maquet, P., Dolan, R. J., & Rugg, M. D. (2002). Brain activity underlying encoding and retrieval of source memory. *Cerebral Cortex, 12*(10), 1048-1056.

Carey, S., & Bartlett, E. (1978). Acquiring a single new word. *Proceedings of the Stanford Child Language Conference, 15*, 17–29.

Carson, M. J., Thrash, J. C., & Walter, B. (2006). The cellular response in neuroinflammation: the role of leukocytes, microglia and astrocytes in neuronal death and survival. *Clinical neuroscience research*, *6*(5), 237-245.

Ciaramelli, E., Grady, C. L., & Moscovitch, M. (2008). Top-down and bottom-up attention to memory: a hypothesis (AtoM) on the role of the posterior parietal cortex in memory retrieval. *Neuropsychologia*, *46*(7), 1828-1851.

Cipolotti, L., Bird, C., Good, T., Macmanus, D., Rudge, P., & Shallice, T. (2006). Recollection and familiarity in dense hippocampal amnesia: A case study. *Neuropsychologia*, *44*(3), 489-506.

Clark, R. E., Manns, J. R., & Squire, L. R. (2002). Classical conditioning, awareness, and brain systems. *Trends in cognitive sciences*, *6*(12), 524-531.

Cohen, G. (1979). Language comprehension in old age. *Cognitive psychology*, *11*(4), 412-429.

Cohen, N. J., & Eichenbaum, H. (1993). *Memory, Amnesia, and The Hippocampal System. Cambridge*, MA, MIT Press.

Cohen, N. J., & Squire, L. R. (1980). Preserved learning and retention of pattern-analyzing skill in amnesia: dissociation of knowing how and knowing that. *Science*, *210*(4466), 207-210.

Cools, R., Clark, L., & Robbins, T. W. (2004). Differential responses in human striatum and prefrontal cortex to changes in object and rule relevance. *The Journal of Neuroscience*, *24*(5), 1129-1135.

Corbetta, M., & Shulman, G. L. (2002). Control of goal-directed and stimulus-driven attention in the brain. *Nature reviews neuroscience*, *3*(3), 201-215.

Corkin, S. (1984, January). Lasting consequences of bilateral medial temporal lobectomy: Clinical course and experimental findings in HM. In *Seminars in Neurology* (Vol. 4, No. 2, pp. 249-259).

Costafreda, S. G., Fu, C. H., Lee, L., Everitt, B., Brammer, M. J., & David, A. S. (2006). A systematic review and quantitative appraisal of fMRI studies of verbal fluency: role of the left inferior frontal gyrus. *Human brain mapping*, *27*(10), 799-810.

Courtney, S. M., Ungerleider, L. G., Keil, K., & Haxby, J. V. (1997). Transient and sustained activity in a distributed neural system for human working memory. *Nature*, *386*(6625), 608-611.

Cusack, R. (2005). The intraparietal sulcus and perceptual organization. *Journal of cognitive neuroscience*, *17*(4), 641-651.

Davachi, L., Mitchell, J. P., & Wagner, A. D. (2003). Multiple routes to memory: distinct medial temporal lobe processes build item and source memories. *Proceedings of the National Academy of Sciences, 100*(4), 2157-2162.

Davies, M., Machin, P. E., Sanderson, D. J., Pearce, J. M., & Aggleton, J. P. (2007). Neurotoxic lesions of the rat perirhinal and postrhinal cortices and their impact on biconditional visual discrimination tasks. *Behavioural brain research*, *176*(2), 274-283.

Deisseroth, K., Singla, S., Toda, H., Monje, M., Palmer, T. D., & Malenka, R. C. (2004). Excitation-neurogenesis coupling in adult neural stem/progenitor cells. *Neuron*, *42*(4), 535-552.

Demonet, J. F., Chollet, F., Ramsay, S., Cardebat, D., Nespoulous, J. L., Wise, R., ... & Frackowiak, R. (1992). The anatomy of phonological and semantic processing in normal subjects. *Brain*, *115*(6), 1753-1768.

Deng, W., Aimone, J. B., & Gage, F. H. (2010). New neurons and new memories: how does adult hippocampal neurogenesis affect learning and memory?. *Nature Reviews Neuroscience*, *11*(5), 339-350.

De Visscher, A., Berens, S. C., Keidel, J. L., Noël, M. P., & Bird, C. M. (2015). The interference effect in arithmetic fact solving: An fMRI study. *NeuroImage*, *116*, 92-101.

De Visscher, A., & Noël, M. P. (2014). Arithmetic facts storage deficit: the hypersensitivity-to-interference in memory hypothesis. *Developmental science*, *17*(3), 434-442.

DeVito, L. M., Kanter, B. R., & Eichenbaum, H. (2010). The hippocampus contributes to memory expression during transitive inference in mice. *Hippocampus*, *20*(1), 208-217.

DeWitt, I., & Rauschecker, J. P. (2012). Phoneme and word recognition in the auditory ventral stream. *Proceedings of the National Academy of Sciences*, *109*(8), E505-E514.

DeWitt, I., & Rauschecker, J. P. (2013). Wernicke's area revisited: parallel streams and word processing. *Brain and language*, *127*(2), 181-191.

Dienes, Z. (2011). Bayesian versus orthodox statistics: which side are you on?. *Perspectives on Psychological Science*, *6*(3), 274-290.

Diguet, E., Gross, C. E., Tison, F., & Bezard, E. (2004). Rise and fall of minocycline in neuroprotection: need to promote publication of negative results. *Experimental neurology*, *189*(1), 1-4.

Dodel, R., Spottke, A., Gerhard, A., Reuss, A., Reinecker, S., Schimke, N., ... & Eggert, K. (2010). Minocycline 1-year therapy in multiple-system-atrophy: Effect on clinical symptoms and [11C](R)-PK11195 PET (MEMSA-trial).*Movement Disorders*, *25*(1), 97-107.

Doeller, C. F., & Burgess, N. (2008). Distinct error-correcting and incidental learning of location relative to landmarks and boundaries. *Proceedings of the National Academy of Sciences*, *105*(15), 5909-5914.

Doeller, C. F., King, J. A., & Burgess, N. (2008). Parallel striatal and hippocampal systems for landmarks and boundaries in spatial memory. *Proceedings of the National Academy of Sciences*, *105*(15), 5915-5920.

Domercq, M., & Matute, C. (2004). Neuroprotection by tetracyclines. *Trends in pharmacological sciences*, *25*(12), 609-612.

Donner, T. H., Kettermann, A., Diesch, E., Ostendorf, F., Villringer, A., & Brandt, S. A. (2002). Visual feature and conjunction searches of equal difficulty engage only partially overlapping frontoparietal networks. *NeuroImage*, *15*(1), 16-25.

du Boisgueheneuc, F., Levy, R., Volle, E., Seassau, M., Duffau, H., Kinkingnehun, S., ... & Dubois, B. (2006). Functions of the left superior frontal gyrus in humans: a lesion study. *Brain*, *129*(12), 3315-3328.

Duff, M. C., Hengst, J., Tranel, D., & Cohen, N. J. (2006). Development of shared information in communication despite hippocampal amnesia. *Nature neuroscience*, *9*(1), 140-146.

Dusek, J. A., & Eichenbaum, H. (1997). The hippocampus and memory for orderly stimulus relations. *Proceedings of the National Academy of Sciences*, *94*(13), 7109-7114.

Eacott, M. J., Machin, P. E., & Gaffan, E. A. (2001). Elemental and configural visual discrimination learning following lesions to perirhinal cortex in the rat. *Behavioural brain research*, *124*(1), 55-70.

Eichenbaum, H. (1999). The hippocampus and mechanisms of declarative memory. *Behavioural brain research*, *103*(2), 123-133.

Eichenbaum, H. (2001). The hippocampus and declarative memory: cognitive mechanisms and neural codes. *Behavioural brain research*, *127*(1), 199-207.

Eichenbaum, H., Otto, T., & Cohen, N. J. (1994). Two functional components of the hippocampal memory system. *Behavioral and Brain Sciences*, *17*(03), 449-472.

Eisner, F., McGettigan, C., Faulkner, A., Rosen, S., & Scott, S. K. (2010). Inferior frontal gyrus activation predicts individual differences in perceptual learning of cochlear-implant simulations. *The Journal of Neuroscience*, *30*(21), 7179-7186.

Ekdahl, C. T., Claasen, J. H., Bonde, S., Kokaia, Z., & Lindvall, O. (2003). Inflammation is detrimental for neurogenesis in adult brain. *Proceedings of the National Academy of Sciences*, *100*(23), 13632-13637.

Ekdahl, C. T., Kokaia, Z., & Lindvall, O. (2009). Brain inflammation and adult neurogenesis: the dual role of microglia. *Neuroscience*, *158*(3), 1021-1029.

Ericsson, A., Liu, C., Hart, R. P., & Sawchenko, P. E. (1995). Type 1 interleukin-1 receptor in the rat brain: Distribution, regulation, and relationship to sites of IL-1–induced cellular activation. *Journal of Comparative Neurology*, *361*(4), 681-698.

Erta, M., Quintana, A., & Hidalgo, J. (2012). Interleukin-6, a major cytokine in the central nervous system. *International journal of biological sciences*, *8*(9), 1254.

Fiorillo, C. D., Tobler, P. N., & Schultz, W. (2003). Discrete coding of reward probability and uncertainty by dopamine neurons. *Science*, *299*(5614), 1898-1902.

Fox, M. D., Snyder, A. Z., Vincent, J. L., Corbetta, M., Van Essen, D. C., & Raichle, M. E. (2005). The human brain is intrinsically organized into dynamic, anticorrelated functional networks. *Proceedings of the National Academy of Sciences of the United States of America*, *102*(27), 9673-9678.

Foxe, J. J., Wylie, G. R., Martinez, A., Schroeder, C. E., Javitt, D. C., Guilfoyle, D., ... & Murray, M. M. (2002). Auditory-somatosensory multisensory processing in auditory association cortex: an fMRI study. *Journal of Neurophysiology*, *88*(1), 540-543.

Frank, M. J., Rudy, J. W., & O'Reilly, R. C. (2003). Transitivity, flexibility, conjunctive representations, and the hippocampus. II. A computational analysis. *Hippocampus*, *13*(3), 341-354.

Friedrich M, & Friederici A. D. (2008) Neurophysiological correlates of online word learning in 14-month-old infants. *NeuroReport 19*, 1757–1761.

Friston, K. J., Buechel, C., Fink, G. R., Morris, J., Rolls, E., & Dolan, R. J. (1997). Psychophysiological and modulatory interactions in neuroimaging. *NeuroImage*, *6*(3), 218-229.

Friston, K. J., Stephan, K. E., Lund, T. E., Morcom, A., & Kiebel, S. (2005). Mixed-effects and fMRI studies. *NeuroImage*, *24*(1), 244-252.

Gaffan, D. (1994). Scene-specific memory for objects: a model of episodic memory impairment in monkeys with fornix transection. *Journal of Cognitive Neuroscience*, *6*(4), 305-320.

Gallagher, M., & Holland, P. C. (1992). Preserved configural learning and spatial learning impairment in rats with hippocampal damage. *Hippocampus*, *2*(1), 81-88.

Gangwani, T., Kachergis, G., & Yu, C. (2010). Simultaneous Cross-situational Learning of Category and Object Names. In S. Ohlsson & R. Catrambone (Eds.), *Proceedings of the 32nd Annual Conference of the Cognitive Science Society* (pp. 1595-1600). Austin, TX: Cognitive Science Society.

Gauthier, I., Tarr, M. J., Anderson, A. W., Skudlarski, P., & Gore, J. C. (1999). Activation of the middle fusiform' face area' increases with expertise in recognizing novel objects. *Nature neuroscience*, *2*(6), 568-573.

Ge, S., Yang, C. H., Hsu, K. S., Ming, G. L., & Song, H. (2007). A critical period for enhanced synaptic plasticity in newly generated neurons of the adult brain. *Neuron*, *54*(4), 559-566.

Gharabaghi, A., Berger, M. F., Tatagiba, M., & Karnath, H. O. (2006). The role of the right superior temporal gyrus in visual search—insights from intraoperative electrical stimulation. *Neuropsychologia*, *44*(12), 2578-2581.

Gläscher, J., Hampton, A. N., & O'Doherty, J. P. (2009). Determining a role for ventromedial prefrontal cortex in encoding action-based value signals during reward-related decision making. *Cerebral cortex*, *19*(2), 483-495.

Grabner, R. H., Ansari, D., Koschutnig, K., Reishofer, G., Ebner, F., & Neuper, C. (2009). To retrieve or to calculate? Left angular gyrus mediates the retrieval of arithmetic facts during problem solving. *Neuropsychologia*, *47*(2), 604-608.

Greene, A. J., Gross, W. L., Elsinger, C. L., & Rao, S. M. (2006). An FMRI analysis of the human hippocampus: inference, context, and task awareness. *Journal of cognitive neuroscience*, *18*(7), 1156-1173.

Greve, A., Cooper, E., & Henson, R. N. (2014). No evidence that ‘fast-mapping’ benefits novel learning in healthy older adults. *Neuropsychologia*, *60*, 52-59.

Griffin, R., Nally, R., Nolan, Y., McCartney, Y., Linden, J., & Lynch, M. A. (2006). The age-related attenuation in long-term potentiation is associated with microglial activation. *Journal of neurochemistry*, *99*(4), 1263-1272.

Hagoort, P. (2005). On Broca, brain, and binding: a new framework. *Trends in cognitive sciences*, *9*(9), 416-423.

Han, J. S., Gallagher, M., & Holland, P. (1998). Hippocampal lesions enhance configural learning by reducing proactive interference. *Hippocampus*, *8*(2), 138-146.

Harrison, N. A., Doeller, C. F., Voon, V., Burgess, N., & Critchley, H. D. (2014). Peripheral inflammation acutely impairs human spatial memory via actions on medial temporal lobe glucose metabolism. *Biological psychiatry*, *76*(7), 585-593.

Hashimoto, K., Tsukada, H., Nishiyama, S., Fukumoto, D., Kakiuchi, T., & Iyo, M. (2007). Protective effects of minocycline on the reduction of dopamine transporters in the striatum after administration of methamphetamine: a positron emission tomography study in conscious monkeys. *Biological psychiatry*, *61*(5), 577-581.

He, Y. I., Appel, S., & Le, W. (2001). Minocycline inhibits microglial activation and protects nigral cells after 6-hydroxydopamine injection into mouse striatum. *Brain research*, *909*(1), 187-193.

Heckers, S., Zalesak, M., Weiss, A. P., Ditman, T., & Titone, D. (2004). Hippocampal activation during transitive inference in humans. *Hippocampus*, *14*(2), 153-162.

Henson, R. N. A., & Penny, W. D. (2003). ANOVAs and SPM. Wellcome Department of Imaging Neuroscience, London, UK.

Hinwood, M., Tynan, R. J., Charnley, J. L., Beynon, S. B., Day, T. A., & Walker, F. R. (2012). Chronic stress induced remodeling of the prefrontal cortex: structural re-organization of microglia and the inhibitory effect of minocycline. *Cerebral Cortex*, 151.

Holdstock, J. S., Hocking, J., Notley, P., Devlin, J. T., & Price, C. J. (2009). Integrating visual and tactile information in the perirhinal cortex. *Cerebral Cortex*, *19*(12), 2993-3000.

Hornak, J., O'Doherty, J. E., Bramham, J., Rolls, E. T., Morris, R. G., Bullock, P. R., & Polkey, C. E. (2004). Reward-related reversal learning after surgical excisions in orbito-frontal or dorsolateral prefrontal cortex in humans. *Cognitive Neuroscience, Journal of*, *16*(3), 463-478.

Horst, J. S. (2009). The Novel Object and Unusual Name (NOUN) database. http://www.sussex.ac.uk/wordlab/noun

Horst, J. S., & Samuelson, L. K. (2008). Fast mapping but poor retention by 24-month-old infants. *Infancy*, *13*(2), 128-157.

Howard, M. W. (2004). Scaling behavior in the temporal context model. *Journal of Mathematical Psychology*, *48*(4), 230-238.

Howard, M. W., Fotedar, M. S., Datey, A. V., & Hasselmo, M. E. (2005). The temporal context model in spatial navigation and relational learning: toward a common explanation of medial temporal lobe function across domains. *Psychological review*, *112*(1), 75.

Howard, M. W., & Kahana, M. J. (2002). A distributed representation of temporal context. *Journal of Mathematical Psychology*, *46*(3), 269-299.

Howard, M. W., Shankar, K. H., & Jagadisan, U. K. (2011). Constructing semantic representations from a gradually changing representation of temporal context. *Topics in Cognitive Science*, *3*(1), 48-73.

Humphries, C., Binder, J. R., Medler, D. A., & Liebenthal, E. (2007). Time course of semantic processes during sentence comprehension: an fMRI study. *NeuroImage*, *36*(3), 924-932.

Hutton, C., Bork, A., Josephs, O., Deichmann, R., Ashburner, J., & Turner, R. (2002). Image distortion correction in fMRI: a quantitative evaluation. *NeuroImage*, *16*(1), 217-240.

Jeffreys, H. (1961). Theory of probability. Oxford University Press: UK.

Johnson, J. D., & Rugg, M. D. (2007). Recollection and the reinstatement of encoding-related cortical activity. *Cerebral Cortex*, *17*(11), 2507-2515.

Joint Formulary Committee & Royal Pharmaceutical Society of Great Britain. (2012). *British national formulary* (Vol. 64). Pharmaceutical Press.

Kachergis, G., Yu, C., & Shiffrin, R. M. (2010). Cross-situational statistical learning: Implicit or intentional. In *Proceedings of the 32nd annual conference of the cognitive science society* (pp. 1189-1194). Austin, TX: Cognitive Science Society.

Kachergis, G., Yu, C., & Shiffrin, R. M. (2012a). An associative model of adaptive inference for learning word–referent mappings. *Psychonomic bulletin & review*, *19*(2), 317-324.

Kachergis, G., Yu, C., & Shiffrin, R. M. (2012b). Cross-situational word learning is better modeled by associations than hypotheses. In *Development and Learning and Epigenetic Robotics (ICDL), 2012 IEEE International Conference on* (pp. 1-6). IEEE.

Kempermann, G., Wiskott, L., & Gage, F. H. (2004). Functional significance of adult neurogenesis. *Current opinion in neurobiology*, *14*(2), 186-191.

King, D. R., de Chastelaine, M., Elward, R. L., Wang, T. H., & Rugg, M. D. (2015). Recollection-Related Increases in Functional Connectivity Predict Individual Differences in Memory Accuracy. *The Journal of Neuroscience*, *35*(4), 1763-1772.

Koffie, R. M., Hyman, B. T., & Spires-Jones, T. L. (2011). Alzheimer's disease: synapses gone cold. *Molecular Neurodegeneration*, *6*(1), 63-63.

Kreutzberg, G. W. (1996). Microglia: a sensor for pathological events in the CNS. *Trends in neurosciences*, *19*(8), 312-318.

Kumaran, D. (2012). What representations and computations underpin the contribution of the hippocampus to generalization and inference?. *Frontiers in human neuroscience*, *6*.

Kumaran, D., Hassabis, D., Spiers, H. J., Vann, S. D., Vargha-Khadem, F., & Maguire, E. A. (2007). Impaired spatial and non-spatial configural learning in patients with hippocampal pathology. *Neuropsychologia*, *45*(12), 2699-2711.

Kumaran, D., & McClelland, J. L. (2012). Generalization through the recurrent interaction of episodic memories: a model of the hippocampal system. *Psychological review*, *119*(3), 573.

Lambon Ralph, M. A., Lowe, C., & Rogers, T. T. (2007). Neural basis of category-specific semantic deficits for living things: evidence from semantic dementia, HSVE and a neural network model. *Brain*, *130*(4), 1127-1137.

Law, J. R., Flanery, M. A., Wirth, S., Yanike, M., Smith, A. C., Frank, L. M., ... & Stark, C. E. (2005). Functional magnetic resonance imaging activity during the gradual acquisition and expression of paired-associate memory. *The Journal of neuroscience*, *25*(24), 5720-5729.

Lawson, L. J., Perry, V. H., Dri, P., & Gordon, S. (1990). Heterogeneity in the distribution and morphology of microglia in the normal adult mouse brain. *Neuroscience*, *39*(1), 151-170.

Lee, A. C., Bussey, T. J., Murray, E. A., Saksida, L. M., Epstein, R. A., Kapur, N., ... & Graham, K. S. (2005). Perceptual deficits in amnesia: challenging the medial temporal lobe 'mnemonic' view. *Neuropsychologia*, *43*(1), 1-11.

Lee, A. C., & Rudebeck, S. R. (2010). Human medial temporal lobe damage can disrupt the perception of single objects. *The Journal of neuroscience*, *30*(19), 6588-6594.

Lee, A. C., Yeung, L. K., & Barense, M. D. (2012). The hippocampus and visual perception. *Frontiers in Human Neuroscience*, *6*.

Leuner, B., & Gould, E. (2010). Structural plasticity and hippocampal function. *Annual review of psychology*, *61*, 111.

Liu, T. T. (2004). Efficiency, power, and entropy in event-related fMRI with multiple trial types: Part II: design of experiments. *NeuroImage*, *21*(1), 401-413.

Lledo, P. M., Alonso, M., & Grubb, M. S. (2006). Adult neurogenesis and functional plasticity in neuronal circuits. *Nature Reviews Neuroscience*, *7*(3), 179-193.

Lu, M. T., Preston, J. B., & Strick, P. L. (1994). Interconnections between the prefrontal cortex and the premotor areas in the frontal lobe. *Journal of Comparative Neurology*, *341*(3), 375-392.

Luppino, G., Matelli, M., Camarda, R., & Rizzolatti, G. (1993). Corticocortical connections of area F3 (SMA-proper) and area F6 (pre-SMA) in the macaque monkey. *Journal of Comparative Neurology*, *338*(1), 114-140.

Macmillan, N. A., & Creelman, C. D. (1991). *Detection theory: a user's guide.* Cambridge University Press.

Maess, B., Koelsch, S., Gunter, T. C., & Friederici, A. D. (2001). Musical syntax is processed in Broca's area: an MEG study. *Nature neuroscience*, *4*(5), 540-545.

Maldjian, J. A., Laurienti, P. J., Kraft, R. A., & Burdette, J. H. (2003). An automated method for neuroanatomic and cytoarchitectonic atlas-based interrogation of fMRI data sets. *NeuroImage*, *19*(3), 1233-1239.

Martins, S., Guillery-Girard, B., Jambaqué, I., Dulac, O., & Eustache, F. (2006). How children suffering severe amnesic syndrome acquire new concepts?. *Neuropsychologia*, *44*(14), 2792-2805.

Masson, M. E. (2011). A tutorial on a practical Bayesian alternative to null-hypothesis significance testing. *Behavior research methods*, *43*(3), 679-690.

McClelland, J. L. (2013). Incorporating rapid neocortical learning of new schema-consistent information into complementary learning systems theory. *Journal of Experimental Psychology: General*, *142*(4), 1190.

McClelland, J. L., & Goddard, N. H. (1996). Considerations arising from a complementary learning systems perspective on hippocampus and neocortex. *Hippocampus*, *6*(6), 654-665.

McClelland, J. L., McNaughton, B. L., & O'Reilly, R. C. (1995). Why there are complementary learning systems in the hippocampus and neocortex: insights from the successes and failures of connectionist models of learning and memory. *Psychological review*, *102*(3), 419.

McCloskey, M., & Cohen, N. J. (1989). Catastrophic interference in connectionist networks: The sequential learning problem. *The psychology of learning and motivation*, *24*(109-165), 92.

McEchron, M. D., Bouwmeester, H., Tseng, W., Weiss, C., & Disterhoft, J. F. (1998). Hippocampectomy disrupts auditory trace fear conditioning and contextual fear conditioning in the rat. *Hippocampus*, *8*(6), 638-646.

McLaren, D. G., Ries, M. L., Xu, G., & Johnson, S. C. (2012). A generalized form of context-dependent psychophysiological interactions (gPPI): a comparison to standard approaches. *NeuroImage*, *61*(4), 1277-1286.

McMurray, B., Horst, J. S., & Samuelson, L. K. (2012). Word learning emerges from the interaction of online referent selection and slow associative learning. *Psychological review*, *119*(4), 831.

Medina, T. N., Snedeker, J., Trueswell, J. C., & Gleitman, L. R. (2011). How words can and cannot be learned by observation. *Proceedings of the National Academy of Sciences*, *108*(22), 9014-9019.

Middleton, F. A., & Strick, P. L. (1996). The temporal lobe is a target of output from the basal ganglia. *Proceedings of the National Academy of Sciences*, *93*(16), 8683-8687.

Monje, M. L., Toda, H., & Palmer, T. D. (2003). Inflammatory blockade restores adult hippocampal neurogenesis. *Science*, *302*(5651), 1760-1765.

Monti, M. M., Osherson, D. N., Martinez, M. J., & Parsons, L. M. (2007). Functional neuroanatomy of deductive inference: a language-independent distributed network. *NeuroImage*, *37*(3), 1005-1016.

Monti, M. M., Parsons, L. M., & Osherson, D. N. (2009). The boundaries of language and thought in deductive inference. *Proceedings of the National Academy of Sciences*, *106*(30), 12554-12559.

Moses, S. N., Ryan, J. D., Bardouille, T., Kovacevic, N., Hanlon, F. M., & McIntosh, A. R. (2009). Semantic information alters neural activation during transverse patterning performance. *NeuroImage*, *46*(3), 863-873.

Moses, S. N., Ostreicher, M. L., Rosenbaum, R. S., & Ryan, J. D. (2008). Successful transverse patterning in amnesia using semantic knowledge. *Hippocampus*, *18*(2), 121-124.

Moshagen, M. (2010). multiTree: A computer program for the analysis of multinomial processing tree models. *Behavior Research Methods*, *42*(1), 42-54.

Musso, M., Moro, A., Glauche, V., Rijntjes, M., Reichenbach, J., Büchel, C., & Weiller, C. (2003). Broca's area and the language instinct. *Nature neuroscience*, *6*(7), 774-781.

Nadel, L., & Moscovitch, M. (1997). Memory consolidation, retrograde amnesia and the hippocampal complex. *Current opinion in neurobiology*, *7*(2), 217-227.

Nelson, S. M., Dosenbach, N. U., Cohen, A. L., Wheeler, M. E., Schlaggar, B. L., & Petersen, S. E. (2010). Role of the anterior insula in task-level control and focal attention. *Brain structure and function*, *214*(5-6), 669-680.

Nimmerjahn, A., Kirchhoff, F., & Helmchen, F. (2005). Resting microglial cells are highly dynamic surveillants of brain parenchyma in vivo. *Science*, *308*(5726), 1314-1318.

Nobre, A. C., Gitelman, D. R., Dias, E. C., & Mesulam, M. M. (2000). Covert visual spatial orienting and saccades: overlapping neural systems. *NeuroImage*, *11*(3), 210-216.

Noppeney, U., Patterson, K., Tyler, L. K., Moss, H., Stamatakis, E. A., Bright, P., ... & Price, C. J. (2007). Temporal lobe lesions and semantic impairment: a comparison of herpes simplex virus encephalitis and semantic dementia. *Brain*, *130*(4), 1138-1147.

Obleser, J., Wise, R. J., Dresner, M. A., & Scott, S. K. (2007). Functional integration across brain regions improves speech perception under adverse listening conditions. *The Journal of Neuroscience*, *27*(9), 2283-2289.

O'Kane, G., Kensinger, E. A., & Corkin, S. (2004). Evidence for semantic learning in profound amnesia: an investigation with patient HM. *Hippocampus*, *14*(4), 417-425.

O'Reilly, R. C., & McClelland, J. L. (1994). Hippocampal conjunctive encoding, storage, and recall: avoiding a trade-off. *Hippocampus*, *4*(6), 661-682.

Perry, V. H., Cunningham, C., & Holmes, C. (2007). Systemic infections and inflammation affect chronic neurodegeneration. *Nature Reviews Immunology*, *7*(2), 161-167.

Poldrack, R. A., Clark, J., Pare-Blagoev, E. J., Shohamy, D., Moyano, J. C., Myers, C., & Gluck, M. A. (2001). Interactive memory systems in the human brain. *Nature*, *414*(6863), 546- 550.

Poldrack, R. A., Prabhakaran, V., Seger, C. A., & Gabrieli, J. D. (1999). Striatal activation during acquisition of a cognitive skill. *Neuropsychology*, *13*(4), 564.

Polyn, S. M., & Kahana, M. J. (2008). Memory search and the neural representation of context. *Trends in cognitive sciences*, *12*(1), 24-30.

Polyn, S. M., Natu, V. S., Cohen, J. D., & Norman, K. A. (2005). Category-specific cortical activity precedes retrieval during memory search. *Science*, *310*(5756), 1963-1966.

Preston, A. R., Shrager, Y., Dudukovic, N. M., & Gabrieli, J. D. (2004). Hippocampal contribution to the novel use of relational information in declarative memory. *Hippocampus*, *14*(2), 148-152.

Raivich, G., Bohatschek, M., Kloss, C. U., Werner, A., Jones, L. L., & Kreutzberg, G. W. (1999). Neuroglial activation repertoire in the injured brain: graded response, molecular mechanisms and cues to physiological function. *Brain Research Reviews*, *30*(1), 77-105.

Rakic, P. (2002). Adult neurogenesis in mammals: an identity crisis. *The Journal of Neuroscience*, *22*(3), 614-618.

Rescorla, L. A. (1980). Overextension in early language development. *Journal of Child Language*, *7*(02), 321-335.

Rodriguez-Moreno, D., & Hirsch, J. (2009). The dynamics of deductive reasoning: an fMRI investigation. *Neuropsychologia*, *47*(4), 949-961.

Rogers, R. L., Andrews, T. K., Grasby, P. M., Brooks, D. J., & Robbins, T. W. (2000). Contrasting cortical and subcortical activations produced by attentional-set shifting and reversal learning in humans. *Journal of Cognitive Neuroscience*, *12*(1), 142-162.

Rolls, E. T. (2013). The mechanisms for pattern completion and pattern separation in the hippocampus. *Frontiers in systems neuroscience*, *7*.

Rudy, J. W., & Sutherland, R. J. (1995). Configural association theory and the hippocampal formation: an appraisal and reconfiguration. *Hippocampus*, *5*(5), 375-389.

Rushworth, M. F., Noonan, M. P., Boorman, E. D., Walton, M. E., & Behrens, T. E. (2011). Frontal cortex and reward-guided learning and decision-making. *Neuron*, *70*(6), 1054-1069.

Saksida, L. M., & Bussey, T. J. (2010). The representational–hierarchical view of amnesia: Translation from animal to human. *Neuropsychologia*, *48*(8), 2370-2384.

Saksida, L. M., Bussey, T. J., Buckmaster, C. A., & Murray, E. A. (2007). Impairment and facilitation of transverse patterning after lesions of the perirhinal cortex and hippocampus, respectively. *Cerebral Cortex*, *17*(1), 108-115.

Sanderson, D. J., Pearce, J. M., Kyd, R. J., & Aggleton, J. P. (2006). The importance of the rat hippocampus for learning the structure of visual arrays. *European Journal of Neuroscience*, *24*(6), 1781-1788.

Saxe, M. D., Battaglia, F., Wang, J. W., Malleret, G., David, D. J., Monckton, J. E., ... & Drew, M. R. (2006). Ablation of hippocampal neurogenesis impairs contextual fear conditioning and synaptic plasticity in the dentate gyrus. *Proceedings of the National Academy of Sciences*, *103*(46), 17501-17506.

Schafer, G., & Plunkett, K. (1998). Rapid word learning by fifteen-month-olds under tightly controlled conditions. *Child development*, 309-320.

Schmidt-Hieber, C., Jonas, P., & Bischofberger, J. (2004). Enhanced synaptic plasticity in newly generated granule cells of the adult hippocampus. *Nature*, *429*(6988), 184-187.

Sederberg, P. B., Schulze-Bonhage, A., Madsen, J. R., Bromfield, E. B., Litt, B., Brandt, A., & Kahana, M. J. (2007). Gamma oscillations distinguish true from false memories. *Psychological Science*, *18*(11), 927-932.

Seger, C. A., & Cincotta, C. M. (2005). The roles of the caudate nucleus in human classification learning. *The Journal of Neuroscience*, *25*(11), 2941-2951.

Sescousse, G., Redouté, J., & Dreher, J. C. (2010). The architecture of reward value coding in the human orbitofrontal cortex. *The Journal of Neuroscience*, *30*(39), 13095-13104.

Shafritz, K. M., Gore, J. C., & Marois, R. (2002). The role of the parietal cortex in visual feature binding. *Proceedings of the National Academy of Sciences*, *99*(16), 10917-10922.

Sharon, T., Moscovitch, M., & Gilboa, A. (2011). Rapid neocortical acquisition of long-term arbitrary associations independent of the hippocampus. *Proceedings of the National Academy of Sciences*, *108*(3), 1146-1151.

Shohamy, D., & Wagner, A. D. (2008). Integrating memories in the human brain: hippocampal-midbrain encoding of overlapping events. *Neuron*, *60*(2), 378-389.

Simons, J. S., Verfaellie, M., Galton, C. J., Miller, B. L., Hodges, J. R., & Graham, K. S. (2002). Recollection-based memory in frontotemporal dementia: implications for theories of long-term memory. *Brain, 125*(11), 2523-2536.

Skotko, B. G., Kensinger, E. A., Locascio, J. J., Einstein, G., Rubin, D. C., Tupler, L. A., ... & Corkin, S. (2004). Puzzling thoughts for HM: Can new semantic information be anchored to old semantic memories? *Neuropsychology*, *18*(4), 756.

Smith, A. C., & Brown, E. N. (2003). Estimating a state-space model from point process observations. *Neural Computation*, *15*(5), 965-991.

Smith A., C., Frank L., M., Wirth S., Yanike M., Hu D., Kubota Y., Graybiel A. M., Suzuki W. A., Brown E., N. (2004) Dynamical analysis of learning in behavior experiments. *Journal of Neuroscience, 24*, 447-461.

Smith, C. N., Urgolites, Z. J., Hopkins, R. O., & Squire, L. R. (2014). Comparison of explicit and incidental learning strategies in memory-impaired patients. *Proceedings of the National Academy of Sciences*, *111*(1), 475-479.

Smith, K., Smith, A. D., & Blythe, R. A. (2011). Cross-situational learning: An experimental study of word-learning mechanisms. *Cognitive Science*, *35*(3), 480-498.

Smith, L., & Yu, C. (2008). Infants rapidly learn word-referent mappings via cross-situational statistics. *Cognition*, *106*(3), 1558-1568.

Squire, L. R., & Alvarez, P. (1995). Retrograde amnesia and memory consolidation: a neurobiological perspective. *Current opinion in neurobiology*, *5*(2), 169-177.

Squire, L. R., Knowlton, B., & Musen, G. (1993). The structure and organization of memory. *Annual review of psychology*, *44*(1), 453-495.

Squire, L. R., Slater, P. C., & Chace, P. M. (1975). Retrograde amnesia: temporal gradient in very long term memory following electroconvulsive therapy. *Science*, *187*(4171), 77-79.

Sriram, K., Miller, D. B., & O'Callaghan, J. P. (2006). Minocycline attenuates microglial activation but fails to mitigate striatal dopaminergic neurotoxicity: role of tumor necrosis factor-α. *Journal of neurochemistry*, *96*(3), 706-718.

Staresina, B.P. and Davachi, L. (2009). Mind the gap: Binding experiences across space and time in the human hippocampus. *Neuron 63*(2): 267 - 276.

Stence, N., Waite, M., & Dailey, M. E. (2001). Dynamics of microglial activation: A confocal time-lapse analysis in hippocampal slices. *Glia*, *33*(3), 256-266.

Strand, F., Forssberg, H., Klingberg, T., & Norrelgen, F. (2008). Phonological working memory with auditory presentation of pseudo-words—an event related fMRI Study. *Brain research*, *1212*, 48-54.

Sutherland, R. J., & Rudy, J. W. (1989). Configural association theory: The role of the hippocampal formation in learning, memory, and amnesia. *Psychobiology*, *17*(2), 129-144.

Swanson, L. W. (1982). The projections of the ventral tegmental area and adjacent regions: a combined fluorescent retrograde tracer and immunofluorescence study in the rat. *Brain research bulletin*, *9*(1), 321-353.

Tanaka, S. C., Doya, K., Okada, G., Ueda, K., Okamoto, Y., & Yamawaki, S. (2004). Prediction of immediate and future rewards differentially recruits cortico-basal ganglia loops. *Nature neuroscience*, *7*(8), 887-893.

Tettamanti, M., Rotondi, I., Perani, D., Scotti, G., Fazio, F., Cappa, S. F., & Moro, A. (2009). Syntax without language: Neurobiological evidence for cross-domain syntactic computations. *Cortex*, *45*(7), 825-838.

Thompson, R. F., & Kim, J. J. (1996). Memory systems in the brain and localization of a memory. *Proceedings of the national academy of sciences*, *93*(24), 13438-13444.

Tikka, T. M., Fiebich, B. L., Goldsteins, G., Keinänen, R., & Koistinaho, J. E. (2001). Minocycline, a tetracycline derivative, is neuroprotective against excitotoxicity by inhibiting activation and proliferation of microglia. *The journal of Neuroscience*, *21*(8), 2580-2588.

Tikka, T. M., & Koistinaho, J. E. (2001). Minocycline provides neuroprotection against N-methyl-D-aspartate neurotoxicity by inhibiting microglia. *The Journal of Immunology*, *166*(12), 7527-7533.

Trueswell, J. C., Medina, T. N., Hafri, A., & Gleitman, L. R. (2013). Propose but verify: Fast mapping meets cross-situational word learning. *Cognitive psychology*, *66*(1), 126-156.

Tse, D., Langston, R. F., Kakeyama, M., Bethus, I., Spooner, P. A., Wood, E. R., ... & Morris, R. G. (2007). Schemas and memory consolidation. *Science*, *316*(5821), 76-82.

Tulving, E. (1972). Episodic and semantic memory 1. *Organization of Memory. London: Academic*, *381*(e402), 4.

Tzourio-Mazoyer, N., Landeau, B., Papathanassiou, D., Crivello, F., Etard, O., Delcroix, N., ... & Joliot, M. (2002). Automated anatomical labeling of activations in SPM using a macroscopic anatomical parcellation of the MNI MRI single-subject brain. *NeuroImage*, *15*(1), 273-289.

UKCRN (2014). *Minocycline in Alzheimer's Disease Efficacy (MADE) trial*. Retrieved from: http://public.ukcrn.org.uk/search/StudyDetail.aspx?StudyID=14866.

Van der Jeugd, A., Goddyn, H., Laeremans, A., Arckens, L., D'Hooge, R., & Verguts, T. (2009). Hippocampal involvement in the acquisition of relational associations, but not in the expression of a transitive inference task in mice. *Behavioral neuroscience*, *123*(1), 109.

van Eimeren, L., Grabner, R. H., Koschutnig, K., Reishofer, G., Ebner, F., & Ansari, D. (2010). Structure-function relationships underlying calculation: a combined diffusion tensor imaging and fMRI study. *NeuroImage*, *52*(1), 358-363.

van Kesteren, M. T., Ruiter, D. J., Fernández, G., & Henson, R. N. (2012). How schema and novelty augment memory formation. *Trends in neurosciences*, *35*(4), 211-219.

van Praag, H., Shubert, T., Zhao, C., & Gage, F. H. (2005). Exercise enhances learning and hippocampal neurogenesis in aged mice. *The Journal of Neuroscience*, *25*(38), 8680-8685.

Vargha-Khadem, F., Gadian, D. G., & Mishkin, M. (2001). Dissociations in cognitive memory: the syndrome of developmental amnesia. *Philosophical Transactions of the Royal Society B: Biological Sciences*, *356*(1413), 1435-1440.

Viviani, B., Bartesaghi, S., Gardoni, F., Vezzani, A., Behrens, M. M., Bartfai, T., ... & Marinovich, M. (2003). Interleukin-1β enhances NMDA receptor-mediated intracellular calcium increase through activation of the Src family of kinases. *The Journal of neuroscience*, *23*(25), 8692-8700.

Wagner, I. C., van Buuren, M., Kroes, M. C., Gutteling, T. P., van der Linden, M., Morris, R. G., & Fernández, G. (2015). Schematic memory components converge within angular gyrus during retrieval. *ELife, 4*, e09668.

Wardak, C., Olivier, E., & Duhamel, J. R. (2002). Saccadic target selection deficits after lateral intraparietal area inactivation in monkeys. *The Journal of neuroscience*, *22*(22), 9877-9884.

Warren, D. E., & Duff, M. C. (2014). Not so fast: Hippocampal amnesia slows word learning despite successful fast mapping. *Hippocampus*, *24*(8), 920-933

Warrington, E. K. (1975). The selective impairment of semantic memory. *The Quarterly journal of experimental psychology*, *27*(4), 635-657.

Warrington, E. K., & Duchen, L. W. (1992). A re-appraisal of a case of persistent global amnesia following right temporal lobectomy: a clinico-pathological study. *Neuropsychologia*, *30*(5), 437-450.

Warrington, E. K., & Shallice, T. (1984). Category specific semantic impairments. *Brain*, *107*(3), 829-853.

Wiltgen, B. J., & Silva, A. J. (2007). Memory for context becomes less specific with time. *Learning & Memory*, *14*(4), 313-317.

Winocur, G., Frankland, P. W., Sekeres, M., Fogel, S., & Moscovitch, M. (2009). Changes in context-specificity during memory reconsolidation: selective effects of hippocampal lesions. *Learning & Memory*, *16*(11), 722-729.

Winocur, G., & Moscovitch, M. (2011). Memory transformation and systems consolidation. *Journal of the International Neuropsychological Society*, *17*(05), 766-780.

Winocur, G., Moscovitch, M., & Sekeres, M. (2007). Memory consolidation or transformation: context manipulation and hippocampal representations of memory. *Nature neuroscience*, *10*(5), 555-557.

Wixted, J. T. (2007). Dual-process theory and signal-detection theory of recognition memory. *Psychological review, 114*(1), 152.

Woodroofe, M. N. (1995). Cytokine production in the central nervous system. *Neurology*, *45*(6), S6-S10.

Wunderlich, K., Rangel, A., & O'Doherty, J. P. (2010). Economic choices can be made using only stimulus values. *Proceedings of the National Academy of Sciences*, *107*(34), 15005-15010.

Yassa, M. A., & Stark, C. E. (2011). Pattern separation in the hippocampus. *Trends in neurosciences*, *34*(10), 515-525.

Ye, S. M., & Johnson, R. W. (1999). Increased interleukin-6 expression by microglia from brain of aged mice. *Journal of neuroimmunology*, *93*(1), 139-148.

Yirmiya, R., & Goshen, I. (2011). Immune modulation of learning, memory, neural plasticity and neurogenesis. *Brain, behavior, and immunity*, *25*(2), 181-213.

Yonelinas, A. P. (1999). The contribution of recollection and familiarity to recognition and source-memory judgments: A formal dual-process model and an analysis of receiver operating characteristics. *Journal of Experimental Psychology: Learning, Memory, and Cognition, 25*(6), 1415.

Yonelinas, A. P., Dobbins, I., Szymanski, M. D., Dhaliwal, H. S., & King, L. (1996). Signal-detection, threshold, and dual-process models of recognition memory: ROCs and conscious recollection. *Consciousness and Cognition, 5*(4), 418–441.

Yrjänheikki, J., Keinänen, R., Pellikka, M., Hökfelt, T., & Koistinaho, J. (1998). Tetracyclines inhibit microglial activation and are neuroprotective in global brain ischemia. *Proceedings of the National Academy of Sciences*, *95*(26), 15769-15774.

Yu, C., & Smith, L. B. (2007). Rapid word learning under uncertainty via cross-situational statistics. *Psychological Science*, *18*(5), 414-420.

Zalesak, M., & Heckers, S. (2009). The role of the hippocampus in transitive inference. *Psychiatry Research: Neuroimaging*, *172*(1), 24-30.

Zeithamova, D., Dominick, A. L., & Preston, A. R. (2012). Hippocampal and ventral medial prefrontal activation during retrieval-mediated learning supports novel inference. *Neuron*, *75*(1), 168-179.

Zeithamova, D., & Preston, A. R. (2010). Flexible memories: differential roles for medial temporal lobe and prefrontal cortex in cross-episode binding. *The Journal of Neuroscience*, *30*(44), 14676-14684.

Zeithamova, D., Schlichting, M. L., & Preston, A. R. (2012). The hippocampus and inferential reasoning: building memories to navigate future decisions. *Frontiers in human neuroscience*, *6*.

Zhang, S., Ide, J. S., & Chiang-shan, R. L. (2012). Resting-state functional connectivity of the medial superior frontal cortex. *Cerebral Cortex*, *22*(1), 99-111.

Zhong, Y., Zhou, L. J., Ren, W. J., Xin, W. J., Li, Y. Y., Zhang, T., & Liu, X. G. (2010). The direction of synaptic plasticity mediated by C-fibers in spinal dorsal horn is decided by Src-family kinases in microglia: The role of tumor necrosis factor-α. *Brain, behavior, and immunity*, *24*(6), 874-880.

Ziv, Y., Ron, N., Butovsky, O., Landa, G., Sudai, E., Greenberg, N., ... & Schwartz, M. (2006). Immune cells contribute to the maintenance of neurogenesis and spatial learning abilities in adulthood. *Nature neuroscience*, *9*(2), 268-275.